

**DRUG SCREENING UTILIZING THE VISUAL MOTOR RESPONSE OF
A ZEBRAFISH MODEL OF RETINITIS PIGMENTOSA** by

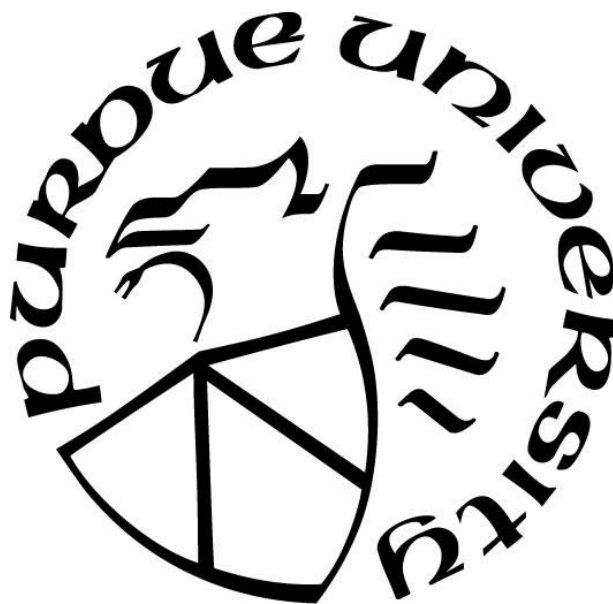
Logan Ganzen

A Dissertation

Submitted to the Faculty of Purdue University

In Partial Fulfillment of the Requirements for the degree of

Doctor of Philosophy



Department of Biological Sciences

West Lafayette, Indiana

May 2020

THE PURDUE UNIVERSITY GRADUATE SCHOOL
STATEMENT OF COMMITTEE APPROVAL

Dr. Yuk Fai Leung, Chair

Department of Biological Sciences

Dr. Donald Ready

Department of Biological Sciences

Dr. Daniel Suter

Department of Biological Sciences

Dr. Connie Weaver

Department of Nutritional Sciences

Approved by:

Dr. Jason Cannon and Dr. Janice Evans

*To my family,
for their love, support, and encouragement to be my best.*

ACKNOWLEDGMENTS

This work would never have been possible without the support of many people. Firstly, I would like to recognize my Ph.D. mentor Dr. Yuk Fai Leung. His support and guidance have helped me to transform into a greater scientist and person. I am thankful for the time I have spent with him as my mentor.

I would like to thank my thesis committee, Dr. Daniel Suter, Dr. Don Ready, and Dr. Connie Weaver for their guidance and patience during my Ph.D. Their guidance has been crucial with keeping my research on track.

This research would not have been completed without the aid and support of many collaborators. Firstly, I would like to thank Dr. Motokazu Tsujikawa for contributing RP zebrafish models to this work. I would also like to thank Dr. Jeff Mumm and Dr. Liyun Zhang for sharing their *nitroreductase* zebrafish lines. The assistance of Dr. Richard Van Rijn for his guidance with developing *in vitro* cell culture assays was crucial to advancing the work. I would also like to thank the assistance of Dr. Ping Ma and his students with statistical analysis of zebrafish behavior.

All of my students have been wonderful mentees during my Ph.D. work. My undergraduate mentees: Khaled Noui-Mehidi, Ryan Wyer, Emre Coskun, Rebecca James, and Truc Kha have made great personal and scientific advancements. I am proud of them all and look forward to seeing them continue to develop in the future.

Finally, I would like to thank my parents, Susan and Jeffery Ganzen, my brother Zachary Ganzen, and my fiancée Dr. MeeJung Ko for their unconditional love and support. None of this work would have been possible without them.

TABLE OF CONTENTS

LIST OF TABLES.....	7
LIST OF FIGURES	8
List of Abbreviations	9
ABSTRACT.....	11
CHAPTER 1. Introduction.....	12
1.1 Retinitis Pigmentosa	12
1.2 The Zebrafish as a Model for RP	16
1.3 <i>In Vivo</i> Drug Screening with Zebrafish	18
1.4 Purpose and Significance of the Study	26
1.5 Scope of the Dissertation	27
CHAPTER 2. Methods.....	29
CHAPTER 3. ROD DEGENERATION AND VISUAL IMPAIRMENT OF THE Q344X ZEBRAFISH	35
3.1 Section Introduction.....	35
3.2 Results.....	35
3.2.1 Anatomical Distribution of Rod Degeneration in the Q344X Zebrafish.....	35
3.2.2 Identification of a Visual Deficit in the Q344X Zebrafish	37
3.2.3 Loss of Scotopic VMR is Specifically Mediated Through Rod Loss	41
3.3 Section Conclusion	43
CHAPTER 4. DRUG SCREENING WITH THE Q344X ZEBRAFISH TO IDENTIFY COMPOUNDS TO TREAT RETINITIS PIGMENTOSA	44
4.1 Section Introduction.....	44
4.2 Results.....	44
4.2.1 Optimization of the Deficient Q344X VMR for Drug Screening	44
4.2.2 Utilizing the VMR Assay with Scotopic Illumination for Drug Screening.....	48
4.2.3 Carvedilol Elicits its Beneficial Effects on the Deficient Q344X VMR Through the Retina	50
4.3 Section Conclusion	54

CHAPTER 5. IDENTIFIATION OF THE MECHANISM OF ACTION OF CARVEDILOL IN THE RETINA	56
5.1 Section Introduction.....	56
5.2 Results.....	56
5.2.1 Carvedilol Treatment Increases Rod Number in the Q344X Retina	56
5.2.2 Carvedilol is the Sole β -Blocker that Gives Rise to the Sustained Scotopic Q344X VMR	61
5.2.3 Carvedilol Treatment does not Alter the Number of TUNEL-positive Cells in Q344X Retinal Cryosections	61
5.2.4 <i>nr2e3</i> Expression Increases in the Lateral and Ventral Retina with Carvedilol Treatment but not in the Medial Retina.....	63
5.2.5 Carvedilol Elicits its Beneficial Effects in the Q344X Retina in a Rod Autonomous Fashion.....	66
5.2.6 Adenylyl Cyclase Inhibition does not Improve the Q344X Scotopic VMR.....	66
5.3 Section Conclusion	70
CHAPTER 6. EXPANDED STUDIES AND FUTURE DIRECTIONS.....	72
6.1 Section Introduction.....	72
6.2 Results.....	72
6.2.1 Screening of FDA-approved Drugs Provides 205 First Pass Hits.....	72
6.2.2 New Zebrafish Models of RP	75
6.3 Section Conclusion	78
CHAPTER 7. DISCUSSION.....	80
REFERENCES	85
VITA.....	105
PUBLICATIONS.....	106

LIST OF TABLES

Table 1. Summary of advantages and drawbacks on using zebrafish visual behaviors for drug screening	24
Table 2. Breakdown of the selection criteria of the ENZO REDOX library	53
Table 3. Rod distribution binning in whole-mount eyes.....	60

LIST OF FIGURES

Figure 1. Simulated sample data of typical light-on and light-off VMR.....	25
Figure 2. Rhodopsin trafficking in a rod photoreceptor	28
Figure 3. Whole-mounted retinæ showing that Q344X zebrafish experience significant rod degeneration by 7dpf.....	36
Figure 4. VMR of Q344X zebrafish larvae at 7dpf	39
Figure 5. Chemical rod photoreceptor ablation disrupts the scotopic light-off VMR.....	42
Figure 6. Optimized VMR protocol to utilize for <i>in vivo</i> high throughput drug screening with the Q344X zebrafish	46
Figure 7. Drug screening of the ENZO REDOX library against Q344X RP model identifies carvedilol as a positive hit.....	51
Figure 8. Carvedilol treatment of the Q344X zebrafish RP model increases rod number in the retina	58
Figure 9. Anatomical distribution of increased rod number in carvedilol-treated Q344X zebrafish larvae	59
Figure 10. TUNEL staining in the Q344X retina is not altered by carvedilol treatment.....	62
Figure 11. <i>nr2e3</i> expression in the Q344X retina is increased in the lateral and ventral retina at 7dpf	64
Figure 12. <i>rhodopsin</i> expression in the Q344X retina is increased in the lateral and ventral retina at 7dpf	65
Figure 13. Carvedilol modulates adrenergic signaling in the rod-like Y79 human retinoblastoma cell line	68
Figure 14. The adenylyl cyclase inhibitor SQ22536 does not improve the deficient Q344X scotopic light-off VMR.....	69
Figure 15. Drugs screened from an FDA-approved compound library against the Q344X scotopic light-off VMR.....	74
Figure 16. Whole-mount eyes of P23H and R135W zebrafish larvae reveal rod degeneration in P23H but not R135W larvae.	76
Figure 17. P23H larvae exhibit a diminished scotopic light-off VMR while R135W larvae display a strong response.	77
Figure 18. Potential Mechanisms of Action of Carvedilol in the Retina.....	83

LIST OF ABBREVIATIONS

AAV	Adeno-associated Virus
ADCY	Adenylyl Cyclase
cAMP	Cyclic Adenosine Monophosphate
CAR	Carvedilol
CT	Carboxyl Terminus
DAPI	4',6-diamidino-2-phenylindole
DMSO	Dimethyl Sulfoxide
Dpf	Days Post-Fertilization
EGFP	Enhanced Green Fluorescent Protein
ERG	Electroretinogram
FDA	Food and Drug Association
Hpf	Hours Post-Fertilization
GCL	Ganglion Cell Layer
GFAP	Glial Fibrillary Acidic Protein
INL	Inner Nuclear Layer
IPL	Inner Plexiform Layer
LCA	Leber Congenital Amaurosis
LED	Light Emitting Diode
MTZ	Metronidazole
NTR	Nitroreductase
OKR	Optokinetic Response
ONL	Outer Nuclear Layer
OMR	Optomotor Response

OPL	Outer Plexiform Layer
PTB	Phototactic Behavior
RNAi	RNA interference
RP	Retinitis Pigmentosa
RPE	Retinal Pigmented Epithelium
RTC	Rhodopsin Transport Carrier
TUNEL	Terminal Deoxynucleotidyl Transferase dUTP Nick End Labeling
VMR	Visual Motor Response
WT	Wildtype

ABSTRACT

Retinitis Pigmentosa (RP) is an incurable inherited retinal degeneration affecting approximately 1 in 4,000 individuals globally. The aim of this dissertation was to identify drugs that can help patients suffering from the disease. To accomplish this goal, the zebrafish was utilized as a model for RP to perform *in vivo* drug screening. The zebrafish RP model expresses a human rhodopsin transgene which contains a premature stop codon at position 344 (*Tg(rho:Hsa.RH1_Q344X)*). This zebrafish model exhibits significant rod photoreceptor degeneration beginning at 7 days post fertilization (dpf). To assess the visual consequence of this rod degeneration the zebrafish behavior visual motor response (VMR) was assayed under scotopic conditions. The Q344X RP model larvae displayed a deficit in this VMR in response to a scotopic light offset. This deficit in behavior was utilized to perform a drug screen to identify compounds that could ameliorate the deficient Q344X VMR. The ENZO SCREEN-WELL® REDOX library was chosen to be screened since oxidative stress may increase RP progression in a non-specific manner. From this library, a β -blocker, carvedilol, was identified as a compound that improved the Q344X VMR behavior. This drug was also able to increase rod number in the Q344X retina. Carvedilol was shown to be capable of working directly on rods by demonstrating that the drug can signal through the adrenergic pathway in the rod-like human Y79 cell line. Since carvedilol is an FDA-approved drug, this screening paradigm was utilized to screen the Selleckchem FDA-approved library to identify more drugs that can potentially be repurposed to treat RP like carvedilol. Additionally, this scotopic VMR assay was used to demonstrate that it can identify behavioral deficits in the P23H RP model zebrafish (*Tg(rho:Hsa.RH1_P23H)*). This dissertation work provides a potential FDA-approved drug for RP treatment and sets the foundation for future drug screening to identify more drugs to treat different forms of RP.

CHAPTER 1. INTRODUCTION

1.1 Retinitis Pigmentosa

Retinitis Pigmentosa (RP) is a form of inherited retinal degeneration that affects approximately 1 in 4,000 individuals globally (Hamel, 2006; Hartong, Berson and Dryja, 2006; O'Neal and Luther, 2019). Clinically, this disease is classified by retinal dystrophies presenting with pigment deposits and photoreceptor death in patients (Fahim, Daiger and Weleber, 1993). Patients can be diagnosed with the symptoms of RP during either their childhood or adult lives. The early symptoms typically include mild night blindness and problems with dark adaptation beginning in the first two decades of life. These symptoms typically progress to loss of peripheral vision and complete night blindness. Patients suffering from peripheral vision loss and night blindness have difficulties performing daily tasks such as driving vehicles and walking through cluttered areas. In progressive cases of RP, patients will eventually lose their vision completely. Individuals suffering from RP have a cost burden of over \$7,000 per year on average higher than healthy individuals (Frick *et al.*, 2012). Overall, cost of vision impairment in adults is reported to be approximately \$51.4 billion annually in the United States (Richman, 2007). Unfortunately, RP is currently an incurable disease with no effective treatment options available.

RP is a genetically heterogeneous disease classification. Firstly, RP is divided into two groups: syndromic and non-syndromic. Syndromic RP occurs with other symptoms causing disease throughout the patient, while non-syndromic RP only presents with degeneration in the retina. Usher syndrome and Bardet-Biedl syndrome are the most common syndromes that include RP as a symptom (Hartong, Berson and Dryja, 2006). Secondly, there are over 65 causative genes that have been identified with multiple mutations that cause RP (RetNet database: <https://sph.uth.edu/RetNet/>) (Hartong, Berson and Dryja, 2006; Daiger, Sullivan and Bowne, 2013; Daiger, Bowne and Sullivan, 2014; Sorrentino *et al.*, 2016). Thirdly, RP exhibits every mode of inheritance including autosomal dominant, autosomal recessive, X-linked, and mitochondrial. Approximately half of all cases are autosomal recessive while approximately 40% of cases are autosomal dominant (Hartong, Berson and Dryja, 2006; Anasagasti *et al.*, 2012). This heterogeneity makes RP a very challenging disease to treat. The majority of the gene mutations causing RP make up a small proportion of the overall affected population, while the majority of

RP cases arise from the genes Rhodopsin (*RHO*), Usherin (*USH2A*), and Retinitis Pigmentosa GTPase Regulator (*RPGR*) (Hartong, Berson and Dryja, 2006). Given the vast number of potential therapeutic target, no single treatment has been developed yet that is capable of broadly treating patients suffering from RP.

Given the heterogeneity of RP, the cellular mechanisms of the disease are dependent on the specific mutation that a gene has gained. However, the symptoms and disease progression of RP are generally the same between patients. Patients generally begin to experience difficulties with dark adaptation and night blindness in adolescents caused by a loss of rod photoreceptors in the peripheral retina (Hartong, Berson and Dryja, 2006). Degenerating rod photoreceptors begin to lose their outer segments and continually break down at the inner segment and finally the synapse (Hamel, 2006). The loss of these rods leads to a loss of peripheral vision in RP patients into adulthood (Hartong, Berson and Dryja, 2006). In progressive cases of RP, peripheral retinal degeneration continues to degenerate the macula and fovea leading to complete blindness (Hamel, 2006). While the specific RP disease mechanism is mutation dependent, most degenerating photoreceptors undergo apoptosis (Cottet and Schorderet, 2009; Parmeggiani *et al.*, 2011). In addition to the specific mechanism, a non-specific mechanism may also play a role in progressing RP. Oxidative stress may be greatly increased in the retina during RP due to the loss of photoreceptors utilizing blood vessels with near-arterial levels of oxygen (Bill, Sperber and Ujiie, 1983; Punzo, Xiong and Cepko, 2012). Managing excessive oxidative stress in the retina due to RP may provide a useful option for treating RP.

While there are no cures for RP and other inherited retinal degenerative diseases, a number of treatments are being developed. Treating retinal degeneration is challenging because humans are unable to innately regenerate photoreceptors once they have degenerated. Therefore, many treatments currently focus on retinal regeneration to restore vision or gene therapy to confer protective effects. Stem cell therapy is being pursued to try to replace degenerated cells and restore vision. Some studies are attempting to utilize photoreceptor precursors created through induced pluripotent stem cells for transplantation into a diseased retina (MacLaren *et al.*, 2006; Pellegrini, De Luca and Arsenijevic, 2007). However, successful integration of photoreceptor precursors into the mature retina has proven to be limited thus far (Young *et al.*, 2000; Sakaguchi, Van Hoffelen and Young, 2003). There are many challenges facing the successful use of stem cell transplantation that still need to be overcome (Pearson, 2014). For example, transplanted photoreceptor precursors

must fully differentiate and synapse with the correct post-synaptic partners. The transplanted photoreceptors are capable of making these connections and restoring vision, however the efficacy of the transplantations is still not ideal (Pearson *et al.*, 2012). One of the challenges facing effective photoreceptor transplantation may include reactive gliosis. Increased amounts of glial fibrillary acidic protein (GFAP) in a degenerating retina prevents successful integration of transplanted photoreceptors (Barber *et al.*, 2013). Stem cell therapy shows promise in potentially restoring vision to a retina degenerated through RP, but there are still many hurdles to overcome before stem cells become a mainstream therapy.

Since RP is mostly an inherited genetic disease, many treatment developments are focusing on utilizing gene therapy to potentially stop the disease. This approach has advantages of being able to treat a variety of RP forms due to the possibility of delivering functional genes or RNA interference (RNAi) constructs with a viral vector. Adeno-associated viruses (AAV) are commonly used to deliver genetic constructs into cells *in vivo*, and AAVs are capable of delivering constructs into the RPE (Pearson *et al.*, 2012). In one recessive form of RP, the gene RPE65 is mutated leading to deficiency in retinoid isomerase activity and retinal degeneration. AAV delivery of functional copies of RPE65 into the retina to offset the deficient retinoid isomerase activity has shown improved visual sensitivity in a clinical trial of three patients (Pearson *et al.*, 2012). This outcome highlights the potential to utilize AAV-mediated gene replacement therapy for treating recessive RP. Autosomal dominant cases of RP that essentially act as a gain of function can be more challenging to target. Rather than introducing another gene, AAVs can be utilized to deliver RNAi constructs to inhibit the translation of targeted genes. However, RNAi will knockdown both the mutated and healthy copy of the gene, so a replacement gene is required to be introduced to compensate. For this gene to avoid the RNAi knockdown, the replacement gene must be codon modified. This strategy has been shown to be feasible by knocking down rhodopsin (RHO) in the mouse retina with RNAi while leaving a codon modified RHO unaffected (O'Reilly *et al.*, 2008). This system has been applied to the autosomal dominant Pro347Ser mouse model of RP to improve the retinal histology and electroretinogram (ERG) of the model (Chadderton *et al.*, 2009). While this system shows promise, there are significant challenges to overcome for successful translation to human patients. AAVs are relatively small and only constructs approximately of 4.8kb can be packaged. This limits the treatment options that require large genes to be delivered. The co-delivery of an RNAi vector as well a codon modified replacement gene

becomes complicated as both constructs need to be successfully integrated which requires an optimal delivery method. Gene therapy has promising implications for treating RP; however, these complications must be overcome before AAV gene delivery becomes a mainstream therapy.

CRISPR/Cas technologies are currently being tested as a form of targeted gene therapy to treat some forms of RP. There are situations when gene replacement therapy is not viable due to the limitation of construct size delivery by AAVs. In one example of syndromic RP, the most common form Leber congenital amaurosis (LCA) arises due to the IVS26 intron mutation in the *CEP290* gene causing a splice site mutation and premature truncation (Ruan *et al.*, 2017). Due to the large size of the gene, it cannot be packaged into an AAV vector. Thus, recent efforts have successfully focused on excising the IVS26 mutation with CRISPR/Cas to result in proper transcription of the gene (Ruan *et al.*, 2017). This technology is currently being tested in clinical trials by Editas Medicine, Inc (NCT03872479) and has been given to patients. Additionally, RP mutations in *RHO* have been targeted with CRISPR/Cas technology also. The P23H mutation leads to autosomal dominant RP and is a candidate for CRISPR/Cas therapy to knockout the P23H allele. This has been shown to be successful in transgenic mice and pigs (Burnight *et al.*, 2017; Li *et al.*, 2018). The future use of CRISPR/Cas technology to treat forms of RP is promising, however, there are specific requirements that must be met for the technology to be used successfully which limits the number of mutations that can be treated.

Once RP has progressed to a stage of advanced degeneration, there are few options available for patients. Retinal prosthesis is one technology that is being developed to restore visual sensation to advanced stage RP patients. The Argus II system is a retinal prosthesis device that requires the surgical implantation of an electrode array onto the surface of the macula (Ahuja *et al.*, 2011). This device has been shown to be capable of improving light sensation and visual acuity in patients implanted with the electrode array (Ho *et al.*, 2015; Duncan *et al.*, 2016). While effective, the system is invasive and relatively expensive costing approximately \$150,000. Some progress has been made by artificially imparting non-photoreceptor retinal neurons photosensation with photoswitches. One example are azobenzene photoswitches that can specifically impart photosensation on OFF-retinal ganglion cells (Tochitsky *et al.*, 2017). These photoswitches are chemicals that are not genetically encoded which improves ease of delivery. Genetically encoded photoswitches have also shown to increase photosensation in a degenerated retina (Tochitsky *et al.*, 2018). However, the photoswitch technology is still in the early stages of development and

might only be capable of restoring basic light sensation. Given all of the potential treatment options available for patients are still experimental and complicated, a need still exists for a cheap, simple, and effective treatment option for RP. This need may be met by utilizing animal models of RP to find drug therapies. The zebrafish (*Danio rerio*) is one of the most popular and powerful animal systems utilized in biomedical research, and they are an appropriate animal to study vision.

1.2 The Zebrafish as a Model for RP

The zebrafish is a highly utilized laboratory animal that is used for biological experiments. Zebrafish offer a number of advantages over other animal models such as ease of handling, low cost and maintenance, amenability to genetic manipulation, and largely transparent embryos (Patton and Zon, 2001). A breeding pair of adult zebrafish embryos are capable of producing between 100 and 200 embryos per week. While mice are more commonly utilized than zebrafish in laboratory settings, mice usually only produce litters of approximately 5 or 6 pups every two months. The large number of embryos that can be collected with batches of adult zebrafish can facilitate performing *in vivo* studies at a high throughput that cannot be feasibly performed with other animals including mice.

Zebrafish eyes have a number of similarities to human eyes which make them appropriate for comparing the fish vision to human vision. Zebrafish utilize predominantly cone-dominant vision to navigate their environment similar to humans (Bilotta, Saszik and Sutherland, 2001). Humans and zebrafish also share the same types of photoreceptors. Humans share short, medium, and long wavelength cones, also known as blue, green, and red cones, with the zebrafish, and the zebrafish also possess a ultra-short wavelength cone able to see into the ultraviolet spectrum (Robinson *et al.*, 1993; Meier, Nelson and Connaughton, 2018). One difference between human and zebrafish cones is that the red and green cones of zebrafish are double cones rather than individual cones (Raymond *et al.*, 2014). In addition to cones, both humans and zebrafish possess rod photoreceptors in the retina. These similarities indicate that similar light information is captured in the retina of humans and zebrafish.

The retina of the zebrafish is laminated in the same order as humans. Both retinas are organized into 3 cellular layers: the outer nuclear layer (ONL), the inner nuclear layer (INL), and the ganglion cell layer (GCL), and two synaptic layers: the inner plexiform layer (IPL) and outer plexiform layer (OPL). The retina is also surrounded by the retinal pigmented epithelium (RPE)

in both humans and zebrafish. Despite these similarities, there are some crucial differences between the zebrafish and human retina that need to be considered. For example, zebrafish eyes are positioned on the side of the head while human eyes are front facing (Chhetri, Jacobson and Gueven, 2014). Another important difference that zebrafish have that must be considered for RP and visual studies is that zebrafish lack a macula and a fovea. In the human retina, the macula is a region which contains a fovea. The fovea contains almost all of the cone photoreceptors (approximately 6 million) in the human retina, and the remainder of the retina is filled with rods (Jonas, Schneider and Naumann, 1992; Purves, Augustine and Fitzpatrick, 2001). In the zebrafish, photoreceptors are organized in highly ordered mosaic evenly throughout the retina (Cameron and Carney, 2000; Fadool, 2003; Salbreux *et al.*, 2012). Despite these anatomical differences, zebrafish are an advantageous model for visual studies relating to human vision over other models. Rodent models that are used for vision studies are nocturnal and utilize a retina composed of 98% rods for perceiving their environment (Bibliowicz, Tittle and Gross, 2011). Similarly, human retinæ are comprised of about 95% rods, but the rods surround the cone-dense fovea. However, zebrafish retinæ contain 60% cones and 40% rods organized in a highly ordered mosaic (Angueyra and Kindt, 2018). Rodents also only possess blue and green cones in contrast to humans and zebrafish. Seminal vision studies have been performed with rodent models, however the differences in rodent vision may not make them suitable for modeling disease in humans.

Since zebrafish have similar visual aspects to humans, they have been utilized to model a variety of retinal degenerations including RP (Tsujikawa and Malicki, 2004; Gross and Perkins, 2008; Y. Sasamoto *et al.*, 2010; Brockerhoff and Fadool, 2011; Morris, 2011; Link and Collery, 2015). Since RP is genetically heterogeneous, the genetic amenability of zebrafish makes it an ideal system to model human degeneration. One of the most commonly mutated genes in RP is RHO (Hartong, Berson and Dryja, 2006) which encodes the photopigment in rods required for the initiation of phototransduction. Approximately 30% of all cases of RP are autosomal dominant, and approximately 30 percent of these cases arise from over 150 mapped mutations in *RHO* (Rossmiller, Mao and Lewin, 2012; Daiger, Bowne and Sullivan, 2014; Athanasiou *et al.*, 2018). A number of transgenic zebrafish lines have been generated with autosomal dominant mutations (Y. Sasamoto *et al.*, 2010). One example of these clinically relevant lines carries a human RHO transgene with a premature stop codon at glutamine 344 (Q344X). Patients with this mutation suffer from an early onset and severe form of the disease

(Jacobson *et al.*, 1991; Sung *et al.*, 1994; Kremmer *et al.*, 1997). This mutated transgene leads to rod degeneration in the zebrafish. Another example of an RP zebrafish model is the RP2 knockdown system. Knockdown of the RP2 orthologue in zebrafish by morpholino injection results in smaller eyes and problems in retinal lamination during development (Shu *et al.*, 2011). These examples highlight how zebrafish can be used to model clinically-relevant forms of RP, and these models can be leveraged to identify new drugs that improve the phenotype of the model.

1.3 *In Vivo* Drug Screening with Zebrafish

Zebrafish have been a common model of choice for performing drug screening to identify compounds that can confer therapeutic effects (Peterson *et al.*, 2000, 2004; Owens *et al.*, 2008; Novodvorsky, Da Costa and Chico, 2013). The zebrafish have many behaviors that can be utilized to develop high-throughput *in vivo* drug screens. One study leveraged wake/wake behavior of zebrafish larvae to screen approximately 5,600 drugs to identify hits that modulated this behavior (Rihel *et al.*, 2010). Another study screened over 24,000 drugs by presenting a variety of light and sound stimuli to larval zebrafish in order to identify novel antipsychotic-like compounds (Bruni *et al.*, 2016). In addition to these examples, a number of recent drug screening projects have been performed which indicates a growing interest in utilizing zebrafish as a tool for *in vivo* drug discovery (Kokel *et al.*, 2010, 2013; Baxendale *et al.*, 2012; Jin *et al.*, 2013; Liu *et al.*, 2014; Dinday and Baraban, 2015; Gallardo *et al.*, 2015; Li *et al.*, 2015; Nath *et al.*, 2016). Since these screens have been able to identify a wide variety of neuroactive compounds, zebrafish can be utilized for screening drugs to treat RP.

There have been no drug screens successful for identifying hits that can treat RP. Two primary methods of drug screening are currently employed to find new treatments (Hughes *et al.*, 2011). Traditionally target-based drug screening is employed with *in vitro* methods which utilize cell line or biochemical assays (Moore and Rees, 2001; An and Tolliday, 2010; Michelini *et al.*, 2010). These types of assays generally provide rapid readouts of luminescence, fluorescence, or colorimetric data (Kasibhatla *et al.*, 2004; Mueller, Kassack and Wiese, 2004; Szymański Paweł and Markowicz and Mikiciuk-Olasik, 2011). These types of approaches are advantageous as they can be drastically scaled up for extremely high-throughput drug screening. For example, modern target-based screens can provide tens of millions of data points on an assay outcome where each data point is a drug tested at a single concentration (Drews, 2000). This level of throughput

allows for screening drug libraries at multiple concentrations. By following this technique, the chances of identifying lead hits by screening as many compounds as possible. However, there are some drawbacks to using target-based screening approaches. Typically, target-based screening focuses on a single target such as protein or a nucleotide sequence that will interact with a drug. However, by focusing on a single target, information on many aspects of the potential drug are missed such as off-target effects and challenges with drug delivery. Target-based screening also does not provide information regarding function of the target cells of lead hits. For example, a hit may interact with a target protein, but it may lead to an unwanted signaling cascade in the affected cell. Given the large number of hits produced by target-based screening, a large number of follow-up studies must be performed to narrow the hits down. This large-scale screening and follow-up experiments require significant resources that are typically only available to large pharmaceutical companies. While large-scale target-based screening has been widely utilized in the pharmaceutical industry, this approach is being associated with declining effectiveness in finding new drugs (Samsdodd, 2005; Terstappen *et al.*, 2007). This decline highlights a need for more a more effective screening approach.

Phenotype-based screening can offset some of the limitations faced by target-based screening. This type of phenotype-based screening is performed *in vivo* to find drugs that can rescue disease phenotypes in a whole animal. For example, fluorescent-based screening can be used to quantify rod degeneration and rescue in the zebrafish retina at a high throughput (Walker *et al.*, 2012). Before high-throughput screening methods were possible, phenotype-based drug screening techniques were used to find drugs to treat disease (Swinney, 2013). The major advantage of this screening technique is that screens can be performed before the disease mechanism in the model system is fully elucidated, and drug hits that are identified through phenotype-based screening are efficacious despite not knowing the mechanism of action (Swinney and Anthony, 2011). Follow-up studies can be performed on the lead hits that have been shown to be useful if required. However, it may not be necessary to investigate detailed mechanisms of action. One study has demonstrated that approximately 82% of FDA approved drugs could not be assigned a specific mechanism of action (Overington, Al-Lazikani and Hopkins, 2006). An example of this would be the anticonvulsant Levetiracetam which was identified in a screen with mice to prevent seizures (Gower *et al.*, 1992). Since the discovery of this drug in 1992, no confirmed mechanism of action has been elucidated for the drug.

Utilizing zebrafish to perform phenotype-based screening may provide a method to identify a drug treatment for RP. Zebrafish display a wide repertoire of behaviors that integrate sensory inputs from multiple sources including sound, touch, olfaction, near-field water movement, and vision. Zebrafish expressing mutations that affect the sensory systems can display altered behaviors. Phenotypic behavior arising from mutations in zebrafish can be leveraged to perform drug screens that can improve the phenotypic behavior (Orger *et al.*, 2004; Rihel and Schier, 2012). Compounds that are identified to ameliorate the phenotypic zebrafish behavior are more likely to be effectively translated since the therapeutic effects are seen on the functional level rather than just on the cellular or molecular signaling level as seen with traditional drug screening. Screening with zebrafish behavior is advantageous over screening for cell survival through methods such as fluorescent-based screening. For example, the ARQiv-HTS screening system has been developed to quantify changes in fluorescence in zebrafish with high throughput (Walker *et al.*, 2012; White *et al.*, 2016). Systems such as this can be used to screen drugs that prevent a loss of fluorescent signal through cell death, however drugs identified with this method do not provide any information regarding the function of the surviving cells. Drugs that can ameliorate phenotypic behaviors arising from mutations in zebrafish immediately provide information about efficacy even though the specific mechanism of the improvement is unknown. Utilizing phenotypic behavioral drug screens with zebrafish models of RP can provide hits that are demonstrably effective in improving the zebrafish vision.

Regarding vision, zebrafish exhibit multiple visually-mediated behaviors that can be used to perform drug screens including the phototactic behavior (PTB), the optokinetic response (OKR), the optomotor response (OMR), and the visual motor response (VMR) (Brockhoff *et al.*, 1995; Neuhauss *et al.*, 1999; Bilotta, 2000; Muto *et al.*, 2005; Emran *et al.*, 2007; Emran, Rihel and Dowling, 2008; Chhetri, Jacobson and Gueven, 2014). PTB is an innate behavior displayed by zebrafish larvae. Generally, zebrafish larvae display positive phototaxis towards illumination while avoiding dark areas (Brockhoff *et al.*, 1995). PTB can be visualized by adapting zebrafish larvae to a dark chamber and then allowing them to migrate to an illuminated chamber. While assessing this behavior can provide significant results, the reliability of the behavior is low. It is reported that $49\% \pm 23\%$ of larvae will migrate from a dark chamber to an illuminated chamber while $36\% \pm 15\%$ of larvae will move between two dark chambers (Brockhoff *et al.*, 1995). The large variation in these distributions would make it difficult for assessing visual phenotypes in RP

zebrafish models. This variation would also compound the difficulty of drug screening on RP models. The OKR and OMR are similar behaviors based upon the visual acuity of zebrafish larvae. These behaviors arise in response to moving striped gradients beginning on 5 days post-fertilization (dpf) for the OKR and 6dpf for the OMR (Brockerhoff *et al.*, 1995; Neuhauss *et al.*, 1999). In the OKR, larvae are generally immobilized in a methylcellulose solution and presented with a rotating grating. Larvae generally follow the striped pattern with their eyes in a slow pursuit motion followed by a rapid reset called a saccade (Huang and Neuhauss, 2008). In the OMR, larvae are placed in a tank with a moving grating below them. The moving grating simulates the direction of a current and causes the larvae to swim against it. Zebrafish that have deficits in the visual system do not perceive these grating stimuli and thus do not display the OKR or OMR (Neuhauss *et al.*, 1999). Drug screens can be performed utilizing the OKR and OMR to rescue mutant behavior, but there are limitations in applying the behaviors. Drug screening with the OKR may provide hits that improve visual acuity, however the throughput of OKR experiments is quite low and not amenable to high throughput. The OKR may be better suited for secondary screening after candidate compound have been identified. The OMR can be used to identify drug-mediated changes in zebrafish vision (Richards *et al.*, 2008), however false positives and negatives may require additional testing and screening which will lower efficiency. To date, neither the OKR nor OMR have been able to screen for drugs that improve the visual acuity of visual mutant zebrafish. These assays also need to be tuned for the best spatial frequency, contrast, and grating speed with the tested illumination levels (Rinner, Rick and Neuhauss, 2005).

A useful behavior to use for drug screening with RP zebrafish models at high throughput is the VMR. The VMR is characterized by a visual startle response that can be elicited by a sudden change in environmental illumination (Emran *et al.*, 2007; Emran, Rihel and Dowling, 2008; Gao *et al.*, 2014, 2016; Liu *et al.*, 2015; Ganzen *et al.*, 2017). This behavior is first exhibited by 3dpf and can be strongly elicited by 5dpf (Emran, Rihel and Dowling, 2008; Liu *et al.*, 2015; Gao *et al.*, 2016). To assay the VMR, zebrafish larvae are typically placed into a multi-well plate (commonly 96-well plate format) and are placed in a light-proof environment with a light source (Colwill and Creton, 2011; Ingebretson and Masino, 2013; Zhou *et al.*, 2014). Larvae are illuminated by IR light in their plates so that they may be tracked by camera. While it currently is not believed that zebrafish can perceived IR light, one study has suggested that zebrafish larvae may be sensitive to near-IR illumination (Hartmann *et al.*, 2018). The tracked larvae are presented with a white light

stimulus, and the swimming behavior is tracked and recorded. There are systems that are commercially available to assay the VMR ('Viewpoint LifeSciences', no date; 'Noldus', no date), and systems are also able to be built in-house (Maurer *et al.*, 2010; Zhou *et al.*, 2014).

The VMR behavior is comprised of two components: a startle response to light onset (light-on VMR), and a startle response to light offset (light-off VMR) (Figure 1) (Emran, Rihel and Dowling, 2008; Liu *et al.*, 2015; Zhang *et al.*, 2016). The light-on VMR of zebrafish larvae is displayed by a sharp and immediate increase in swimming behavior (on the millisecond scale) followed by a decline in swimming. Likewise, the light-off VMR also is characterized by a rapid swimming behavior immediately after light change, however, larvae increase swimming behavior after the light offset rather than reduce swimming. The VMR behavior can be assayed by repeating light onset and offset stimuli to create multiple trials with the same group of fish, or by testing multiple groups of fish as biological replicates. While this behavior provides useful information regarding light sensation, the VMR does not provide information about the visual acuity of the zebrafish. However, light sensation should be sufficient for a phenotypic drug screen utilizing RP zebrafish models. Light sensation is required for zebrafish visual acuity, so testing for light sensation is a logical first step before testing for visual acuity.

VMR experiments usually record the zebrafish behavior in terms of movement over time as well as larval displacement (Emran *et al.*, 2007; Emran, Rihel and Dowling, 2008; Rihel *et al.*, 2010; Ali, Champagne and Richardson, 2012; de Esch *et al.*, 2012; Fernandes *et al.*, 2012; Beker van Woudenberg *et al.*, 2013; Vignet *et al.*, 2013; Lange *et al.*, 2013; Deeti, O'Farrell and Kennedy, 2014; Gao *et al.*, 2014, 2016; Liu *et al.*, 2015; Zhang *et al.*, 2016). Tracking software generally detects larvae as pixels that are darker than background above a certain threshold. Computer software analyzes the pixel locations per frame to determine the activity of the fish. Thresholds can be set base on either pixel change activity or velocity to bin the activity of the fish into different groups such as low, medium, and high activity. Utilizing these bins may reveal changes in zebrafish behavior in response to drug treatments. Since the VMR represents the behavioral result of all of the neural signaling involved upon light stimulation of the zebrafish, it is an appropriate method to assay the behavioral effects of mutations on the fish visual system as well as the effects of drug treatment.

The VMR is an attractive behavior to perform drug screening for RP for a number of reasons. Firstly, throughput can be very high considering that the screen is performed *in vivo*. 96-

well plates can be used to assay the VMR of multiple larvae simultaneously, and multiple plates can be run in a day depending on the utilized protocol. Secondly, assessing the VMR of zebrafish larvae is relatively simple and does not require many resources. This simplicity coupled with the relatively inexpensive cost of maintaining a zebrafish colony makes the ability to perform VMR assays available to smaller research groups that do not necessarily have the resources of large-scale pharmaceutical industries. This behavior is also less laborious to assay than other visual behaviors in zebrafish such as the (OKR) (Brockhoff *et al.*, 1995, 1997; Easter and Gregory Nicola, 1997; Brockhoff, 2006). Thirdly, as previously discussed, any positive drug hits would indicate improved light sensation. Utilizing the zebrafish VMR for phenotypic screening with RP zebrafish models would provide positive hits that can functionally restore vision. Fourthly, drug treatment of zebrafish larvae is uncomplicated. Drugs can be dissolved in water or a DMSO vehicle and added directly to the zebrafish media. It is believed that zebrafish exposed to this manner can absorb the drugs directly through the skin or ingested through gut epithelium (Zhang *et al.*, 2015). One example that this VMR screening technology can identify drugs that improves zebrafish vision in a retinal degeneration model utilized the *pde6c* splice site mutant. This mutant models a cone-rod dystrophy disease and cannot perceive photopic light (Stearns *et al.*, 2007; Lewis *et al.*, 2010). Treatment of the *pde6c* mutant with the natural compound schisandrin B improved VMR and changed rod morphology (Zhang *et al.*, 2016). This study indicates that the zebrafish used to model RP can be used to leverage a phenotypic VMR to screen and identify drugs that will ameliorate the behavior.

Table 1. Summary of advantages and drawbacks on using zebrafish visual behaviors for drug screening

Visual Behavior	Earliest Displayed Stage	Advantages	Drawbacks
Phototactic Behavior (PTB)	7dpf	PTB can be assessed simply without complex tracking software or hardware setups. Provides information on light sensation.	PTB is difficult to reliably measure since choice behavior is complex. Difficult to scale for high throughput.
Optokinetic Response (OKR)	5dpf	OKR provides information on the visual acuity of zebrafish larvae which is a good indicator of the quality of vision.	Larvae must be restrained for assessment which results in low throughput. Many factors including spatial frequency, contrast, stimulus speed, and illumination must be considered.
Optomotor Response (OMR)	6dpf	The OMR behavior can provide information on visual acuity in a freely moving zebrafish larvae. May be scaled up for high throughput.	False positives and negatives may be an issue to overcome for drug screening. Factors including spatial acuity, stimulus speed, contrast, and illumination must be considered.
Visual Motor Response (VMR)	3dpf becoming robust at 5dpf	VMR provides information on the light sensation of zebrafish and is amenable to high throughput. Behavior is driven solely by changes in environmental illumination.	No information provided on zebrafish visual acuity. Optimization with adaptation times and illumination required.

Zebrafish visual behaviors can be utilized to perform phenotypic drug screening. The PMR, OKR, OMR, and VMR have inherent advantages and disadvantages for screening use as summarized in Table 1.

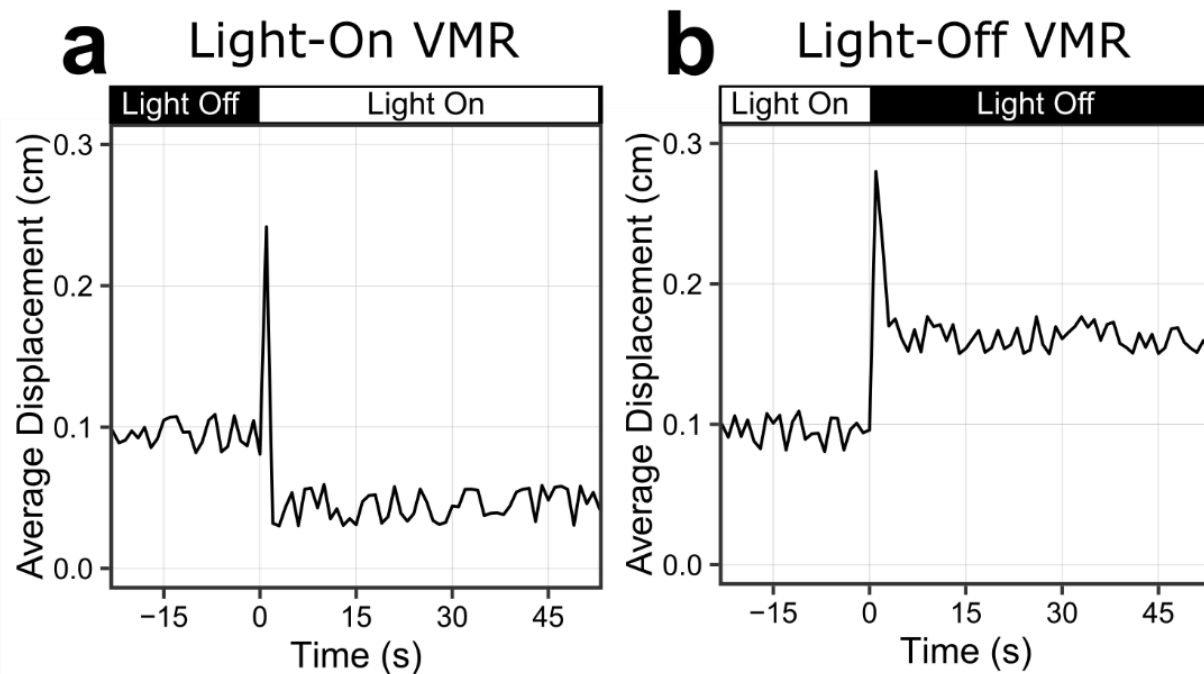


Figure 1. Simulated sample data of typical light-on and light-off VMR

Simulated example of a typical light-on VMR profile and a light-off VMR profile from a change in bright illumination. a) Sample data showing the expected shape of a light-on VMR. Zebrafish larvae will generally display a fast startle response within one second of the light onset followed by a brief period of reduced swimming activity. b) Sample data showing the expected shape of a light-off VMR. Zebrafish larvae display a fast startle response immediately after light offset followed by a brief increase in swimming.

1.4 Purpose and Significance of the Study

The ultimate goal of this study is to identify a compound, or multiple compounds, that can be translated to human patients suffering from RP. To accomplish this goal, the transgenic zebrafish line expressing a truncated *rhodopsin* transgene at glutamine 344 (Q344X) was utilized. Q344X RHO is a catalytically active protein, yet it lacks a VXPX ciliary trafficking motif on the carboxy terminus (CT) tail which is required for RHO to traffic properly to the outer segment of rod photoreceptors (Figure 2). RHO that lacks the VXPX motif mislocalizes to the inner segment and synaptic terminal of the rods (Sung *et al.*, 1994; Concepcion and Chen, 2010). The general trafficking of RHO includes being folded in the ER and packaged into post-Golgi vesicles known as rhodopsin transport carriers (RTCs) in the Golgi Apparatus (Nemet, Ropelewski and Imanishi, 2015). Once RHO is packaged into an RTC, the GTPase ARF4 binds to CT of RHO and acts as a scaffold for the binding of other trafficking components (Deretic *et al.*, 2005). ARF4 recruits the proteins RAB8, RABIN8, RAB11, and ASAP1 to the RTC (Wang *et al.*, 2012). This complex is necessary for the trafficking of the RTC to the connecting cilium for incorporation into outer segment discs. Q344X RHO follows the same trafficking pathway, but Q344X-containing RTCs do not exit the Golgi correctly. The Q344X RHO is properly folded in the ER aided by the Hsp70 chaperone BiP (Athanasidou *et al.*, 2012). However, once Q344X RTCs are ready to exit the Golgi, ARF4 is unable to bind to the CT of Q344X RHO. As a result, the ARF4 trafficking complex cannot form, and the Q344X RTCs cannot be trafficked to the connecting cilium (Figure 2). Q344X RHO becomes incorporated into the plasma membrane in the inner segment and synapse. Rods expressing Q344X RHO undergo apoptosis and cause retinal degeneration (Portera-Cailliau *et al.*, 1994).

To investigate the Q344X mutation and find therapies, a transgenic model was created with zebrafish which express human Q344X *RHO* in rods under the control of the zebrafish *rho* promoter (Y. Sasamoto *et al.*, 2010; Nakao *et al.*, 2012). Similar to patients that exhibit early onset RP, Q344X zebrafish exhibit significant rod degeneration beginning on 5dpf and becomes severe at 7dpf. In order to utilize the model, the transgenic fish expresses an EGFP reporter in the transgene which allows for Q344X zebrafish to be identified by 2dpf, and it eliminates the need for post hoc genotyping to confirm the presence of the transgene. Since Q344X RHO is

catalytically active, it is hypothesized that mislocalized activation of rhodopsin activates adenylyl cyclase (ADCY) through G protein signaling (Nakao *et al.*, 2012). The aberrant ADCY signaling outside of the outer segment in the rod likely causes apoptosis through a cAMP signaling cascade (Alfinito and Townes-Anderson, 2002; Nakao *et al.*, 2012). Previous experiments utilizing the Q344X zebrafish demonstrated that ADCY inhibition led to some rod survival (Nakao *et al.*, 2012). However, the presence of the mislocalized Q344X RHO may also cause degeneration in the absence of light activation. Work with *Xenopus* has indicated that rods will still degenerate in the presence of Q344X RHO without any light stimulation (Tam *et al.*, 2006). Even though that rods degenerate in the dark, the degeneration is lessened in Q344X mice reared in darkness indicating that mislocalized RHO catalytic activity causes severe degeneration (Concepcion and Chen, 2010). These studies suggest that there are multiple disease mechanisms in play regarding the Q344X RHO mutation.

1.5 Scope of the Dissertation

In this work, the Q344X RP model zebrafish was utilized to develop an *in vivo* drug screening platform to identify drug treatments to treat RP. Chapter 3 describes how the Q344X model exhibits rod degeneration, and that Q344X-expressing zebrafish larvae have a diminished light-off VMR in response to a scotopic light stimulus. Chapter 4 elaborates on the optimization of the diminished Q344X VMR for the purposes of drug screening. This optimized protocol was used to screen for compounds that ameliorate attenuated Q344X VMR, and the FDA-approved drug carvedilol was identified as a positive hit. Chapter 5 details efforts to identify carvedilol's mechanism of action in the retina to determine how the drug improves the Q344X zebrafish RP model. Chapter 6 describes future directions and preliminary data utilizing the drug screening platform.

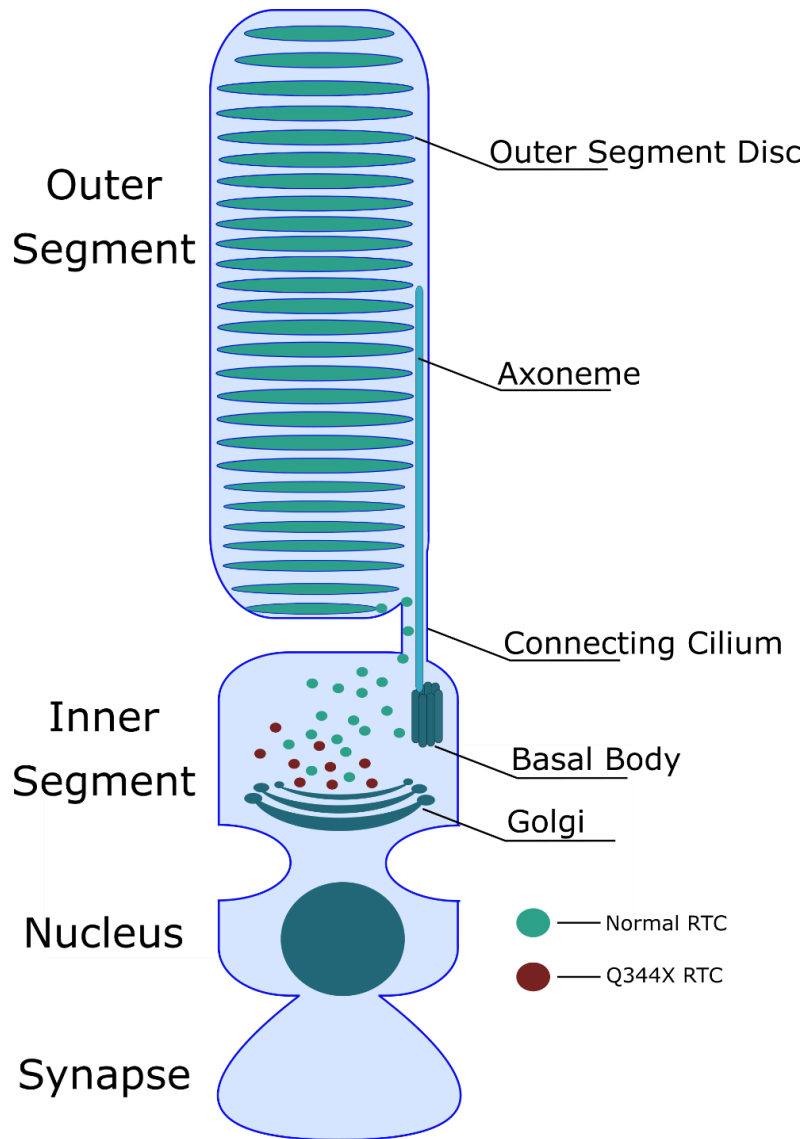


Figure 2. Rhodopsin trafficking in a rod photoreceptor

Diagram of a rod photoreceptor highlighting the trafficking of the rod opsin rhodopsin. Rhodopsin is translated in the ER and trafficked to the Golgi. Rhodopsin transport carriers (RTCs) bud from the Golgi and are trafficked to the basal body. RTCs are then sent through the connecting cilium to be incorporated into outer segment discs in outer segment of the rod. This trafficking of RHO is critical for the proper formation of the outer segment and function of the phototransduction cascade. This trafficking is dependent on presence of a VXPX ciliary trafficking motif on the carboxy terminus of RHO. The loss of this trafficking motif due to a premature stop codon at position 344 (Q344X) prevents proper localization of the RTC. Q344X-containing RTCs are mislocalized to the inner segment and synapse of the rod rather than the outer segment.

CHAPTER 2. METHODS

Animals:

Zebrafish of the AB background were utilized for all experiments (<https://zfin.org/ZDB-GENO-960809-7>). Adult and larval zebrafish were maintained and bred using standard procedure (Westerfield, 2007). Adult fish were placed in breeding tanks the night before breeding after receiving all meals. Adult fish began spawning after the beginning of the light cycle at 9:00am, and embryos were collected before 10:30am. Larval zebrafish were reared until 7 days post-fertilization (dpf) in E3 medium in an incubator at 28°C. The fish incubator was kept on a 14hr light and 10hr dark cycle. E3 medium was changed daily, and healthy embryos were kept for experiments. All protocols were approved by the Purdue University Institutional Animal Care and Use Committee.

Transgenic Animals:

Tg(rho:Hsa.RH1_Q344X), *Tg(rho:Hsa.RH1_P23H)* and *Tg(rho:Hsa.RH1_R135W)* transgenic animals were generated previously (Y. Sasamoto *et al.*, 2010; Nakao *et al.*, 2012) and are referred to here as Q344X, P23H, and R135W respectively. Q344X, P23H, and R135W larvae were identified on 2dpf through the expression of EGFP under the control of 1.1kbp promoter of *olfactory marker protein (omp)* contained in the transgenic cassette. Their genotype was verified via PCR with the following primers: 5'-CCAGCGTGGCATTCTACATC-3' and 5'-AACGCTTACAATTTACGCCT-3'. The rods in the Q344X, P23H, and R135W lines were labeled with the *Tg(-3.7rho:EGFP)* transgene (Hamaoka *et al.*, 2002) and is referred to here as *rho:EGFP*. Zebrafish expressing *nitrodreductase* in rod photoreceptors, *Tg(-3.7rho:YFP-nfsB)^{gmc500}*, were generated previously (Walker *et al.*, 2012) and referred to here as *rho:NTR*.

Drug Screening and Treatment:

The ENZO SCREEN-WELL® REDOX library was used for the first screen for drugs that modulate oxidative stress. (ENZO Life Sciences, BML-2835-0100). The Selleckchem FDA-approved Drug Library (Selleckchem, L1300) was utilized for screening FDA-approved drugs. Carvedilol was ordered from ENZO (ENZO Life Sciences, BML-AR112-0100) for further experiments and from MilliporeSigma (MilliporeSigma, C3993-50MG) for confirming the positive effects observed in specific behavioral experiments. All drugs of the ENZO library were

dissolved in DMSO and were compared to DMSO controls. The Selleckchem library contained drugs dissolved both in DMSO and water, and the corresponding control was utilized for comparison. The maximum DMSO percentage zebrafish larvae were exposed to was 0.1%. Thirty larvae were exposed per drug dissolved in 15mL E3 media in a 15mm petri dish. The treatment began on 5dpf unless otherwise stated. The media were not refreshed during experiment. The treated larvae were directly transferred into the 96-well plate with their corresponding E3 medium with drugs to ensure consistent drug dosing throughout the treatment period.

Rod Ablation in *rho:NTR* Zebrafish:

To chemically ablate rods, we used the zebrafish line expressing *nitroreductase* (NTR) under the control of the rhodopsin promoter (Walker *et al.*, 2012) (*rho:NTR*). Treatment with the prodrug metronidazole (MTZ) specifically ablates rod photoreceptors. Specifically, NTR-expressing larvae were treated with 2.5mM MTZ from 5dpf to 7dpf. Their VMR was compared with the untreated larvae on 7dpf.

Retinal Histology and Imaging:

All larvae were fixed in 4% paraformaldehyde (PFA) overnight at 4°C. For retinal cryosections, fixed larvae were infiltrated with 30% sucrose overnight at 4°C prior to imbedding in Tissue Freezing Medium (GeneralData, TFM). Ten micrometers-thick cryosections were collected on Fisherbrand Superfrost Plus Microscope Slides (Thermo Fisher Scientific, 12-550-15). The sections containing the optic nerve were analyzed for anatomical reference. Sections were counterstained with 0.25mg/mL DAPI (Molecular Probes, D1306), and rods were imaged by EGFP expressing through the *Tg(-3.7rho:EGFP)* transgene.

TUNEL Staining

TUNEL labeling was carried out on collected cryosections with Roche *In Situ* Cell Death Detection Kit, TMR Red (Roche, 12156792910). The positive controls were WT samples treated with DNase I (New England Biolabs, M0303S) at a concentration of 3 units/mL for 10 minutes at room temperature. The negative controls were samples stained with the TdT (terminal deoxynucleotidyl transferase)-negative solution. All samples were counterstained with 0.25mg/mL DAPI (Molecular Probes, D1306) for 30 minutes at room temperature, and mounted with VECTASHIELD Mounting Medium (VWR, 101098-042).

Whole-animal Preparation

To visualize rod distribution in the retina, PFA-fixed larvae were bleached with 1% KOH/3% H₂O₂ for 40 minutes at room temperature to bleach the black pigment from the retinal pigment epithelium. The bleached embryos were imbedded a 3% methyl cellulose solution for observation. Rods were visualized with the *Tg(-3.7rho:EGFP)* transgene.

Microscope and Camera

All samples were imaged with an Olympus BX51 microscope (Olympus) and a SPOT RT3 Color Slider camera (SPOT Imaging).

In Situ Hybridization

In situ hybridization was performed using the ZFIN protocol as a guide (<https://wiki.zfin.org/display/prot/Whole-Mount+In+Situ+Hybridization>). Zebrafish larvae were collected and treated with PTU (phenylthiourea) by 24 hours post-fertilization to inhibit black pigment formation in the eye, and larvae were drug treated as described above. Larvae were fixed in 4% PFA overnight at 4°C. Fixed larvae were washed 5 times in PBST (phosphate buffered saline with 0.1% Tween 20). Washed larvae were dehydrated and permeabilized stepwise in 30%, 50%, 70%, and 100% MeOH/PBST solution and rehydrated in reverse order. Rehydrated embryos were further permeabilized with proteinase K treatment for 1 hour at room temperature (RT). Proteinase K treated larvae were fixed again with 4% PFA at RT for 30 minutes. Fixed larvae were washed 5 times in PBST. Larvae were then pre-hybridized in hybridization (HYB) solution plus 5mg/mL torula RNA and 50µg/mL heparin (HYB+) overnight at 65°C. DIG-labeled RNA probes were added to HYB+ solution. Pre-hybridized larvae were treated with pre-warmed probe solution and incubated overnight at 65°C. Hybridized embryos were washed twice with 50% formamide/2x SSCT (saline sodium citrate plus 0.1% Tween 20) at 65°C for 20 minutes. Embryos were then washed in succession with 2x SSCT once and 0.2X SSCT twice for 20 minutes at 65°C. Washed embryos were further washed twice in PBST at RT. Washed larvae were blocked for 1 hour at RT and stained with anti-DIG-alkaline phosphatase antibody (Roche, 1093274) at 1:3000 dilution overnight at 4°C. Larvae were washed 5 times in PBST at RT followed by three washes in staining buffer for 5 minutes. Washed larvae were stained with NBT/BCIP at RT until signal was visible. Stained larvae were washed three times in PBST and fixed with 4% PFA to halt the staining reaction. Non-specific signal was removed by destaining larvae. Larvae were successively washed in 30%, 50%, 70%, and 100% MeOH/PBST solution. Larvae were then destained with 66% benzyl alcohol/33% benzo benzoate in glass containers for 2 minutes. Destained larvae were rehydrated

in opposite order of MeOH/PBST washing and further washed with PBST three times. Signal was analyzed at this point.

Visual Motor Response Assay:

A ZebraBox system from ViewPoint Life Sciences was utilized for the Visual Motor Response (VMR) assay. Individual zebrafish larvae were placed in 96-well plate format using Whatman UNIPlate square 96-well plates (VWR, 13503-152). In order to produce a scotopic stimulus, the ZebraBox was modified to attenuate the light intensity beyond its lowest limit by fitting neutral-density filters in the light path. Seven neutral density filters (BarnDoor Film and Video Lighting, E209R), each allowing approximately 40% transmittance, were stacked between the light source and the plate holder until a final intensity of 0.01 lux was attained. In our scotopic experiments, the machine was also powered at 5% in order to prevent instability from the LED light source. The larval displacement was collected by the tracking mode which binned the activity every second. To conduct the scotopic VMR assay, larvae were sorted and grown in 100x15mm petri dishes (VWR, 25384-088) with 15mL E3 media in a density of 30 larvae from 2dpf to 5dpf. Larvae were transferred to 96-well plates with one larva per well on the morning of 6dpf and dark adapted overnight. On 7dpf, the dark-adapted larvae were placed in the ZebraBox and their scotopic VMR was measured. For drug-treated larvae, this procedure was the same except larvae were exposed to drugs in petri dishes on 5dpf. In this study, the following protocol was used: 30 minutes in the dark followed by a 60-minute scotopic light illumination at 0.01 lux, and then a light offset for 5 minutes (Fig.1a). All VMR experiments were conducted between the 9am and 6pm to minimize the effect of circadian rhythm on vision (Emran *et al.*, 2010).

Light Stimulus Intensity:

Light intensity of the ZebraBox LED spectrum was measured with a SpectriLight ILT950 Spectroradiometer (International Light Technologies). The total irradiance of the LED stimulus over the entire visible spectrum at 5% power output was $3.2\mu\text{W}/\text{cm}^2$ ($0.0105\mu\text{W}/\text{cm}^2$ at 500nm wavelength). The corresponding illuminance was 8.0 lux. The light intensity was further reduced by fitting neutral-density filters in the light path as described above. These neutral-density filters did not alter the color spectrum of the LED light. The light intensity with neutral-density filters was calculated by multiplying the light intensity emitted by the machine with the transmittance of each neutral-density filter. The irradiance of the final scotopic stimulus used in this study was $0.005\mu\text{W}/\text{cm}^2$ ($1.80\text{e-}5\mu\text{W}/\text{cm}^2$ at 500nm). The corresponding illuminance was 0.01 lux.

Y79 Cell Culture and cAMP Assays:

The human Y79 cell line was obtained from American Type Culture Collection (ATCC HTB-18). These cells were cultured in RPMI-1640 Medium (ATCC, 30-2001) with 15% Fetal Bovine Serum (ATCC, 30-2020) at 37°C with 5% CO₂. To measure cAMP levels in the cells, the GloSensor Technology -22F cAMP plasmid (Promega, E2301) was used with GloSensor Assay Reagent (Promega, E1290). Four million cells were seeded into 10cm dishes with 10mL of Opti-MEM Reduced Serum Medium (ThermoFisher, 31985062) for transfection. The cells were transfected with 20µg of GloSensor plasmid utilizing X-tremeGENE HP DNA Transfection Reagent (MilliporeSigma, 6366244001) at a 2:1 ratio of plasmid to X-tremeGENE reagent, according to manufacturer's instructions. These cells were transfected for 24 hours, and then they were transferred back into RPMI for another 24 hours. Twenty-five thousand cells were then seeded into a low-volume white 384-well plate per well (Greiner Bio-one, 784080). The cAMP assay was carried out according to the GloSensor protocol for suspension cells. Cells were either treated with DMSO or carvedilol for 20 minutes at room temperature prior to treatment with isoproterenol. Luminosity was recorded 20 minutes after drug or DMSO vehicle addition with a FlexStation 3 Multi-Mode Microplate Reader (Molecular Devices).

Data Visualization and Statistical Analysis:

General Data and Statistics

All standard statistical analyses were performed with R version 3.6.0 <http://www.r-project.org>.

VMR Data

Statistical analyses and data processing were performed with R version 3.6.0 <http://www.r-project.org>. Raw data from the VMR assay was processed and extracted by Data Workshop (ViewPoint). Data figures were created using “ggplot2 (Wickham, 2016) package in R.

The VMR data were normalized for baseline activity, light-intensity variation per well, and batch effect (i.e. biological replicate) by linear-regression models as previously described (Xie *et al.*, 2019). Additionally, offset values were added to the normalized activity to prevent negative displacement.

To determine if each VMR replicate from drug-treated Q344X larvae during drug screening was consistent with the other replicate, a High-Dimensional Nonparametric Multivariate Test (Chang *et al.*, 2017). This test was chosen because the number of observations (i.e. sample size) for each VMR is less than the dimension of the dataset. The dimension is the length of the time period used

in the analysis and the sample size is the number of drug-treated larvae. The High-Dimensional Hypothesis test was implemented in R with the package “HDtest”.

The Hotelling’s T-squared test (Hotelling, 1931) was used to test significant changes in zebrafish displacement from 1 to 30 seconds after the light change. This test is the multivariate version of the T-test which follows the F-distribution. The test statistic for the Hotelling’s T-squared test is calculated as : $F = \frac{n_1+n_2-\rho-1}{p(n_1+n_2-2)} T^2 \sim F_{p, n_1+n_2-p-1}$ where n_1 and n_2 are the sample size. ρ is the dimension which is the time interval used in the analysis. The Hotelling’s T-squared test was used for VMR analysis due to a number of advantages: 1. The Type I error rate is controlled. 2. The relationship between multiple variables is considered. 3. It can generate an overall conclusion even if multiple (single) t-tests are inconsistent. The null hypothesis for the experiment is the group means for all response variables are equal which means the mean vector of the distance travelled for the two chosen groups are the same ($\mu_1 = \mu_2$). The Hotelling T-squared test analysis was performed on the R package “Hotelling (Curran, 2018)” with some reshape of the dataset.

Y79 cAMP Data

Luminosity data obtained from the Y79 cell line was analyzed and plotted using Graphpad Prism (version 8, GraphPad Software). Data were plotted with the non-linear fit method under “log(agonist) vs. response – Variable slope (three parameters)”. pEC50 (negative log of half maximal effective concentration) and pIC50 (negative log of half maximal inhibitory concentration) were calculated through the above-mentioned non-linear fit.

CHAPTER 3. ROD DEGENERATION AND VISUAL IMPAIRMENT OF THE Q344X ZEBRAFISH

3.1 Section Introduction

This chapter outlines the utilization of the Q344X zebrafish to identify a visual consequence due to rod degeneration. Since this zebrafish line exhibits rod degeneration without any cone degeneration, a behavioral protocol was required that elicited a VMR from rods only. A visual phenotype needed to be ascertained from the Q344X fish in order to utilize it as a behavioral model of RP. In this section, the degeneration of Q344X rod photoreceptors was analyzed, and a behavioral protocol was developed with a scotopic stimulus that identified a deficient light-off VMR due to this rod degeneration. This deficient VMR was found to be a result of rod degeneration.

3.2 Results

3.2.1 Anatomical Distribution of Rod Degeneration in the Q344X Zebrafish

In order to utilize the Q344X zebrafish as an RP model for drug discovery, the progression of rod degeneration was evaluated. Previous characterization of the line indicated that significant rod degeneration began on 5dpf and was severe by 7dpf (Nakao *et al.*, 2012). To determine where rod degeneration progresses, whole-mounted dissected retinæ of WT and Q344X larvae were analyzed. Rods were visualized by a *Tg(-3.7rho:EGFP)* transgene. Q344X fish exhibited severe degeneration throughout most of the retina on 7dpf compared to wildtype (WT) larvae (Figure 3). WT retinæ show the highest densities of rod photoreceptors in the dorsal and ventral retina with the lowest density being seen in the most medial retina. Most of the rod degeneration in the Q344X retina appears to take place primarily medially with only few remaining by 7dpf. These remaining rods appear to have an altered morphology at this stage. Some rods can be still be found in the most lateral areas of the Q344X retina by 7dpf.

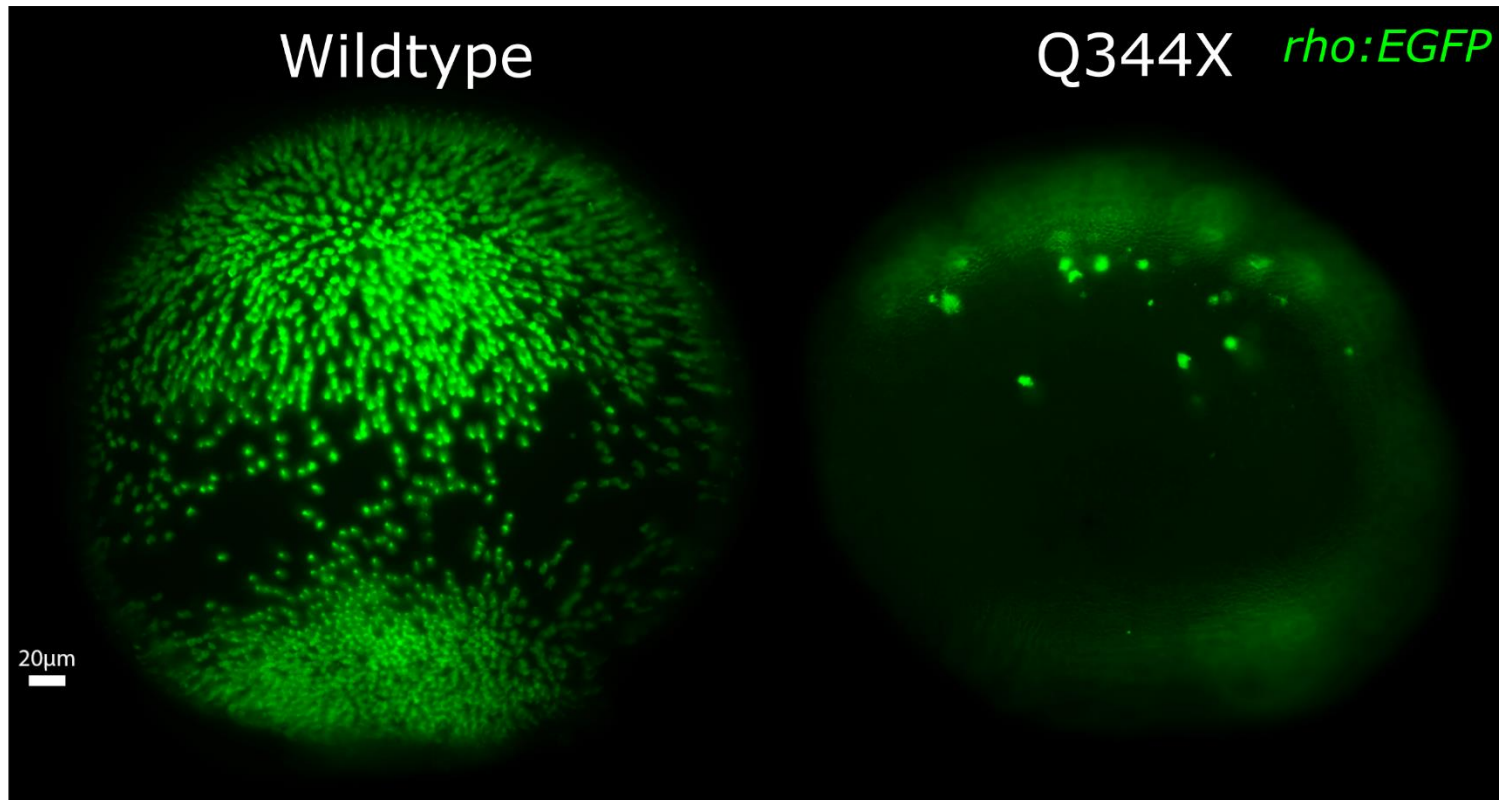


Figure 3. Whole-mounted retinae showing that Q344X zebrafish experience significant rod degeneration by 7dpf

Whole-mount retinae dissected from wildtype and Q344X zebrafish larvae on 7dpf. Rods are imaged with the *Tg(-3.7rho:EGFP)* transgene (shorthand *rho:EGFP*). The retinae are imaged medially. Dorsal is the top of the retina, and ventral is the bottom of the retina. In the wildtype retina, rods are present in the highest densities in the ventral patch and dorsal retina. In the Q344X retina, the vast majority of rods have degenerated with only a few rods present medially.

3.2.2 Identification of a Visual Deficit in the Q344X Zebrafish

Since the Q344X fish experiences rapid rod degeneration, a visual behavior, termed visual motor response (VMR), was utilized to evaluate the light perception of the fish. The zebrafish VMR is a fast startle behavior that can be triggered by a sudden light flash or dark flash. To perform a VMR assay, individual larvae were placed into a clear 96-well plate and exposed to light stimuli. The light stimulus was controlled by a Viewpoint Zebrabox while also tracking the larval zebrafish behavior. The Zebrabox was programmed to generate the following light protocol: dark adaptation for 3 hours, 30 minutes of light and 30 minutes of dark repeated 3 total times. The total time to completion for this VMR protocol is 6.5 hours. This protocol provided 3 technical repeats of light onset and light offset stimuli including a period for sufficient adaptation to the machine environment. The swimming behavior of larvae was recorded as the average distance travelled per second.

Firstly, the VMR of Q344X and WT larvae was assessed utilizing the maximal light intensity of the Zebrabox. At photopic intensities, both WT and Q344X zebrafish displayed a strong VMR to both the light onset and offset stimuli within one second after the light stimulus (light-on VMR and light-off VMR) (Figure 4a and Figure 4b). Since both groups of larvae can perceive the photopic light, the cone phototransduction pathway must be intact and is not being affected by the rod degeneration. To identify a visual phenotype resulting from the rod degeneration in the Q344X zebrafish, a scotopic light stimulus below cone detection threshold was developed. The intensity of the light stimulus of the Zebrabox was lowered to the dimmest stable level, however, this light intensity is still above cone threshold at 8.4 lux. Cones generally require light stimuli at an intensity above 1 lux to exhibit a response (DAVSON, 1973). To further lower the light intensity, neutral density filters were added on the top of the light source. Seven neutral density filters attenuating approximately 60% light intensity each were added to the light source bringing the intensity of the stimulus down to 0.01 lux. The VMR of the Q344X and WT larvae was assessed with this scotopic light. During the scotopic light onset, neither Q344X nor WT larvae displayed a light-on VMR (Figure 4c). However, WT larvae displayed a strong light-off VMR response to the offset of the scotopic light while the Q344X larvae displayed a significantly diminished light-off VMR (Figure 4d). Since the only difference between the Q344X

rhodopsin larvae and WT is the lack of the truncated rhodopsin transgene and rod degeneration, it can be interpreted that the identified phenotype is a result of the rod degeneration. Based on the recorded rod b-waves in larval fish (Moyano, Porteros and Dowling, 2013), and the minimum cone activation threshold in mice (Cachafeiro *et al.*, 2010) at 3.2 lux, it is likely that the developed scotopic stimulus is primarily stimulating rod photoreceptors while leaving cone photoreceptors inactivated. These results indicate that zebrafish larvae are capable of perceiving scotopic light as early as 7dpf.

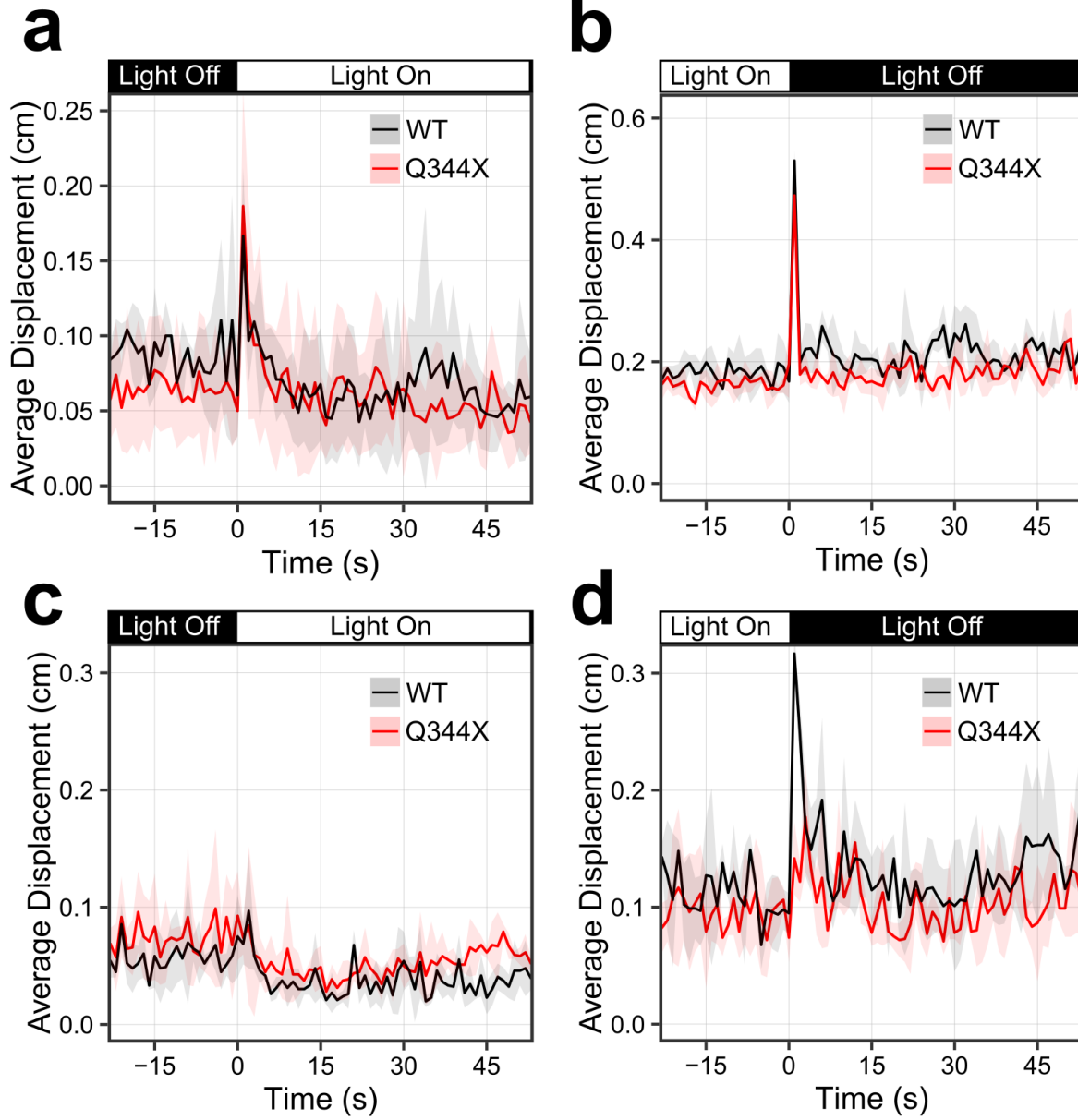


Figure 4. VMR of Q344X zebrafish larvae at 7dpf

Figure 4. continued (a-d): The VMR of wildtype (WT) and Q344X zebrafish was assessed at 7dpf in order to identify a phenotypic behavior due to rod degeneration. First, the VMR of WT and Q344X larvae were assessed under photopic stimuli. a) Both Q344X and WT larvae responded to a photopic light onset stimulus. Both groups of larvae display an increased startle behavior within one second after light onset. The light-on VMR of WT (black trace) and Q344X (red trace) larvae was recorded at 880 lux. The light was turned on at Time = 0. Each trace shows the average larval displacement of 3 technical replicates with 32 larvae per replicate. The corresponding color ribbon indicates ± 1 S.E.M. b) Both Q344X and WT larvae respond to a photopic light offset stimulus. The light-off VMR of WT (black trace) and Q344X (red trace) larvae was recorded at 880 lux. The light was turned off at Time = 0. Each trace shows the average larval displacement of 3 technical replicates with 48 larvae per replicate. The corresponding color ribbon indicates ± 1 S.E.M. Since both WT and Q344X larvae are capable of visualizing light at photopic intensities, a scotopic light source with an intensity below cone threshold was developed to assess scotopic VMR. c) The scotopic light-on VMR of WT (black trace) and Q344X (red trace) larvae was recorded at 0.01 lux. The light was turned on at Time = 0. Each trace shows the average larval displacement of 3 technical replicates with 32 larvae per replicate. The corresponding color ribbon indicates ± 1 S.E.M. Neither WT nor Q344X larvae display a light-on VMR in response to a scotopic light onset. d) WT larvae are capable of perceiving a scotopic light offset stimulus while Q344X larvae are not. The scotopic light-off VMR of WT (black trace) and Q344X (red trace) larvae was recorded at 0.01 lux. The light was turned off at Time = 0. Each trace shows the average larval displacement of 3 technical replicates with 32 larvae per replicate. The corresponding color ribbon indicates ± 1 S.E.M.

3.2.3 Loss of Scotopic VMR is Specifically Mediated Through Rod Loss

Since there is uncertainty about the function of rod photoreceptors at 7dpf, a zebrafish line was utilized to chemically ablate rods to determine if rods are mediating the scotopic VMR. This zebrafish line expresses *nitroreductase* (NTR) under the control of the *rhodopsin* promoter (*rho:NTR*). Nitroreductase converts the prodrug metronidazole (MTZ) into a cytotoxic compound which specifically ablates the rod photoreceptors while not ablating any of the surrounding cells (Walker *et al.*, 2012). rods. The NTR-expressing larvae were exposed to 2.5mM MTZ (*rho:NTR* + MTZ) from 5dpf to 7dpf to ablate rods, and their scotopic light-off VMR was measured at 7dpf. Similar to the Q344X larvae, the (*rho:NTR* + MTZ) rod-ablated larvae exhibited a significantly diminished light-off VMR compared with the untreated (*rho:NTR*) larvae (Figure 5a). The average displacement of *rho:NTR* group one second after the light offset ($0.317 \pm 0.061\text{cm}$) was significantly higher than that of *rho:NTR* + MTZ group ($0.110 \pm 0.062\text{cm}$) (Figure 5b). The diminished scotopic light-off VMR due to rod ablation indicates that this behavior was mediated through rods. This result indicates that rods are functional in zebrafish earlier than previously accepted. Rods are also specifically capable of driving the scotopic VMR.

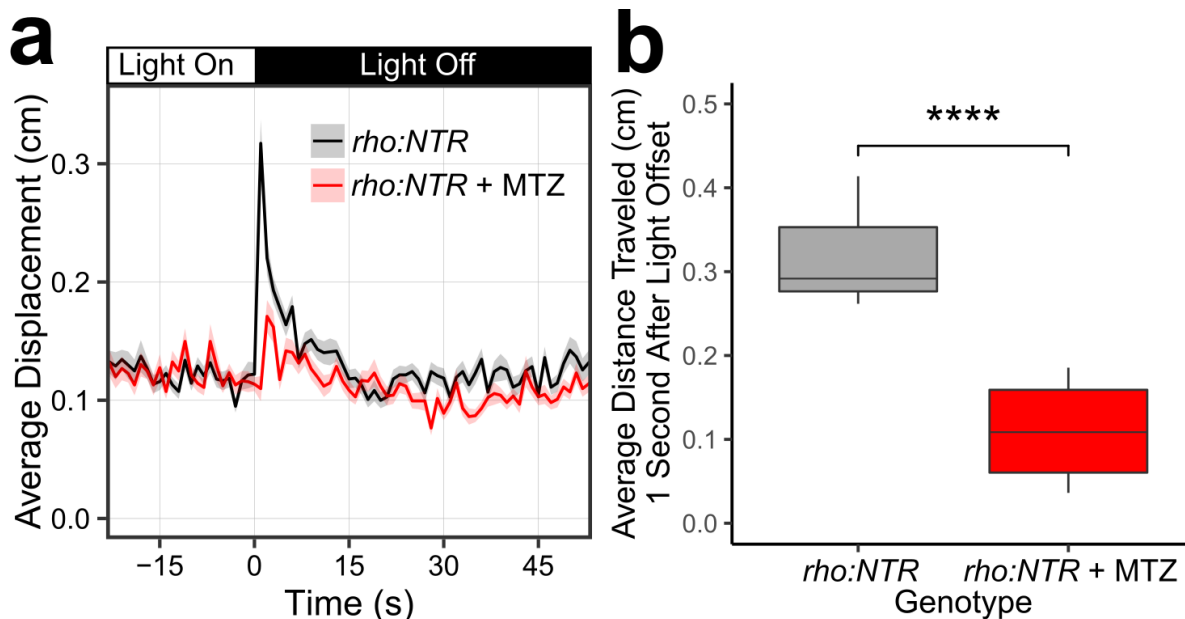


Figure 5. Chemical rod photoreceptor ablation disrupts the scotopic light-off VMR

A zebrafish line expressing *nitroreductase* (NTR) in rod photoreceptors (*rho:NTR*) was utilized to determine if the deficient scotopic light-off VMR displayed by the Q344X zebrafish line is driven by rod photoreceptors. Treatment with the prodrug metronidazole (MTZ) causes NTR to create a toxic byproduct which specifically ablates rods. a) MTZ-mediated ablation of rod photoreceptors leads to the attenuation of the scotopic light-off VMR. The light-off VMR of larvae with *nitroreductase*-expressing rods treated with metronidazole (*rho:NTR + MTZ*, red trace) and without metronidazole (*rho:NTR*, black trace). Each trace shows the average displacement of 6 biological replicates with 24 larvae per condition per replicate. The corresponding color ribbon indicates ± 1 S.E.M. b) Distribution of the average displacement of *rho:NTR* and *rho:NTR + MTZ* larvae one second after light offset. The average displacement of untreated *rho:NTR* larvae ($\mu \pm 1$ Standard Error or the Mean (*S.E.M*): 0.317 ± 0.061 cm, N = 6) was significantly larger than that of *rho:NTR + MTZ* larvae (0.110 ± 0.062 cm, N = 6) (Welch's Two Sample t-test, T = 5.9, df = 10, p-value = 0.00016).

3.3 Section Conclusion

In Chapter 3, the consequence of this rod degeneration was evaluated by assaying the VMR of Q344X larvae. Q344X larvae were capable of responding to photopic light stimuli and displayed a strong VMR. However, when exposed to a scotopic stimulus, WT larvae were able to display a light-off VMR while Q344X larvae did not. Neither WT nor Q344X responded to a scotopic light onset stimulus. This result suggests that rods are driving the scotopic light-off VMR, and the rod degeneration leads to the loss of this behavior. Since Q344X larvae can respond to bright light, the cone pathway in the retina must remain intact despite the rod degeneration. Traditionally, it is not believed that rods contribute to zebrafish behavior until it has developed to 15dpf based primarily on ERG data (Bilotta, Saszik and Sutherland, 2001; Morris and Fadool, 2005; Saade, Alvarez-Delfin and Fadool, 2013). However, a more recent ERG study with the *nof* zebrafish which lacks cone function suggests the rods are functional at 5dpf (Moyano, Porteros and Dowling, 2013). The *nof* zebrafish ERG displays a small a-wave followed by a b-wave of approximately 40 μ V in response to scotopic light stimuli (Moyano, Porteros and Dowling, 2013). Also, VMR work with the *nof* larvae shows that they can behaviorally respond to scotopic stimuli (Venkatraman *et al.*, 2015, 2020). To confirm that rods are driving the scotopic light-off VMR, a zebrafish line expressing *nitroreductase* (NTR) in rod photoreceptors was utilized to specifically chemically ablate rods. Rods are specifically ablated by treatment with metronidazole. NTR-expressing larvae treated with metronidazole showed a loss of the scotopic light-off VMR similar to the Q344X line. These results suggest that rods are capable of driving behavior in zebrafish as early as 7dpf. Since the Q344X zebrafish larvae experience rapid rod degeneration and a robust deficit in VMR by 7dpf, they were utilized to develop a drug screening platform to identify drugs to treat RP.

CHAPTER 4. DRUG SCREENING WITH THE Q344X ZEBRAFISH TO IDENTIFY COMPOUNDS TO TREAT RETINITIS PIGMENTOSA

4.1 Section Introduction

This chapter outlines the optimization and implementation of the deficient Q344X VMR for the purpose of drug screening. The optimization of the original protocol would allow for an increased throughput required for the screening of drugs. It has been suggested that oxidative stress in the retina may exacerbate RP progression (Punzo, Xiong and Cepko, 2012), thus we leveraged this assay to screen ENZO SCREEN-WELL® REDOX library to determine if modulating oxidative stress could ameliorate the Q344X VMR and increase rod survival. A potent antioxidant may be capable of improving the Q344X light-off VMR. Screening this library against the Q344X zebrafish identified carvedilol which improved the scotopic light-off VMR of the Q344X zebrafish as well as improved the rod number in the Q344X retina.

4.2 Results

4.2.1 Optimization of the Deficient Q344X VMR for Drug Screening

The protocol which originally identified the deficient Q344X VMR takes 6.5 hours to complete an experiment. Each experiment is limited to a maximum of 96 larvae per plate, and no more than two of these experiments can be run per day to avoid testing behavior outside the daytime cycle of the circadian rhythm. Zebrafish lose vision and do not exhibit an electroretinogram (ERG) at night (Emran *et al.*, 2010). This protocol would limit screening to two 96-well plates per day. To improve throughput, shorter protocols were designed and tested. While the original protocol included three technical replicates of both light-on and light-off stimuli, a shorter protocol was made to include a single light-off stimulus to increase the ability to perform multiple biological replicates per day. The original protocol also included a long 3.5-hour dark adaptation period after placing the 96-well plate into the Zebrabox. The shorter protocol included a shorter 30-minute dark adaptation period, and larvae in 96-well format were placed overnight in light-proof containers to ensure the rods were completely dark adapted. The final optimized protocol included a 30-minute dark adaptation period, a 1-hour adaptation to the scotopic light,

then a final light offset for 5 minutes (Figure 6a). This optimization demonstrates an improvement in required time from 6.5 total hours to 95 minutes. This protocol utilizes 24 larvae per experiment allowing for high throughput for drug screening while maintaining a high enough sample size to observe a significant difference in VMR between Q344X and WT larvae. The VMR of the Q344X and WT larvae was assessed with this protocol, and the average distance travelled was analyzed one second after the final light offset. WT larvae were able to strongly respond to this optimized protocol upon light off while Q344X larvae did not (Figure 6b). To ensure the optimized protocol is robust, the scotopic light-off VMR of 18 biological replicates of 48 larvae of each Q344X and WT larvae were tested. WT larvae traveled significantly further on average one second after light offset ($0.281 \pm 0.036\text{cm}$) than the Q344X larvae ($0.127 \pm 0.031\text{cm}$) (Figure 6c). Similar to the original protocol, neither WT nor Q344X displayed a VMR to the scotopic light onset (Figure 6d). The average distance travelled one second after light onset was not significantly different between WT and Q344X larvae (Figure 6e). The robust deficient scotopic light-off VMR exhibited by Q344X larvae provides the foundation for drug screening for compounds that ameliorate the phenotypic behavior.

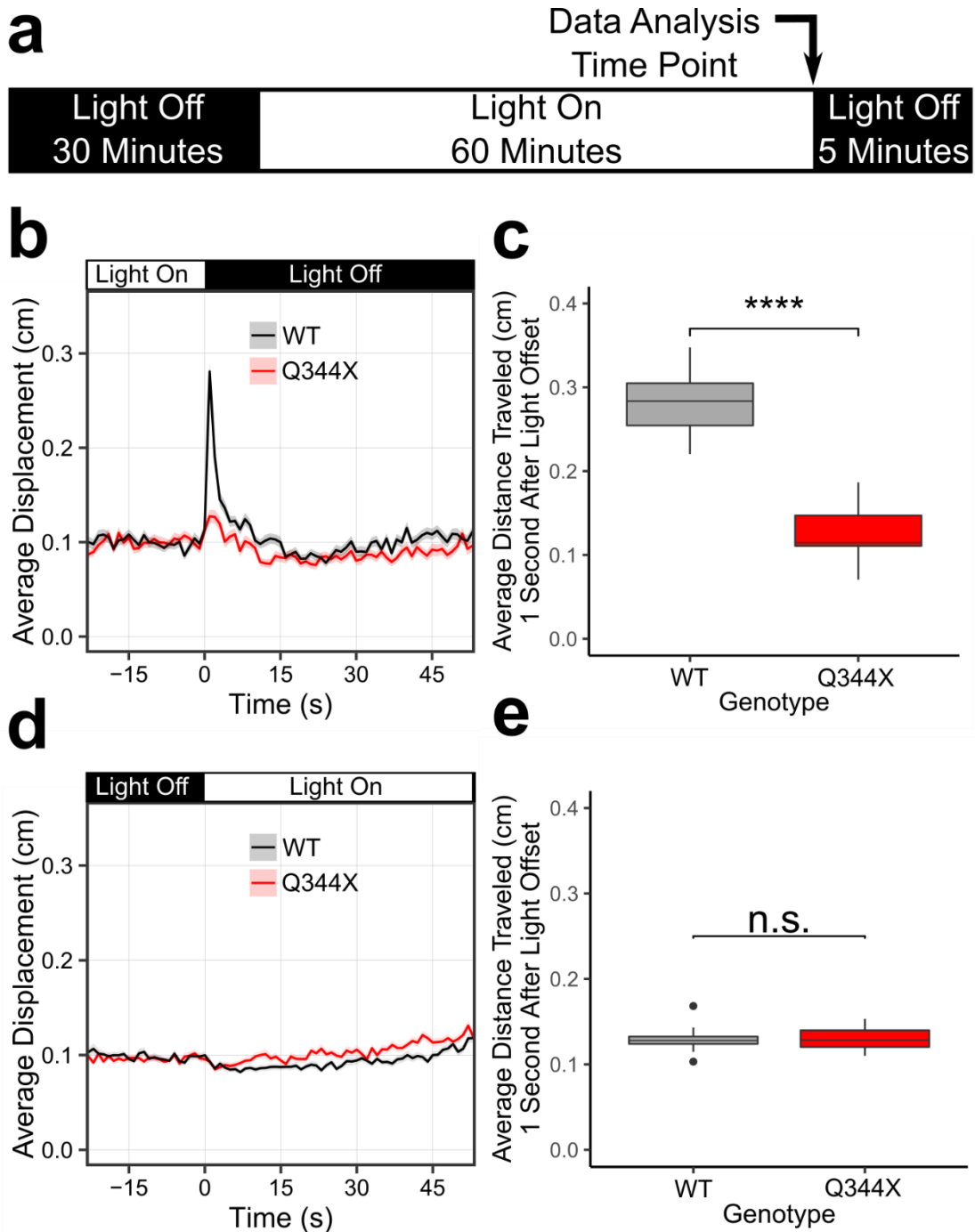


Figure 6. Optimized VMR protocol to utilize for *in vivo* high throughput drug screening with the Q344X zebrafish

Figure 6. continued (a-e): In order to perform drug screening with the Q344X zebrafish, an optimized version of the original 6.5-hour VMR assay protocol was developed to allow for increased throughput for drug screening. a) The optimized protocol consists of a 30-minute dark adaptation period to adapt to the machine environment, a 60-minute light-on period consisting of the scotopic light, and a final light offset of 5 minutes. The light-off VMR was assayed following the light offset indicated by the arrow. As with the original protocol, WT larvae displayed a robust light-off VMR one second after light offset, but Q344X larvae did not. b) The light-off VMR of WT (black trace) and Q344X (red trace) larvae recorded at 0.01 lux. The light was turned off at Time = 0. Each trace shows the average larval displacement of 18 biological replicates with 48 larvae per condition per replicate. The corresponding color ribbon indicates ± 1 S.E.M. c) Distribution of the average larval displacement of WT and Q344X larvae one second after light offset. The average displacement of WT larvae ($\mu \pm 1$ Standard Error or the Mean (*S.E.M*): 0.281 ± 0.036 cm, N = 18) was significantly larger than that of Q344X larvae (0.127 ± 0.031 cm, N = 18)(Welch's Two Sample t-test, T = 13.2, df = 33.2, p-value = $9.006e-15$). Neither WT nor Q344X larvae exhibited a VMR. c) Q344X and WT larvae do not show a VMR to a scotopic light onset stimulus. The scotopic light-on VMR of WT (black trace) and Q344X (red trace) larvae at 0.01 lux. The light was turned on at Time = 0. Each trace shows the average larval displacement of 18 biological replicates with 48 larvae per condition per replicate. The corresponding color ribbon indicates ± 1 S.E.M. d) Boxplot distribution of the average larval displacement of WT and Q344X larvae one second after scotopic light onset. The average displacement of WT larvae ($\mu \pm 1$ (S.E.M): 0.129 ± 0.013 cm, N = 18) was not significantly different from Q344X larvae (0.130 ± 0.013 cm, N = 18)(Welch's Two Sample t-test, T = 0.08, df = 33.8, p-value = 0.93).

4.2.2 Utilizing the VMR Assay with Scotopic Illumination for Drug Screening

With the highly optimized VMR assay developed for the Q344X larval RP model, the next step to finding drug therapies for RP is to utilize this assay in a drug screen. Drug screening is performed under the hypothesis that a compound that is beneficial to the Q344X model will cause the Q344X larvae exhibit a VMR to the stimulus as compared to vehicle or untreated larvae. To improve throughput of this assay, the optimized VMR is utilized at a sample size of $N = 24$ of each group allowing for 4 drugs to be screened per plate. To avoid testing VMR too late into the evening, 6 plates maximum were run per day allowing for a maximum throughput of 24 drugs per day. This assay will allow the Q344X larvae to be screened for compounds that may restore visual function lost by rod degeneration.

One prevailing hypothesis of RP is increased oxidative stress in retina (Komeima *et al.*, 2006). The retina metabolizes more oxygen than any other tissue in the body (Beatty *et al.*, no date), is fed near arterial oxygen levels from choroidal blood vessels, and is exposed to ultraviolet radiation from sunlight. These factors make the retina particularly susceptible to oxidative damage (Punzo, Xiong and Cepko, 2012). Thus, a number of studies have focused on the hypothesis that antioxidant treatments may prevent RP (Rotstein *et al.*, 2003; Komeima *et al.*, 2006; Chucair *et al.*, 2007; Komeima, Rogers and Campochiaro, 2007). The ENZO SCREEN-WELL® REDOX library was screened to address the possibility that oxidative stress may be playing a role in the retinal degeneration and identify new potentially beneficial drugs.

Because rod degeneration in the Q344X model begins at 5dpf (Nakao *et al.*, 2012), this developmental stage was chosen to begin drug treatment. Screening at an earlier developmental stage was avoided to prevent excessive drug toxicity. A common starting concentration for treating zebrafish with drugs is $10\mu\text{M}$ (Wiley, Redfield and Zon, 2017), so that concentration was chosen to screen drugs with the Q344X RP model. 5dpf larvae were treated with the REDOX drugs dissolved E3 for final concentration $10\mu\text{M}$, and the resulting scotopic light-off VMR was tested at 7dpf. The zebrafish larvae were maintained in the drug media throughout the duration of the experiment. Each drug was tested twice with a second-pass screen using embryos collected on different dates. Of the 84 drugs tested, 16 were toxic to the zebrafish at $10\mu\text{M}$. The VMR of the Q344X larvae treated with the remaining 68 drugs was recorded.

With the VMRs of the drug-treated Q344X larvae collected, a method was needed to identify drugs that are effective and should be followed up for further study. Firstly, the VMR of drug treated larvae should be consistent. Drugs that give rise to inconsistent behavioral profiles would make poor treatment options due to unknown variability factors. To determine consistency of drug treated VMR profiles, a High-Dimensional Nonparametric Multivariate Test (Chang *et al.*, 2017) was utilized to compare the swimming behavior of each drug replicate for thirty seconds after the light offset. This test was selected because the sample size of the larvae ($N = 24$) is less than the dimension of the vector (30 seconds of swimming behavior). In this test, a small p-value indicates that drug replicate VMRs are dissimilar and inconsistent while a large p-value indicates that VMR profiles are very similar and consistent. A p-value cut off at 0.9 was selected to identify VMR replicates that are similar. Secondly, the drug treatment should be beneficial to the light sensation of the Q344X zebrafish. To determine drug efficacy, the Hotelling's T-squared test (Liu *et al.*, 2015) was utilized to compare the drug-treated Q344X VMR to control VMR. The Hotelling's T-squared test is a multivariate form of the Student's T test which is appropriate for analyzing high dimensional VMR data over multiple seconds. Because the drugs of the REDOX library are dissolved in DMSO, a control dataset was created by treating Q344X and WT larvae with a matching concentration of 0.1% DMSO. The Hotelling's T-squared test was applied to two timeframes of the VMR: 1 second after light offset to analyze the fast startle response, and from 1 through 30 seconds to detect any changes in sustained swimming activity of the larvae. 5 drug treatments in the 1-second timeframe gave rise to consistent larval behavior, however, none of these drugs were able to give rise to a VMR that was significantly different from the DMSO-treated Q344X dataset. However, 4 drug treatments in the 30-second timeframe were able to give rise to consistent behavior VMR profiles, and of those drugs, 1 drug created a VMR that was significantly different from the DMSO-treated Q344X dataset. These results are summarized in Table 3. The drug that gave rise to both a consistent VMR profile and an improved VMR was the carvedilol. Carvedilol-treated Q344X larvae did not produce a fast startle response one second after light offset, however, the larvae displayed a sustained scotopic light-off VMR compared to DMSO-treated controls (Figure 7a).

4.2.3 Carvedilol Elicits its Beneficial Effects on the Deficient Q344X VMR Through the Retina

Since carvedilol treatment gives rise to an atypical VMR, the drug may have been eliciting a swimming behavior through a sensory mechanism other than vision. Zebrafish express extraocular photoreceptors in the pineal gland that may contribute to behavior. Photoreceptors in the zebrafish pineal gland are thought to regulate circadian rhythm which in turn will affect fish behavior (Li *et al.*, 2012). To address this, the eyeless *chokh/rx3* was utilized to determine if carvedilol works through the retina. Homozygous *chokh/rx3* larvae do not develop eyes due to the loss of function of the Rx3 transcription factor, and any behaviors arising from light stimuli cannot be from the retina (Loosli *et al.*, 2003). The *chokh/rx3* larvae were treated with either carvedilol or DMSO, and their VMR was assessed. Carvedilol treatment of *chokh/rx3* larvae did not result in the increased swimming VMR as seen in carvedilol treated Q344X larvae (Figure 7b). This result indicates that retina must be intact in order for carvedilol to elucidate its beneficial effects. To further assess the possibility that carvedilol is inducing the sustained swimming activity in a non-specific way, WT larvae were treated with 10 μ M carvedilol and the scotopic light-off VMR was tested. The WT larvae treated with carvedilol did not display a sustained swimming behavior like in carvedilol-treated Q344X larvae, but the distance travelled one second after light offset was reduced.

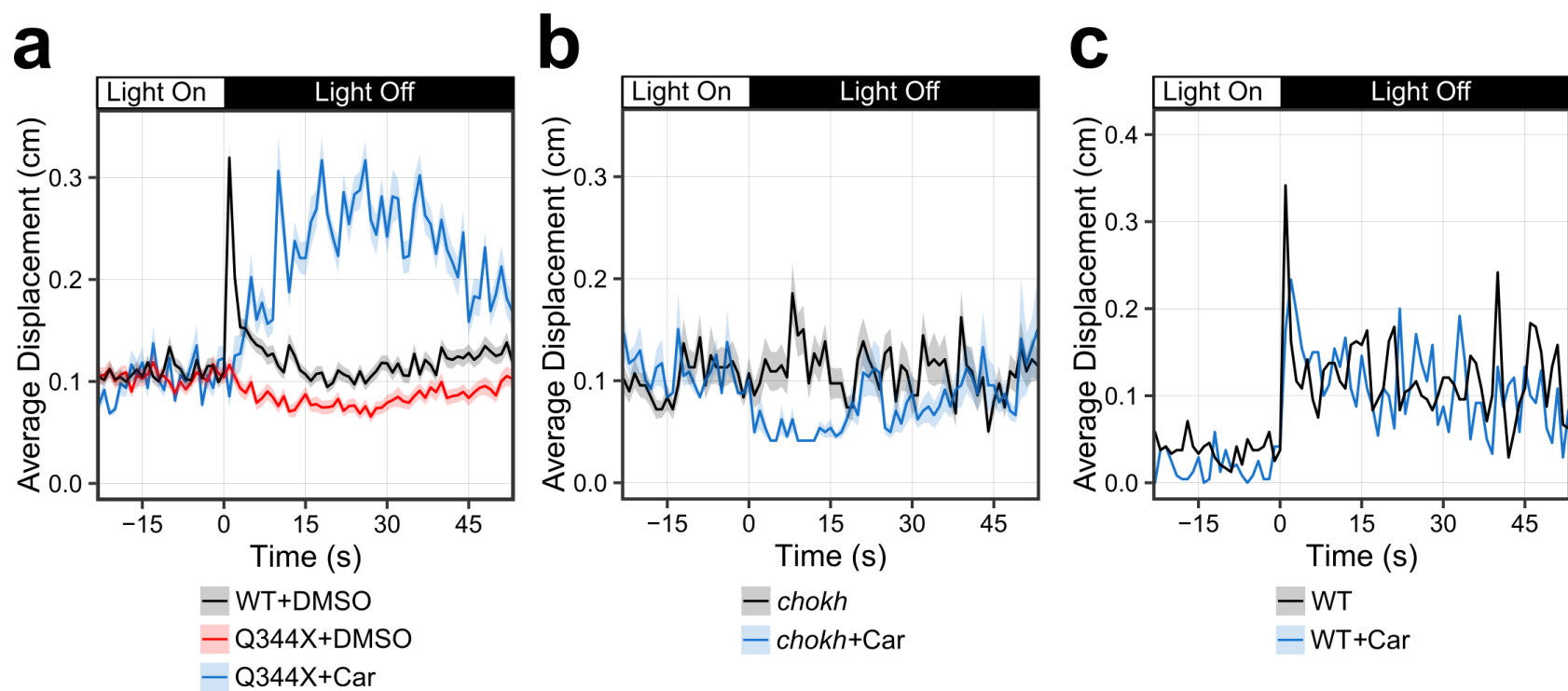


Figure 7. Drug screening of the ENZO REDOX library against Q344X RP model identifies carvedilol as a positive hit

Figure 7. continued (a-c): To find drugs that can treat RP, the ENZO REDOX library was screened to identify hits that can improve the deficient Q344X scotopic light-off VMR. Since the drugs of this library were dissolved in DMSO as a vehicle, drugs were compared to Q344X larvae treated with DMSO. Out of all of the drugs tested in this library, only one drug was identified as a positive hit: carvedilol. Carvedilol treatment of Q344X larvae results in a scotopic light off VMR that is characterized by a sustained swimming activity rather than a sharp WT-like response. a) Carvedilol treatment on Q344X larvae resulted in a sustained scotopic light-off VMR (blue trace indicates average distance travelled, N = 2 replicates of 24 larvae) compared to that of both DMSO-treated WT larvae and DMSO-treated Q344X larvae (black and red trace respectively indicates average distance travelled, N = 9 replicates of 48 larvae). The two carvedilol replicates were highly consistent and not different from each other (High-Dimensional Nonparametric Multivariate Test, N = 24, $T_{HD} = 1.78$, p-value = 0.91). Each replicate demonstrated a significant change in behavior for the duration of 30 seconds after light offset above DMSO-treated Q344X larvae (Hotelling's T-squared test, N = 24, T = 378.0 and 456.0, df = 30, p-value < 0.00001 for each replicate). b) To determine if carvedilol's effects are elicited through the retina, eyeless *chokh* fish were treated with carvedilol (blue trace indicates average distance travelled) and their VMR was compared with untreated control (black trace indicates average distance travelled). Carvedilol treatment did not increase the *chokh* VMR (Hotelling's T-squared test, N = 24 larvae per condition, T = 37.8, df = 30, p-value = 0.946). Ribbon indicates ± 1 S.D. c) WT larvae were treated with carvedilol to determine if carvedilol imparts a sustained swimming activity with a healthy retina. WT larvae (black trace indicates average distance travelled, N = 24 larvae) display the typical fast startle response at light offset. WT larvae treated with 10 μ M carvedilol (blue trace indicates average distance travelled, N = 24 larvae) display a reduced VMR at light offset, but still display a fast response.

Table 2. Breakdown of the selection criteria of the ENZO REDOX library

	1 Second Timeframe	30 Second Timeframe
Number of Starting Drugs in the Library	84	84
Number of Drugs Not Toxic	68	68
Number of Drugs Which Induced Consistent Light-off Scotopic VMR in Both Replicates	5	4
Number of Drugs Which Induced Consistent Light-off Scotopic VMR in Both Replicates, and Significantly Different from DMSO-treated controls (p-value < 0.05)	0	1

The 84 drugs in the ENZO Redox library were each applied to the Q344X larvae at 10 μ M (N = 24 larvae) in two independent replicates. Of these 84 drugs, 16 were toxic. The two replicates were then compared to each other with a High-Dimensional Nonparametric Multivariate Test to determine similarity in either 1-second or 30-second timeframe. The drugs that induced consistent light-off scotopic VMR were compared to DMSO-treated Q344X controls to determine if they caused a significant change in behavior (p-value < 0.05). In the 1-second timeframe, no drugs met all criteria, but in the 30 second timeframe, one drug (carvedilol) was both consistent in both replicates and caused a significant change in light-off scotopic VMR compared to controls.

4.3 Section Conclusion

In Chapter 4, the Q344X zebrafish RP model is leveraged to create a drug screening platform utilizing the deficient scotopic VMR. The protocol that was originally used to discover the deficit in the Q344X scotopic light-off VMR took 6.5 hours to complete and included 3 technical replicates of light onset and light offset. With this protocol, only a single 96-well plate could be run at a time. Given the limitations of zebrafish behavior in regard to the circadian rhythm (Emran *et al.*, 2010), this protocol could only be performed twice in one day spanning the course of 13 hours. Firstly, this protocol would be limited to two plates per day, totaling the number of larvae tested per day at 192. If drugs are tested in batches of 24 larvae, it would take 13 hours to screen 8 drugs per day. Secondly, 13 hours to complete 8 drugs requires manpower spanning much longer than the traditional 8-hour day. Some of these challenges can be overcome by keeping different groups of zebrafish on opposite light-dark cycles to continuously run VMR assays within the circadian rhythm. Alternating personnel to perform these assays can keep screens running. However, these two modifications come at a high expense relative to the increased throughput gained. In order to improve throughput without increasing the need for additional resources, sample size and protocol time was altered. An optimized protocol requiring 95 minutes to complete with a sample size of 24 larvae was developed to increase throughput. This optimized protocol assays a single scotopic light offset which allows for a larger number of biological replicates to be performed. Lowering the sample size per group doubles the effective throughput available for drug screening. Combining the lower sample size with the quicker protocol, the effective throughput is increased to 24 drugs in 9.5 hours. This paradigm allows for these experiments to be carried out in a single day, by a single person, and stay within the light cycle of the zebrafish circadian rhythm. Most importantly, the scotopic light-off VMR remains robust with the optimized protocol, and the deficit in the Q344X VMR is recapitulated.

The optimized protocol was utilized to screen the ENZO REDOX library to identify potential drugs to treat RP. Since oxidative stress has been shown to play a role in RP progression (Punzo, Xiong and Cepko, 2012), drugs that may have an antioxidant effect may improve the deficient Q344X VMR. Larvae were drug treated beginning on 5dpf at a concentration of 10 μ M for each drug. The decision to begin drug treatment at 5dpf was made due to the beginning of rod degeneration in Q344X mutant, and the zebrafish visual system as developed to a point where

larvae display a variety of visual behaviors including the VMR and OKR (Easter and Nicola, 1997; Emran *et al.*, 2007; Chhetri, Jacobson and Gueven, 2014; Liu *et al.*, 2015). This stage also was chosen to allow the larvae to developmentally mature to a stage as far as possible to minimize potential toxicity from drugs. Unexpectedly, carvedilol was a β -blocker identified as a positive hit from this library. Rather than a fast startle VMR, carvedilol-treated Q344X larvae exhibited a sustained swimming behavior in response to the scotopic light offset. This type of behavior is different from the expected WT-like fast startle immediately after light offset; however, the sustained VMR of the carvedilol-treated Q344X indicates light sensation in the RP model. Any behavioral change due to increased light sensation in an RP model can be considered an improvement. An eyeless zebrafish larva was utilized to confirm that carvedilol is working through the retina and not exerting an off-target effect. Homozygous *chokh/rx3* zebrafish do not develop eyes which makes them ideal for testing the contributions of extraocular photoreceptors on behavior. Carvedilol-treated *chokh/rx3* did not recapitulate the sustained VMR seen with carvedilol-treated Q344X retina. This result suggests that carvedilol is working through the retina of the Q344X fish, and that the retina must be intact for carvedilol to alter the Q344X VMR. To determine if carvedilol causes the sustained swimming behavior non-specifically, WT larvae were treated with carvedilol. Since the carvedilol-treated WT larvae did not display a sustained swimming activity, the sustained swimming behavior seen with the treated Q344X larvae is likely specific to the model. Carvedilol can improve the Q344X scotopic light-off VMR, however the mechanism behind the improvement is not immediately known.

CHAPTER 5. IDENTIFICATION OF THE MECHANISM OF ACTION OF CARVEDILOL IN THE RETINA

5.1 Section Introduction

This chapter outlines the efforts made to determine the mechanism of action of carvedilol in the retina. Since carvedilol increases the light sensation of the Q344X zebrafish, the number of rods remaining in the Q344X was analyzed to determine if the carvedilol-treated Q344X VMR is a result of a change in rod number. Q344X rod numbers were found to be increased with carvedilol treatment, so the source of these rods was investigated by TUNEL-staining to assess carvedilol's effects on apoptosis, and *in situ* hybridization was performed to determine if new rods were being generated due to drug treatment. Since β -adrenergic signaling is not well characterized in the retina, a rod-like human cell line was utilized to determine if carvedilol may work directly on rods. Because aberrant ADCY signaling is associated with mislocalized activation of Q344X RHO, and that inhibition of ADCY has shown to improve rod survival, an ADCY inhibitor was tested to determine if it would also improve the Q344X VMR.

5.2 Results

5.2.1 Carvedilol Treatment Increases Rod Number in the Q344X Retina

The Q344X RP model exhibits a deficient scotopic light-off VMR due to rod degeneration, carvedilol may be improving the VMR through increasing the number of rods in the retina. To visualize rods in the retina, an EGFP transgene under the control of the *rhodopsin* promoter (*Tg(-3.7rho:EGFP)*) was utilized. The number of rods in the retina was quantified on whole-mounted and cryosectioned retinæ. Retinal cryosections were made containing the optic nerve to consistently compare samples. With cryosections, Q344X retinæ showed significant rod degeneration on 5dpf (Figure 8a and Figure 8b) which is consistent with previously reported results (Nakao *et al.*, 2012). At this 5dpf stage, the Q344X larvae were treated with 10 μ M carvedilol and the rod number was quantified at 6dpf and 7dpf. Carvedilol-treated Q344X larvae exhibited an increased number of rods compared to DMSO-treated Q344X larvae on 6dpf and 7dpf (Figure 8c

and Figure 8d). The majority of increased rod number can be seen in the ventral patch and the dorsal retina.

To determine the anatomical distribution of the increased number of rods in the carvedilol-treated Q344X retina, whole-mounted retinæ were imaged on 7dpf to assess rod distribution. WT larvae have a high density of rods in the lateral retina and ventral patch on 7dpf while Q344X exhibited excessive rod degeneration in these areas (Figure 9). Carvedilol-treated Q344X retinæ exhibited increased rods in the lateral retina and the ventral patch. While the carvedilol treatment increased rods, it did not bring the rod number to wildtype levels. The carvedilol-treated larvae displayed gaps in the rod distribution in the lateral retina, and there are some rods extending medially. To quantify these observations, WT, Q344X, and carvedilol-treated Q344X were binned into these 3 classifications based on the distribution of EGFP signal: Strong, Intermediate, and Weak (Table 3). All WT larvae were classified as Strong. The carvedilol-treated Q344X larvae had significantly more Intermediate phenotypes in the lateral and ventral views compared to the DMSO-treated Q344X group. No larvae from the carvedilol or DMSO-treated Q344X groups was classified as Strong. The correlation between rod increase and enhanced light-off VMR of Q344X larvae suggests that the extra rods mediated the visual improvement.

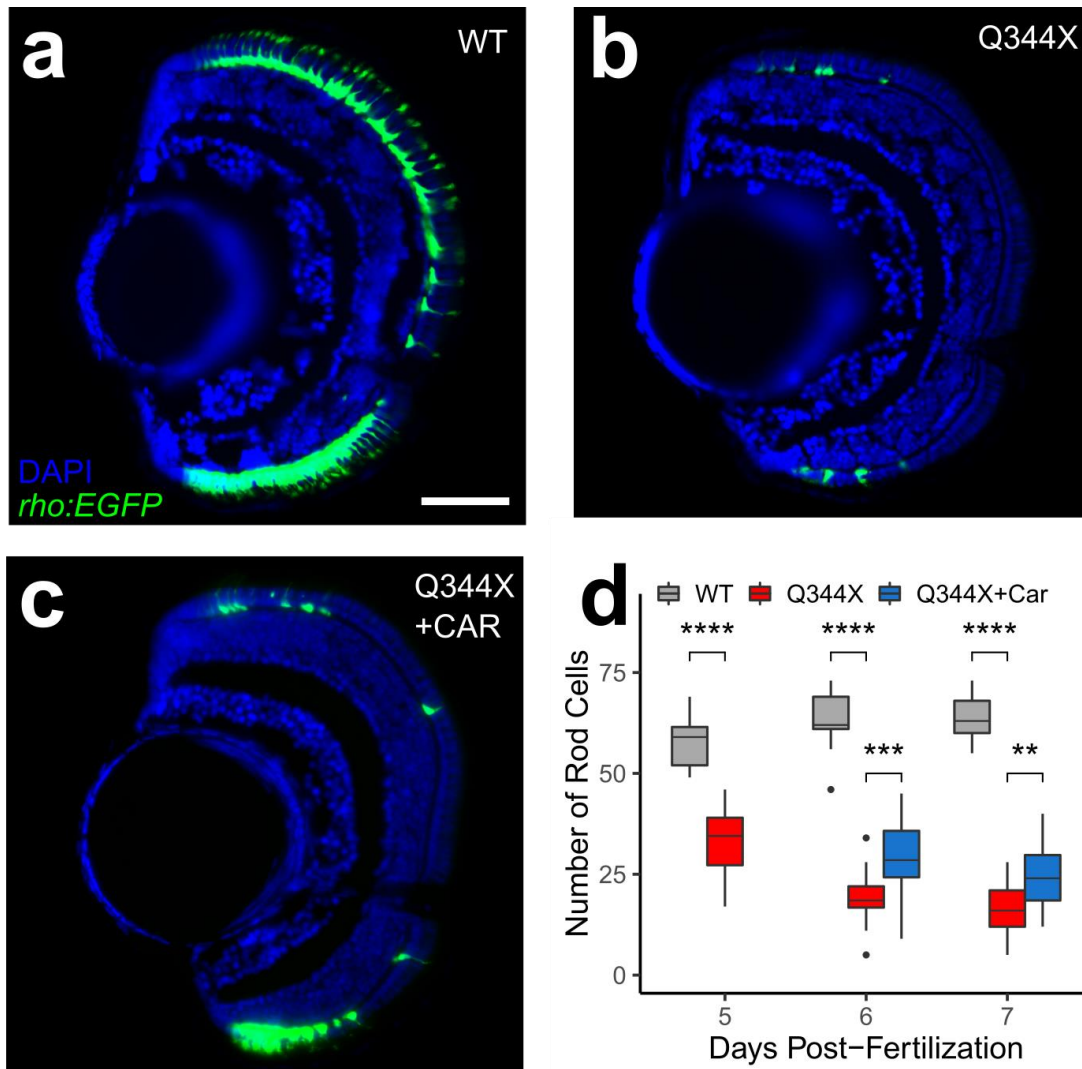


Figure 8. Carvedilol treatment of the Q344X zebrafish RP model increases rod number in the retina

Carvedilol treatment increased rod numbers in the Q344X larvae. Representative retinal cryosection of a (a) wildtype (WT), (b) Q344X, and (c) carvedilol-treated Q344X (Car) larva at 7dpf. Rods were labeled by EGFP expression driven by *rho* promoter (*rho:EGFP*), and the nuclei were counterstained with DAPI. Scale = 50 μ m. d) Quantification of rod number in WT, Q344X, and carvedilol-treated Q344X retinal cryosections from 5dpf to 7dpf. Q344X larvae have significantly fewer rods compared with WT starting at 5dpf (WT, N = 11; Q344X, N=16; Welch's Two Sample t-test, T = 8.7, df =23.8, p-value = 7.2e-09), at 6dpf (WT, N = 9; Q344X, N =20; Welch's Two Sample t-test, T = 14.0, df =12.1, p-value = 7.7e-09), and at 7dpf (WT, N = 9; Q344X, N =17; Welch's Two Sample t-test, T = 18.9, df =17.7, p-value = 3.7e-13). Carvedilol treatment beginning on 5dpf results in significantly more rods in the Q344X retina compared to untreated Q344X at 6dpf (Q344X, N = 20; Car, N =21; Welch's Two Sample t-test, T = 4.1, df =36.3, p-value = 0.0002) and at 7dpf (Q344X, N = 17; Car, N =11; Welch's Two Sample t-test, T = 3.2, df =24.9, p-value = 0.003).

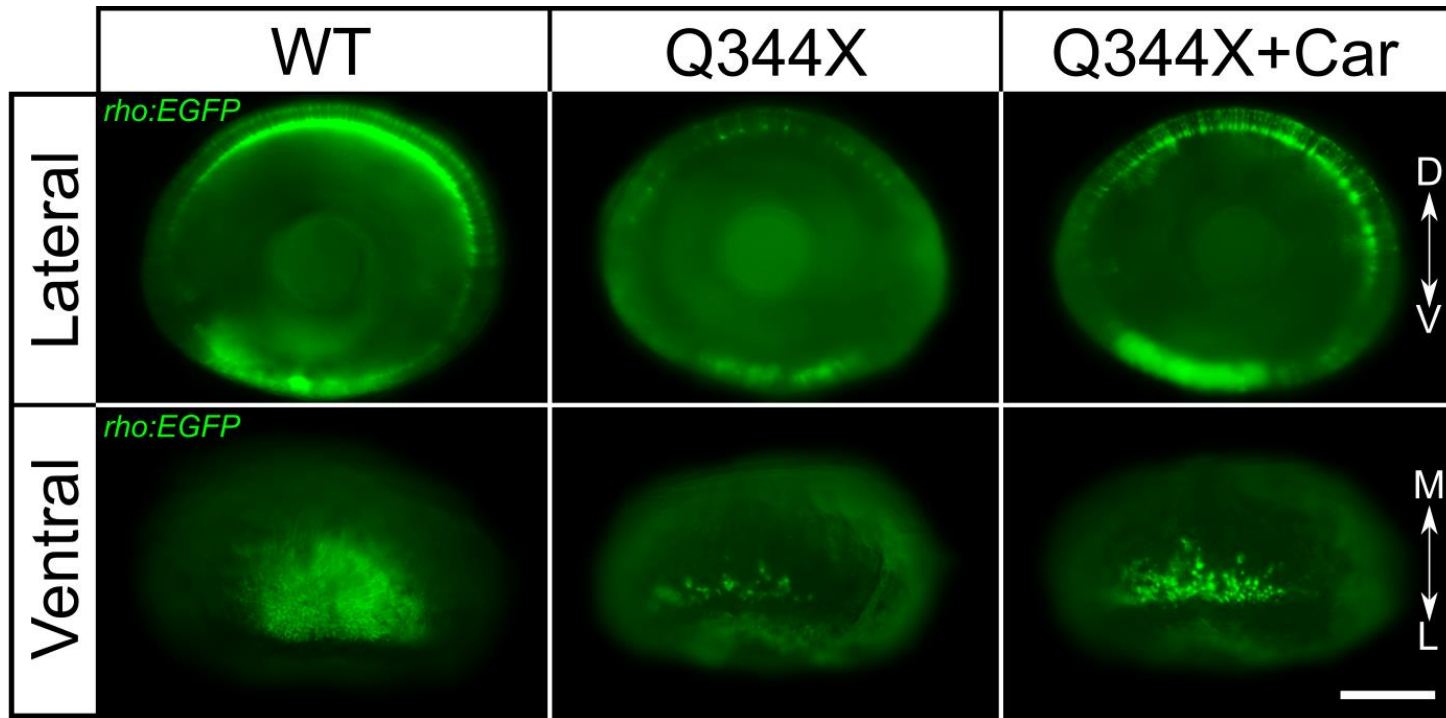


Figure 9. Anatomical distribution of increased rod number in carvedilol-treated Q344X zebrafish larvae

Representative whole-eye images of WT, Q344X, and carvedilol-treated Q344X larvae at 7dpf. Rods were labeled by EGFP expression. Left column: WT rods were mainly found on dorsal and ventral retina (top). They were abundantly present in the ventral patch of the retina extending medially (bottom). Middle column: Q344X rods were mostly degenerated at the same stage (top). There were only a thin line of rods remaining near the lateral edge of the Q344X retina (bottom). Right column: Carvedilol treatment increased the number of Q344X rods on both dorsal and ventral retina (top); however, gaps of missing rods were still apparently on dorsal retina. More rods were observed in the ventral patch of the carvedilol-treated retina (bottom). Scale = 100 μ m. D = Dorsal, V = Ventral, M = Medial, L = Lateral.

Table 3. Rod distribution binning in whole-mount eyes

	Strong	Intermediate	Weak
WT Lateral	10	0	0
Q344X Lateral	0	9	15
Q344X+Car Lateral	0	16	8
WT Ventral	10	0	0
Q344X Ventral	0	8	16
Q344X+Car Ventral	0	16	8

Rod number analysis on whole-mount eyes. All larvae were bleached and examined from the lateral and ventral sides. The signal were classified into 3 categories by the extent of *rho:EGFP* fluorescence. The Strong group contains the samples with high rod number/signal intensity in the lateral retina and ventral patch; the Intermediate group contains the samples with distinct rods in the lateral retina with noticeable gaps, and some rods in the ventral patch extending medially; and the Weak group contains the samples with sparse rods in the lateral retina and the most lateral edge of the ventral patch. A representative image of Strong, Intermediate and Weak type can be found in the left, middle and right column in Fig. 3e respectively. Carvedilol treatment increased the number of Q344X larvae with Intermediate phenotypes and reduced the number of Weak phenotypes in both the lateral (Chi-square test, $\chi^2 = 4.09$, $df = 1$, p -value = 0.043) and ventral views (Chi-square test, $\chi^2 = 5.33$, $df = 1$, p -value = 0.020). No Q344X larvae was classified as Strong with or without carvedilol treatment.

5.2.2 Carvedilol is the Sole β -Blocker that Gives Rise to the Sustained Scotopic Q344X VMR

Since screening of the ENZO REDOX library revealed the β -blocker carvedilol as a positive hit, adrenergic signaling is implicated in the mechanism of improving the Q344X VMR. To see if other β -blockers are capable of eliciting the same type of sustained Q344X VMR as carvedilol, all commercially available β -blockers was selected to test on the Q344X RP model. However, none of the tested β -blockers were able to improve the deficient Q344X VMR. This indicates that carvedilol is unique in the ability to improve the Q344X VMR.

5.2.3 Carvedilol Treatment does not Alter the Number of TUNEL-positive Cells in Q344X Retinal Cryosections

Carvedilol treatment increases the number of rods in the Q344X retina; however, the source of these rods is unknown. Previous work has promoted apoptosis as the mechanism of cell death for Q344X rods (Alfinito and Townes-Anderson, 2002; Nakao *et al.*, 2012). One hypothesis is that carvedilol is preventing apoptotic signaling to preserve Q344X rods. To assess apoptosis in the Q344X retina, apoptotic cells were stained with a TUNEL (terminal deoxynucleotidyl transferase dUTP nick end labeled) assay. Retinal cryosections from WT, DMSO-treated Q344X, and carvedilol-treated Q344X larvae were stained from 5dpf to 7dpf. Any TUNEL-positive cells in the outer nuclear layer (ONL) were quantified (Figure 10). Q344X retinæ showed significant amounts of TUNEL-positive cells in the ONL compared to WT retinæ at all developmental stages. However, carvedilol treatment did not alter the number of TUNEL-positive cells compared to DMSO-treatment on 6dpf or 7dpf. It is possible that this lack of change in apoptosis could be that the apoptotic cells in the zebrafish retina are rapidly cleared by macrophages within 45 minutes (Mitchell, Lovel and Lambert, 2019). The rapid clearance of apoptotic cells in cryosections likely results in only few detectable TUNEL-positive cells.

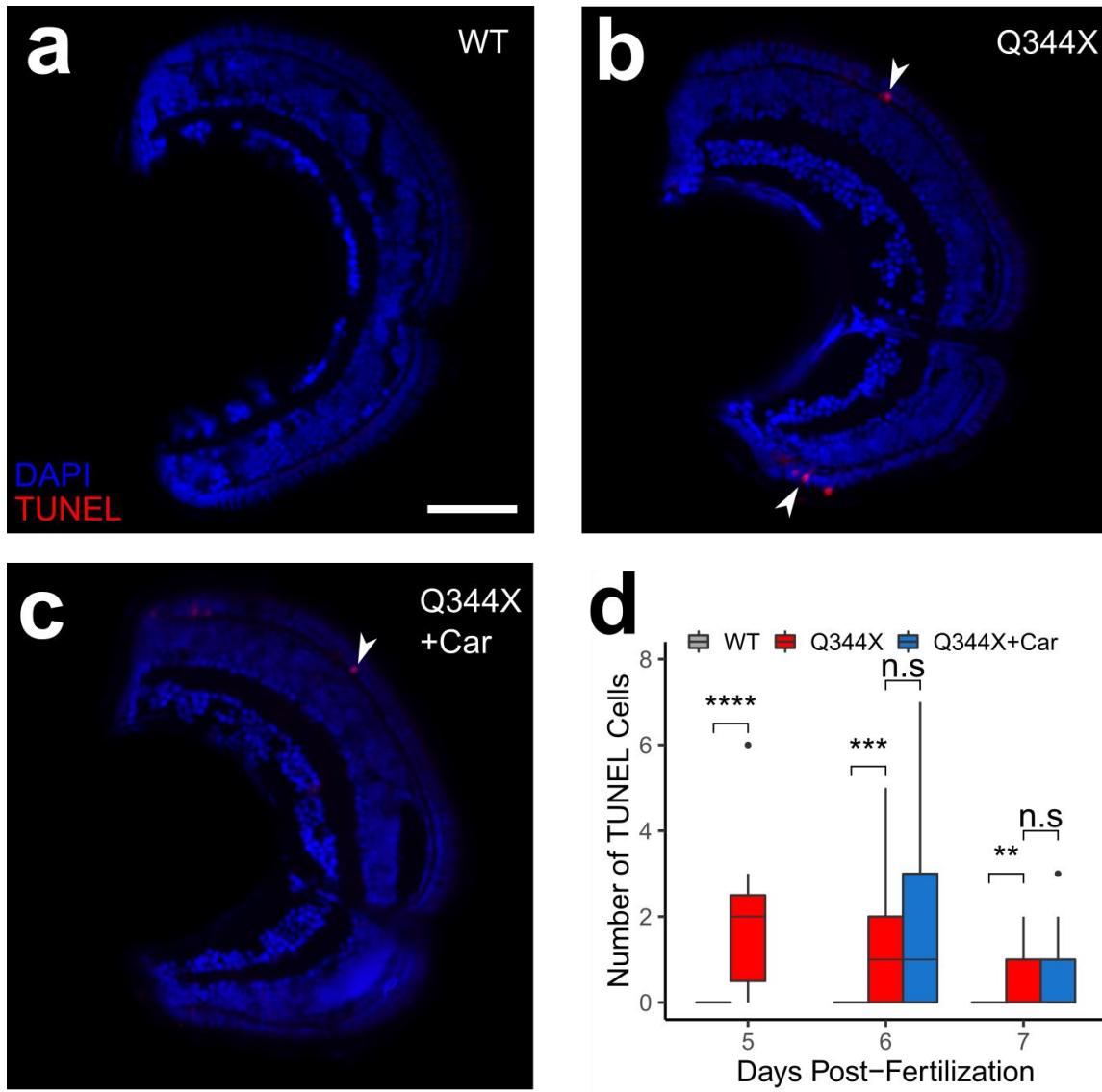


Figure 10. TUNEL staining in the Q344X retina is not altered by carvedilol treatment

TUNEL-staining of Wildtype (WT), Q344X, carvedilol-treated Q344X retinal cryosections revealed that carvedilol does not lower the detectable number of TUNEL-positive cells. Representative retinal cryosection of a (a) WT, (b) Q344X, and (c) carvedilol-treated Q344X (Q344X+Car) larva at 7dpf. For all sections, lateral is to the left and dorsal is up. TUNEL-positive cells were labeled in red, and the nuclei were counterstained with DAPI. The arrows indicate the TUNEL-positive cells in the outer nuclear layer. Scale = 50 μ m. D) Quantification of TUNEL-positive cells in WT, Q344X, and Q344X+Car retinal cryosections from 5dpf to 7dpf. Compared to WT, the Q344X retinae had more TUNEL-positive cells at 5dpf (WT, N = 11; Q344X, N = 19; Welch's Two Sample t-test, T = 5.0, df = 18.0, p-value = 9.8e-05), at 6dpf (WT, N = 9; Q344X, N = 25; Welch's Two Sample t-test, T = 4.3, df = 24, p-value = 0.0003), and at 7dpf (WT, N = 8; Q344X, N = 22; Welch's Two Sample t-test, T = 3.5, df = 21.1, p-value = 0.002). Carvedilol treatment beginning at 5dpf did not alter the number of TUNEL-positive cells at 6dpf (Q344X, N = 25; Car, 6dpf N = 24; Welch's Two Sample t-test, T = 0.9, df = 41.3, p-value = 0.36), or at 7dpf (Q344X, N = 22; Car, N = 14; Welch's Two Sample t-test, T = 0.2, df = 21.5, p-value = 0.81)

5.2.4 *nr2e3* Expression Increases in the Lateral and Ventral Retina with Carvedilol Treatment but not in the Medial Retina

Since zebrafish are capable of regenerating photoreceptors throughout their lifetime (Angueyra and Kindt, 2018), the question arises whether the increased rod number in Q344X larvae are surviving rod photoreceptors or new rods differentiating from progenitors. TUNEL-staining was inconclusive to determine the source of the increased rods in carvedilol-treated Q344X larvae, so *in situ* hybridization was used to analyze genes related to photoreceptor development with and without drug treatment. The gene *nr2e3* was selected since it is a transcription factor that promotes that transcription of rod-specific genes and suppresses the transcription of cone-specific genes (Kobayashi *et al.*, 1999; Morris *et al.*, 2008). Nr2e3 also promotes *rhodopsin* transcription. If *nr2e3* transcription is seen in area of the retina that has experienced severe rod degeneration without *rhodopsin* expression, this could indicate new rods differentiating. The expression of *nr2e3* (Figure 11) and *rhodopsin* (Figure 12) was assessed on 7dpf.

Expression of *nr2e3* in the WT retina can be seen around the lateral retina near the ciliary marginal zone extending medially. The *nr2e2* expression in the ventral patch and lateral retina of Q344X larvae appears to be increased with carvedilol treatment matching the increased rods visualized with EGFP. However, no *nr2e3* expression is seen medially towards the optic nerve with carvedilol treatment. Expression of *rhodopsin* is prevalent throughout the WT on 7dpf including strong staining in the ventral and dorsal retina. No *rhodopsin* signal was seen in the medial area of the retina in Q344X larvae, and only faint staining was present in the lateral retina and ventral patch. Carvedilol treatment increased rhodopsin staining in the lateral retina and ventral patch similar to *nr2e3* pattern.

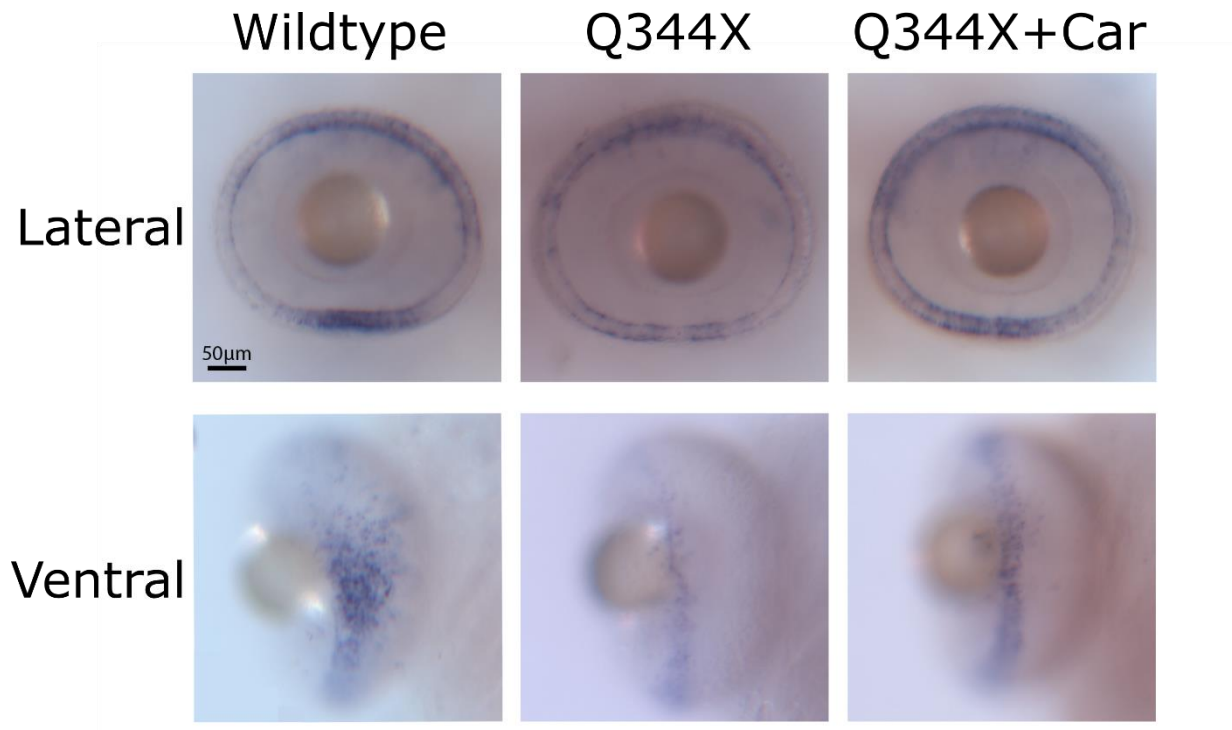


Figure 11. *nr2e3* expression in the Q344X retina is increased in the lateral and ventral retina at 7dpf

Representative images of in situ hybridization was performed to determine if carvedilol treatment is inducing the generation of new rods. The expression of the gene *nr2e3* was investigated as it would indicate the differentiation of rod progenitors. Wildtype retinae displayed strong *nr2e3* expression in the proliferative zones in the lateral retina and ventral patch. In the Q344X retina, *nr2e3* expression is still present in the lateral retina, but it has become severely diminished in the ventral patch. Carvedilol treatment of Q344X larvae increases some staining signal in both the lateral retina and ventral patch. However, no new staining is seen extending medially in the retina with carvedilol which suggests that new rods are not being generated.

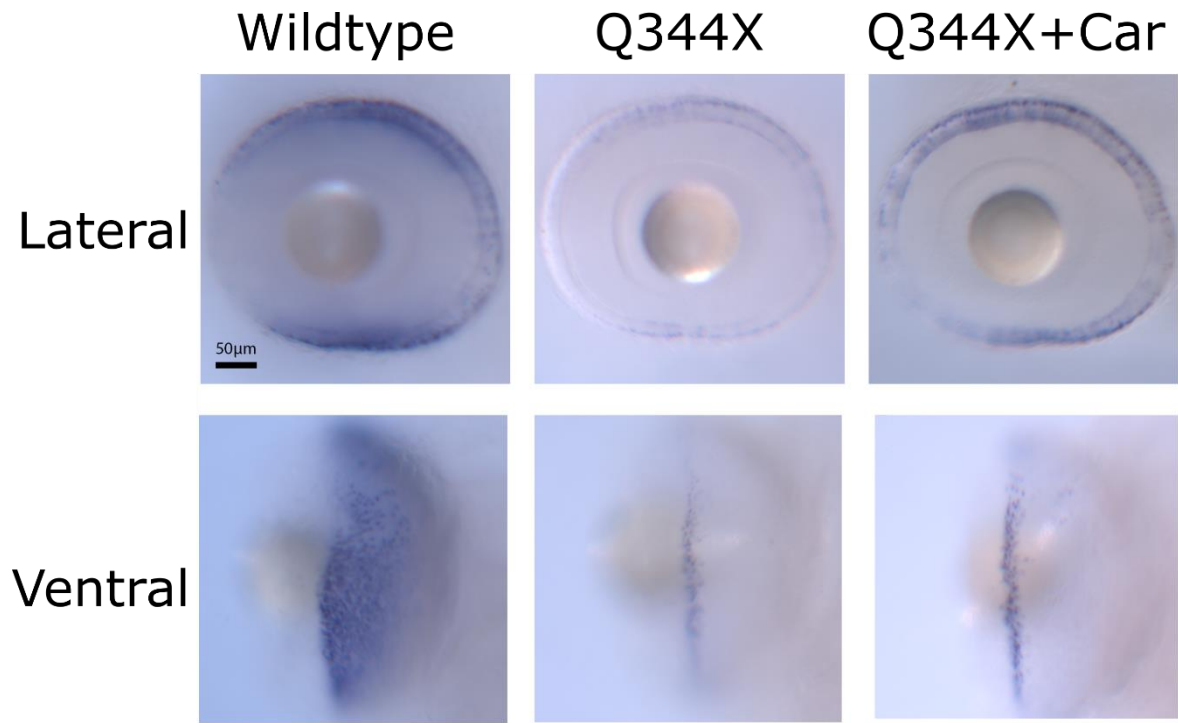


Figure 12. *rhodopsin* expression in the Q344X retina is increased in the lateral and ventral retina at 7dpf

Representative images of in situ hybridization was performed to determine if carvedilol treatment is creating new, mature rods. The expression of the *rhodopsin* was investigated as since it only labels mature rods. The staining results of *rhodopsin* are similar to imaging the rods expressing EGFP. Wildtype retinæ display strong staining in the lateral retina and in the ventral patch extending medially. Almost all of this staining is gone in both the lateral retina and ventral patch of Q344X larvae. Carvedilol treatment increased the amount of staining in the ventral patch and lateral retina. However, no mature rods were seen extending medially in the retina which indicates that no new functional rods are being generated with carvedilol treatments.

5.2.5 Carvedilol Elicits its Beneficial Effects in the Q344X Retina in a Rod Autonomous Fashion

Carvedilol is a β -blocker that binds to β adrenergic receptors and inhibits adrenergic signaling. However, its retinal target is unknown, and it may act directly on rods. To evaluate this possibility, we examined the effect of carvedilol treatment on a rod-like cell line, the Y79 human retinoblastoma line which uniquely expresses rod-specific genes (Di Polo and Farber, 1995). The level of adrenergic signaling was determined by GPCR-modulated changes in cAMP levels as measured by a cAMP-sensitive luciferase. First, the Y79 cells were transfected with the luciferase reporter, and then they were exposed to a half-log dose-response curve of isoproterenol, a β -adrenergic receptor agonist. Isoproterenol was capable of inducing cAMP signaling in the transfected Y79 cells with a pEC50 of 7.49 ± 1.07 (Figure 13a). The cAMP level was not increased in controls treated with matching DMSO percentage. The relative cAMP level did not increase much above $10\mu\text{M}$ isoproterenol. To determine if carvedilol treatment can inhibit this isoproterenol-mediated cAMP increase, the transfected Y79 cells were pretreated with a half-log dose-response curve of carvedilol and then challenged with a dose of $10\mu\text{M}$ isoproterenol that would induce saturating relative cAMP level according to Fig. 12a. Carvedilol pretreatment was able to prevent isoproterenol-mediated cAMP signaling with a pIC50 of 6.51 ± 0.67 (Figure 13b). Therefore, carvedilol likely bound to the β -adrenergic receptors and directly elicited its beneficial effects on rods.

5.2.6 Adenylyl Cyclase Inhibition does not Improve the Q344X Scotopic VMR

Since the mislocalized activation of the Q344X Rhodopsin likely can stimulate ADCY activity and cAMP production, inhibition of this signaling cascade should prevent the death of the rod. Previous work with the Q344X zebrafish line has shown that inhibition of ADCY with the inhibitor SQ22536 does in fact increase rod number (Nakao *et al.*, 2012). To determine if this increase in rods can translate to improved vision, the Q344X zebrafish was treated with SQ22536 from 5dpf to 7dpf and the scotopic light-off VMR was tested on 7dpf. Interestingly, the ADCY inhibitor did not improve the Q344X VMR at the 30 second time frame (Figure 14). This lack of

efficacy might be caused by unintended effects of treating an entire zebrafish larva with an ADCY inhibitor that affected the VMR.

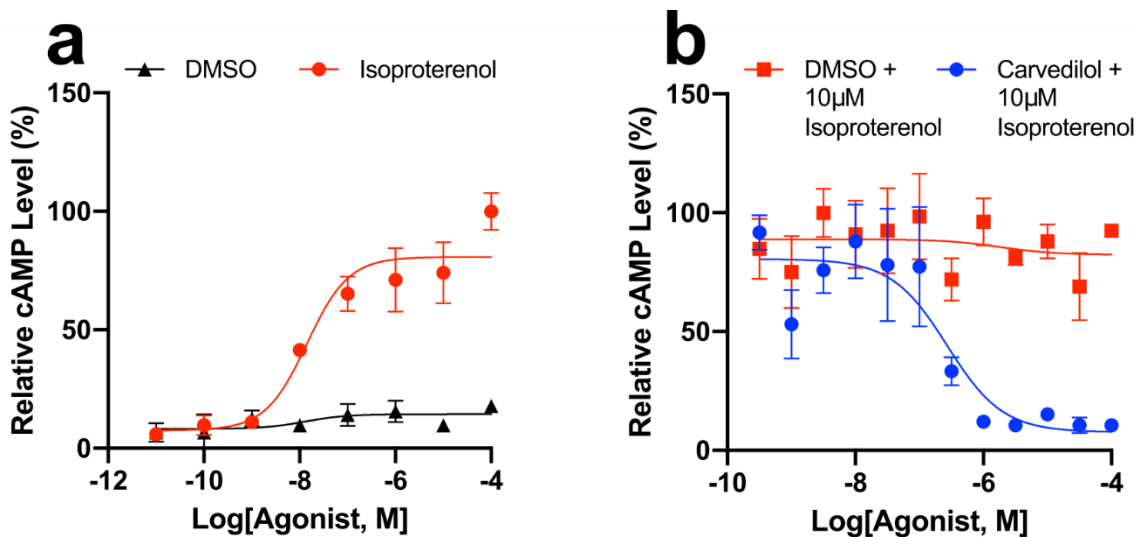


Figure 13. Carvedilol modulates adrenergic signaling in the rod-like Y79 human retinoblastoma cell line

Carvedilol treatment might directly act on rods cells. To determine the extent to which carvedilol act directly on rods, we conducted a GloSensor cAMP assay with rod-like human Y79 cells. A) Representative dose-response curves of GloSensor-transfected Y79 cells treated with half-log concentrations of isoproterenol (red trace; N = 4) or percentage-matched DMSO (black trace; N = 4). These plots were normalized to the maximum average luminescent level recorded per experiment. Error bars show ± 1 S.E.M. Isoproterenol was capable of increasing cAMP signaling through β -adrenergic receptor binding with an pEC50 of 7.49 ± 1.07 . B) Representative dose-response curves of GloSensor-transfected Y79 cells pretreated with half log doses of carvedilol (blue trace; N = 4) or percentage-matched DMSO (red trace; N = 4). Cells were then challenged with a 10 μ M isoproterenol that could induce maximal cAMP response, as shown in Fig. A. Carvedilol pretreatment was capable of preventing isoproterenol-mediated cAMP increases with an pIC50 of 6.51 ± 0.67 .

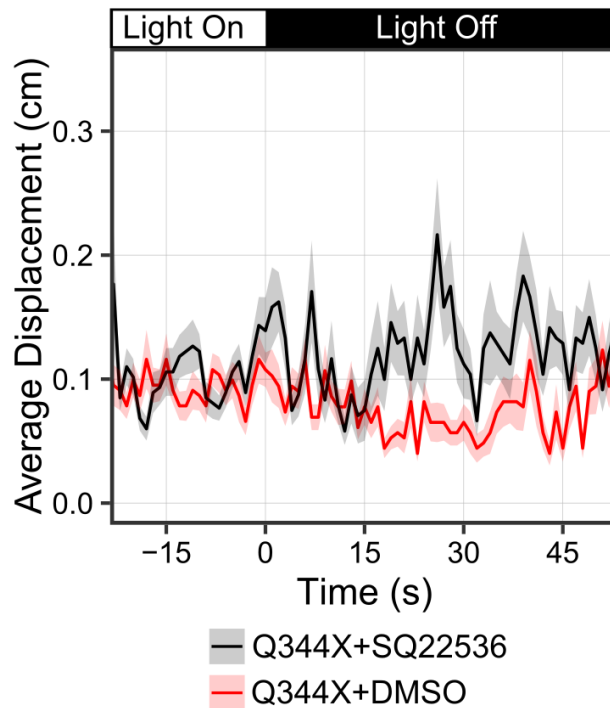


Figure 14. The adenylyl cyclase inhibitor SQ22536 does not improve the deficient Q344X scotopic light-off VMR

Q344X larvae were treated with the adenylyl cyclase (ADCY) inhibitor SQ22536 (black trace) to determine if inhibiting ADCY would improve the VMR compared to DMSO treatment (red trace). The optimized scotopic protocol was utilized, and the scotopic light offset occurs at $T = 0$. Treatment with SQ22536 did not significantly improve the Q344X VMR (Hotelling's T-squared test, $N = 24$ larvae per condition, $T = 40.7$, $df = 30$, $p\text{-value} = 0.952$). Ribbon indicates ± 1 Standard Deviation.

5.3 Section Conclusion

Chapter 5 describes the efforts taken to determine how carvedilol is improving light sensation in the Q344X RP model. Firstly, since the Q344X zebrafish loses light sensation due to rod degeneration, the retina of carvedilol-treated larvae was investigated to determine if increased rod number is resulting in the improved VMR. Retinal cryosections were made in order to count the number of rods with EGFP in center of the retina beginning on 5dpf and continuing through 7dpf. Cryosections were made containing the optic nerve to allow for consistent comparison between samples. Carvedilol treatment significantly increased the rod count in the Q344X retina, but this number does not reach WT levels. It may be possible that this intermediate number of functional rods present is causing the sustained swimming VMR in carvedilol-treated Q344X larvae rather than electing a fast startle response. Whole-mount eyes were examined to determine the anatomical location of the increased rod number in the entire retina. Carvedilol was able to increase the number of rods in the lateral retina and ventral patch compared to no treatment. Like seen with cryosections, carvedilol treatment did not improve the Q344X retina to wildtype morphology. Gaps in the rod distribution can still be seen in the lateral retina, and only moderate improvement occurs in the ventral patch. These areas of the retina are proliferative for rods and witnessing an increased rod number in these areas suggests that carvedilol is acting on younger rods in these areas. Since carvedilol is primarily referred to as a β -blocker, all the commercially available β -blockers were tested to see if β -blockers in general are able to improve the Q344X VMR. However, no β -blocker other than carvedilol could improve the Q344X VMR.

Since carvedilol treatment increases rod number of the Q344X retina, the source of these rods was investigated by analyzing cell death and gene expression. Since Q344X rods likely die through apoptotic mechanisms (Alfinito and Townes-Anderson, 2002; Nakao *et al.*, 2012), the progression of apoptosis was investigated using TUNEL labeling. TUNEL staining labels fragmented DNA which is seen at the last stages of apoptosis. Q344X larvae showed significant numbers of TUNEL-positive cells compared to WT between 5dpf and 7dpf. However, TUNEL staining was unable to show any significant difference in TUNEL-positive cells in the Q344X retina with carvedilol treatment. One reason for this could be that apoptotic cells in the zebrafish retina are rapidly cleared by macrophages in as little as 45 minutes (Mitchell, Lovel and Lambert, 2019). These cryosections are also approximately 10 μ m in thickness which encompasses only a

few cell layers. Rapid clearance of apoptotic cells coupled with thin cryosections might result in only few detectable TUNEL-positive cells. Future studies should utilize a method that assesses whole-retina apoptosis such as expressing a transgenic reporter for an earlier stage of the apoptotic pathway. Alternatively, it may be possible that carvedilol is inducing the creation of new rod photoreceptors. To assess the possibility of new rods, in situ hybridization was performed with larvae to examine the expression of the gene *nr2e3*. This gene is the precursor to *rhodopsin* expression, and it labels rod progenitor cells. In the Q344X retina, *nr2e3* is significantly diminished by 7dpf compared to WT, and some increased staining can be seen with carvedilol treatment. This staining occurs in the lateral retina and ventral patch similar to the location of increased rod number seen with EGFP. No changes in staining were seen in the older medial areas of the retina which would suggest that no new rods are being generated through carvedilol treatment. Taken together, these results most strongly suggest that carvedilol is preventing cell death of younger rods in the proliferative areas of the zebrafish retina.

CHAPTER 6. EXPANDED STUDIES AND FUTURE DIRECTIONS

6.1 Section Introduction

This chapter outlines the expansion of the scotopic light-off VMR system to screen for more drugs beneficial for treating RP and the characterization of new zebrafish models of RP. Since carvedilol is an FDA-approved drug, it can easily be repurposed to treat RP. To find more drugs that can potentially be repurposed, an FDA-approved library from Selleckchem was screened against the Q344X model. Since the Q344X RP model represents only a single type of mutation in *rhodopsin*, two more mutations in *rhodopsin* were in the zebrafish to determine if modeled similar disease progression occurs relative to the Q344X model. The P23H and R135W mutations were inserted into zebrafish as transgenes. The retinæ of these models were assessed for rod degeneration, and their scotopic light-off VMR was tested.

6.2 Results

6.2.1 Screening of FDA-approved Drugs Provides 205 First Pass Hits

In addition to the ENZO REDOX library, two other drug screening libraries have been selected for screening. Since carvedilol discovered through the ENZO REDOX library is FDA-approved, an FDA-approved drug library containing 1,440 compounds was chosen to be screened. FDA-approved drugs that improve the deficient Q344X VMR can be rapidly prescribed off-label by physicians to treat RP. This fact combined with the confirmed bioactivity of these compounds provides a good chance for attaining multiple hits from this library. All 1,440 compounds have been screened against the Q344X model at a concentration of 10 μ M beginning on 5dpf. The lead hits of the first pass were identified by the scotopic light-off VMR peak value provided 1 second after light offset. Compounds that fell outside of the untreated Q344X distribution of the distance travelled one second after light offset of each replicate were selected as hits. The largest value at travelled by untreated Q344X larvae in this data set is 0.214cm. By using this value as the lower limit for selection criteria, there are 205 drugs that caused Q344X larvae to have a startle response above this level (Figure 15). However, this measure does account for drugs that increase sustained

swimming behavior similar to the carvedilol VMR profile. This provides a first-pass hit rate of this library of approximately 14.2%. Drug-treated VMR values falling within the Q344X control distribution were not selected for further follow up, while drugs-treated VMR values above this distribution and within the WT control VMR distribution were selected for second-pass screening. Approximately 15% of the drugs in this library were toxic to the zebrafish larvae at 10 μ M concentration. These 205 drugs replicates will be tested for consistency with the High-Dimensional Nonparametric Multivariate Test and tested for efficacy with the Hotelling's T-squared test. This work should identify multiple FDA-approved drug hits that can be used to treat RP. Future studies will include follow up experiments on these drugs to investigate rod number in the Q344X retina and other possible mechanisms of action.

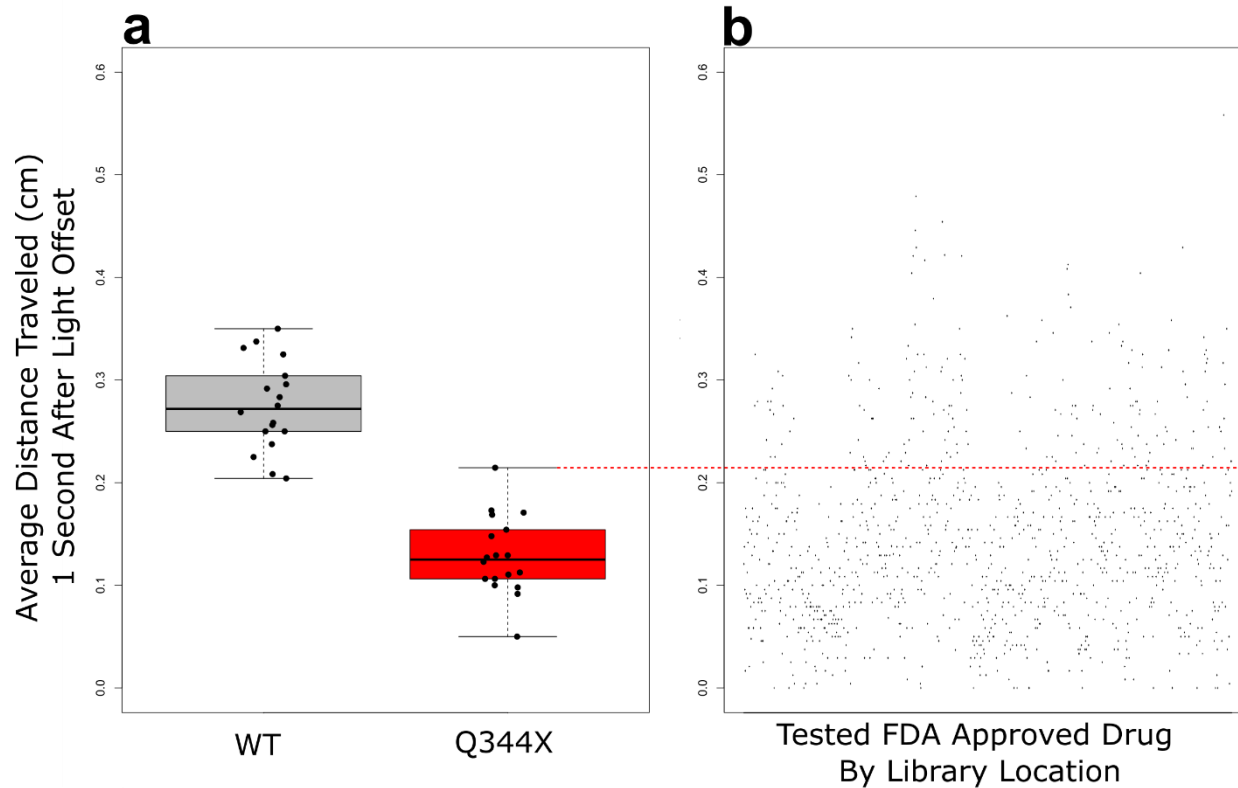


Figure 15. Drugs screened from an FDA-approved compound library against the Q344X scotopic light-off VMR

Given that carvedilol is an FDA approved drug, a library containing 1,440 FDA-approved drugs were screened against the Q344X zebrafish line. A) The distribution of WT and Q344X scotopic light-off VMR one second after light offset was used to determine which drugs should be followed up with a second pass. Any drugs that fall outside of the Q344X distribution indicates that a drug is having an effect on VMR. Since only drugs that increase the Q344X scotopic light-off VMR would be of interest, a cutoff was created at the maximum of the Q344X distribution (red dashed line). B) Representation of the VMR of Q344X larvae treated with drugs of the FDA-approved library. The x-axis represents the drug location in the order stored in the library. 205 drugs in the FDA library resulted in VMRs above the Q344X distribution indicated by the red dashed line.

6.2.2 New Zebrafish Models of RP

The Q344X RP zebrafish model has proven useful in identifying deficits in vision due to rod degeneration. However, this model only represents one mutation of a single gene that causes RP. In order to expand screening to identify drugs that can treat RP arising from different mutations, models carrying specific mutations need to be utilized. Since over 150 mutations have been mapped in rhodopsin leading to RP (Rossmiller, Mao and Lewin, 2012; Daiger, Bowne and Sullivan, 2014; Athanasiou *et al.*, 2018), more transgenic zebrafish models of RP containing mutations in *RHO* are being developed (Y. Sasamoto *et al.*, 2010). Two zebrafish autosomal dominant RP models carrying mutations in addition to Q344X are available to be investigated for disease recapitulation. The P23H *Tg(rho:Hsa.RH1_P23H)* and R135W *Tg(rho:Hsa.RH1_R135W)* mutations in *RHO* were assessed for an RP phenotype. The P23H point mutation leads to a misfolding of the protein which causes *RHO* to become stuck in the ER (Olsson *et al.*, 1992). Rods expressing P23H *RHO* are believed to die through ER stress triggered by the unfolded protein response. The P23H mutation is the most common RP mutation found in North America (Daiger, Bowne and Sullivan, 2007). The R135W mutation causes hyperphosphorylation and decreased binding to 11-*cis* retinal (Chuang *et al.*, 2004). Additionally, R135W *RHO* binds visual arrestin with increased affinity causing disruption in the endocytic pathway. This disruption in endocytosis is believed to lead to death of R135W-expressing rods. Transgenic zebrafish carrying these two mutations were analyzed for rod death and a deficient scotopic light-off VMR. P23H larvae exhibited apparent rod degeneration in the ventral patch beginning on 5dpf and progressively became worse by 7dpf compared to WT larvae (Figure 16). However, the R135W larvae did not display any apparent rod degeneration between 5dpf and 7dpf. To determine if these mutations lead to a visual defect, the scotopic light-off VMR was assessed of these two transgenic lines. As expected, P23H larvae exhibited a diminished scotopic light-off VMR due to rod degeneration (Figure 17a). R135W larvae displayed a fast startle behavior in response to the scotopic light offset (Figure 17b). It is likely that R135W larvae displayed a strong response at this stage due to the lack of any apparent rod degeneration. Future studies with these and other zebrafish RP models will need to consider the disease mechanism in order to develop screening methods optimized for the particular carried mutation.

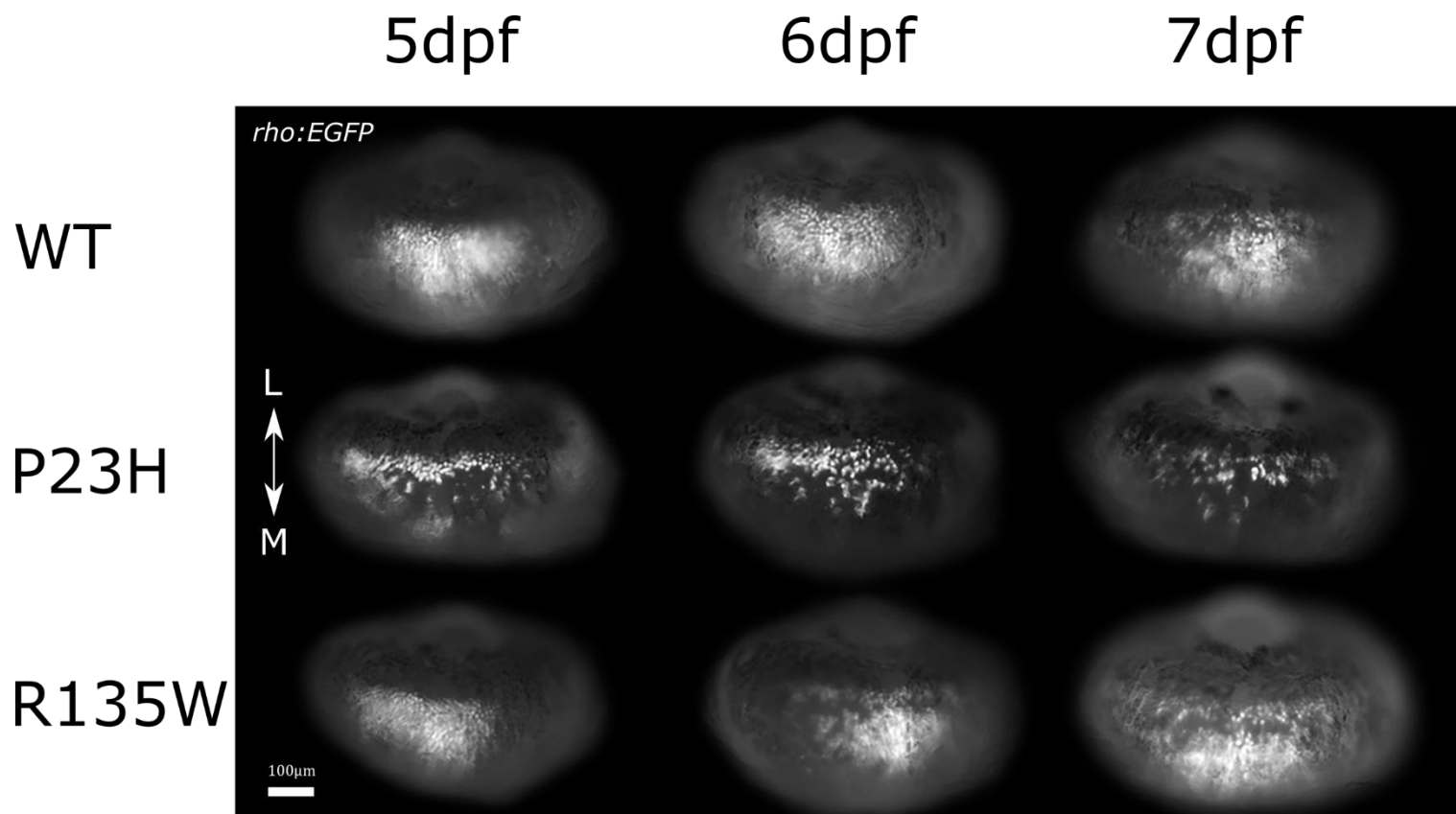


Figure 16. Whole-mount eyes of P23H and R135W zebrafish larvae reveal rod degeneration in P23H but not R135W larvae.

Transgenic zebrafish expressing P23H and R135W RHO were assessed for rod degeneration utilizing a *rho:EGFP* transgene. Rod degeneration was evaluated from 5dpf to 7dpf of WT (top row), P23H (middle row), and R135W (bottom row) in the ventral patch (L=Lateral, M=Medial). P23H larvae displayed rod degeneration in the ventral patch beginning on 5dpf and progressing through 7dpf compared to WT. Patches of missing rods appear to extend medially in P23H retinæ. However, no obvious degeneration could be identified in R135W larvae. The rod pattern of R135W larvae did not appear to differ from that of WT larvae at all stages.

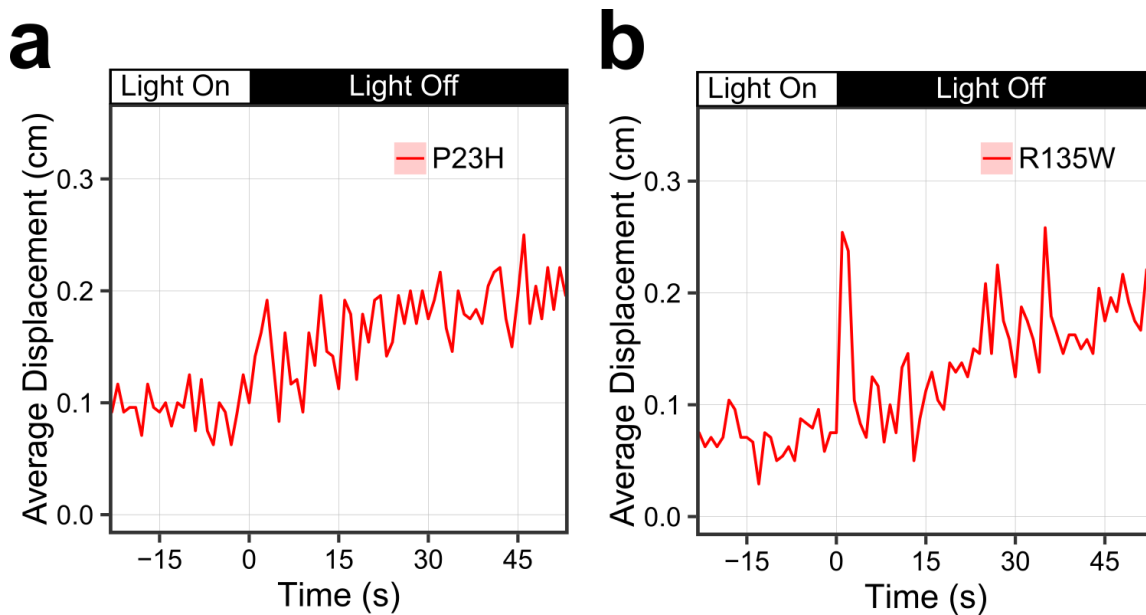


Figure 17. P23H larvae exhibit a diminished scotopic light-off VMR while R135W larvae display a strong response.

To determine if the P23H and R135W RP models have any visual defects, the scotopic light-off VMR was assessed. The optimized scotopic protocol was utilized, and the scotopic light offset occurs at $T = 0$. a) Scotopic light-off VMR of 24 P23H larvae. P23H larvae do not exhibit a strong startle response immediately after offset of the scotopic light. This lack of VMR correlates with the loss of rod photoreceptors. b) Scotopic light-off VMR of 24 R135W larvae. Unlike P23H larvae, the R135W larvae show a rapid scotopic light-off VMR immediately after the light offset.

6.3 Section Conclusion

Chapter 6 highlights the expansion of the optimized scotopic VMR assay to screen a larger number of FDA approved drugs, and the utilization of the optimized assay to investigate new zebrafish models of RP. The discovery of the FDA-approved drug carvedilol highlighted the advantage of repurposing already approved drugs to treat RP. Since each individual mutation that leads to RP can be considered a unique disease with a unique mechanism, it is not practical to complete the FDA approval process for a new drug that treats each individual mutation. Clinical trials and FDA approval may take upwards of 10 years for a new drug, however repurposed drugs may be prescribed off-label by physicians almost immediately given that safety can be demonstrated. To identify more FDA-approved drugs that may treat RP, a library containing 1,440 FDA-approved drugs was screened with the Q344X RP model to identify drugs that may improve the model's deficient scotopic light-off VMR. Since this library is large, it would take significant time and resources to perform a second-pass screen of the entire library. To improve efficiency, drugs that resulted in a fast startle VMR profile with an average distance travelled that falls outside of the Q344X peak VMR distribution were selected for second-pass screening. There are 205 drugs that fall above the Q344X distribution cutoff line. Future work will compare the second-pass drug VMR profiles for consistency as well as with the Hotelling's T-squared test. The result of this screen should provide a multitude of drug candidates which may be able to treat RP. Having a pool of candidate drugs is advantageous compared to only focusing on a single drug. A pool of candidates increases the likelihood that at least one drug will show efficacy when translated into mice RP models and eventually human patients. This pool of potentially effective RP drugs may also be utilized as a smaller, first-pass screening library for different zebrafish RP models to increase the likelihood of a rapid drug discovery.

In addition to expanding drug discovery, the optimized scotopic light-off VMR assay can be utilized to assess new zebrafish models of RP. In addition to Q344X, the mutations P23H and R135W in RHO were assessed with transgenic zebrafish to identify any rod degeneration and consequential visual phenotype. The misfolded P23H RHO led to rod degeneration beginning on 5dpf and progressing through 7dpf in fashion similar to the Q344X model. Also, like the Q344X model, the P23H mutation led to a deficit in the scotopic light-off VMR on 7dpf. This result indicates that the P23H model may be immediately used for drug discovery utilizing the optimized

scotopic light-off VMR assay. However, the R135W model did not exhibit any visible rod degeneration or visual phenotype in the first week of development. Future studies may require investigating the model at a later developmental stage to determine if a rod degeneration phenotype is present. Also, more sensitive techniques such as electrophysiology may be needed to detect subtle changes in rod or retinal physiology due to this mutation. The analysis performed on these two models suggests that there will be variation in the severity of disease progression in different models of zebrafish RP that must be considered when designing methods of finding new treatments.

CHAPTER 7. DISCUSSION

There are no cures for RP, and all current treatment options lack efficacy or feasibility. To identify drugs that could treat RP, the zebrafish was utilized as a model system to perform *in vivo* drug screening. To model RP, the transgenic zebrafish line expressing human Q344X RHO was used due to its rapid rod degeneration. The Q344X RP zebrafish model displayed a deficient light-off VMR when presented with a scotopic light offset at 7dpf. To confirm the deficient zebrafish behavior was due to rod degeneration, rods expressing *nitroreductase* (rho:NTR) were chemically ablated with metronidazole, and the scotopic light-off VMR was tested. As with the Q344X line, the rod-ablated rho:NTR line also displayed a deficient scotopic light-off VMR. This result indicates that rod photoreceptors are functional and contributing to visual behavior as early as 7dpf in the zebrafish. Moreover, the deficient Q344X scotopic light-off VMR can be utilized to test RP therapies that should improve the behavior. The Q344X scotopic light-off VMR was leveraged to screen drug libraries to identify compounds that improved the Q344X behavior. These drugs can potentially then be translated to human patients. The β -blocker carvedilol was identified as a positive hit from the ENZO REDOX library that improved the Q344X scotopic light-off VMR. This improvement was correlated with an increase in rod number in the Q344X zebrafish retina at 6dpf and 7dpf. This result suggests that the increased number of rods is improving the visual perception of the Q344X zebrafish. However, it is not known what the minimum number of rods is required to impart visual information. The source of the increased rod number was investigated with TUNEL and *in situ* hybridization staining. There was no change in the number of TUNEL-positive cells with carvedilol treatment, and the rod progenitor *nr2e3* staining was only seen in the peripheral retina and a thin strip on the ventral patch. The lack in change of the TUNEL-positive cells may be due to the rapid progression of apoptosis and thin cryosections (Mitchell, Lovel and Lambert, 2019). Since *nr2e3* staining is only present and increased in the proliferative zones of the retina with carvedilol treatment, it is likely that carvedilol is not inducing new rod generation. Thus, the most likely source of the increased rod number from carvedilol treatment is through preventing rod degeneration.

Few studies are available that provide information regarding adrenergic signaling in the retina. One of carvedilol's target receptors, the β -1 adrenergic receptor, is expressed in mouse rods (Siebert *et al.*, 2012); however, it is not known if β -blockers are able to work directly on rods. To

determine if carvedilol is capable of working directly on rods, the rod-like human Y79 retinoblastoma line was utilized to test carvedilol *in vitro*. These cells were transfected with a cAMP-sensitive luciferase that becomes brighter in the presence of increased cAMP levels. To determine if the adrenergic signaling pathway is intact in this cell line, the epinephrine analog isoproterenol was applied to the cells in a dose-dependent manner. Isoproterenol is a strong β -adrenergic receptor agonist which stimulates the production of cAMP through G α -mediated activation of ADCY. Isoproterenol treatment increased cAMP levels in the Y79 cell line which indicates that the rod-like cells express functional β -adrenergic receptors. To determine if carvedilol can inhibit this isoproterenol-mediated G protein signaling, the Y79 cells were pre-treated with carvedilol and then challenged with a single concentration of isoproterenol. Carvedilol was able to inhibit the increased levels of cAMP in a dose-dependent manner. These results suggest that β -adrenergic signaling is present and functional in rod photoreceptors, and this signaling pathway may serve as a target for carvedilol to treat RP.

This work with carvedilol suggests that targeting GPCR signaling through adrenergic receptors is an attractive method for the treating Q344X RP. While the full disease mechanism is unknown, it is believed that mislocalized activation of rhodopsin in the inner segment of Q344X rods induces ADCY activation resulting in cAMP increase and apoptosis (Portera-Cailliau *et al.*, 1994; Sung *et al.*, 1994; Concepcion and Chen, 2010; Nakao *et al.*, 2012). This highlights ADCY as a potential drug target. Previous work with the Q344X zebrafish, as well as the Stargardt Disease mouse, has shown that inhibition of ADCY with the inhibitor SQ22536 improved photoreceptor survival (Nakao *et al.*, 2012; Chen *et al.*, 2013). However, Q344X larvae did not display an improved VMR with SQ22536 treatment. This may be due to unintended effects of globally treating the entire zebrafish larvae with an ADCY inhibitor that affected the VMR. Future work with ADCY as a target may require a drug with more specificity to see beneficial effects in the Q344X RP model.

Carvedilol is effective in improving light sensation and rod number in the Q344X retina, yet despite being able to work directly on rods, the molecular mechanism of carvedilol in respect to Q344X RHO signaling remains unknown. In addition to having antioxidant activity, carvedilol has several known modes of action. It is primarily classified as a β -blocker; however, it has also been demonstrated to act as an α 1-blocker, a calcium channel agonist at high concentration, and a free radical scavenger (Giannattasio *et al.*, 1992; McTavish, Campoli-Richards and Sorkin, 1993).

Carvedilol may mediate its visual benefit through some of these pathways. Traditionally, β -blockers are seen only as β -antagonists that prevent epinephrine from binding β -adrenergic receptors. Epinephrine is present in the mouse subretinal space and increases with light exposure (Hadjiconstantinou, Cohen and Neff, 1983). Blocking epinephrine signaling can potentially lower cAMP levels in the Q344X rods by preventing endogenous ADCY signaling. Interestingly, carvedilol also acts as an atypical β -blocker which is capable of inducing biased signaling (Wisler *et al.*, 2007). Specifically, carvedilol can promote β -arrestin signaling while acting as an inverse agonist towards G protein signaling (Wang *et al.*, 2017). This type of β -arrestin signaling has been shown to have anti-apoptotic effects (DeFea *et al.*, 2000; Povsic, Kohout and Lefkowitz, 2003; Ahn *et al.*, 2009) that may prevent Q344X rod death. Carvedilol-mediated β -arrestin signaling can induce downstream effects such as epidermal growth factor receptor (EGFR) transactivation that may confer therapeutic properties (Noma *et al.*, 2007; Kim *et al.*, 2008). β -arrestin is capable of inducing signaling as an adaptor protein through pathways such as mitogen-activated protein kinase (MAPK), protein kinase B (AKT), and the tyrosine kinase SRC (Revankar *et al.*, 2004; Rajagopal, Rajagopal and Lefkowitz, 2010). Carvedilol may also exert protective effects on Q344X rods through α 1 blockade since selectively blocking Gs-coupled α 1-adrenergic receptors can prevent photoreceptor degeneration in a Stargardt Disease model (Chen *et al.*, 2013, 2016). Endogenous agonism of α 1-adrenergic receptors are capable of inducing phospholipase C-mediated (PLC) apoptosis (Gilman, 1987; Chen *et al.*, 2013). Carvedilol's α -blocking ability may prevent PLC-mediated apoptosis of rod cells. It is unlikely that carvedilol is acting as a calcium channel blocker since it would likely stop the larval zebrafish heart beating and kill the larva before its VMR could be measured (Stainier, 2001; Chopra *et al.*, 2010). Since no other hits were identified from this REDOX library, carvedilol probably did not exert its visual benefit on the Q344X model as a radical-scavenging antioxidant. The potential mechanisms of action that carvedilol may be eliciting in the retina are diagrammed in Figure 18.

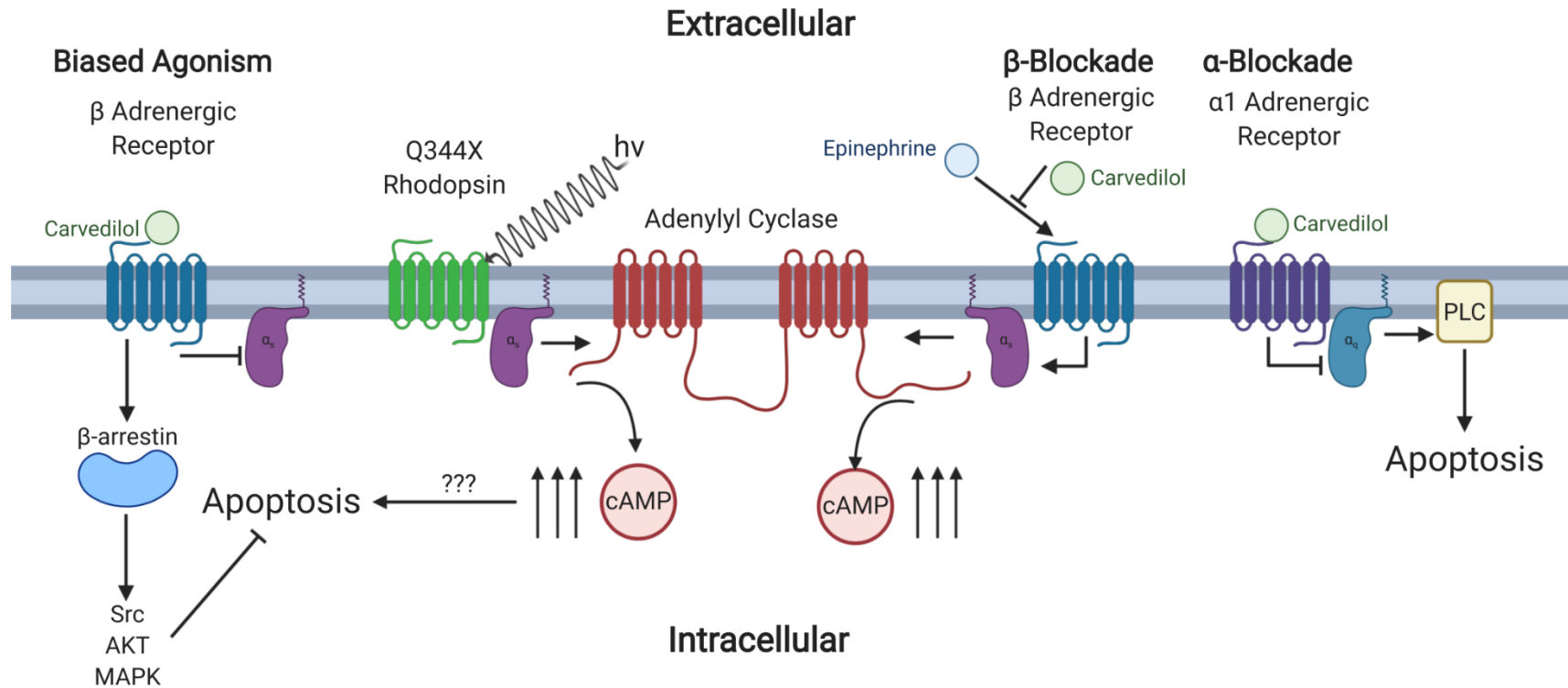


Figure 18. Potential Mechanisms of Action of Carvedilol in the Retina

There are more than one potential mechanisms of action that carvedilol may elicit beneficial effects in the Q344X retina (listed in bold). Aberrant activation of Q344X RHO activates adenylyl cyclase through $G\alpha$ signaling leading to a drastic increase in cAMP. Since carvedilol acts as a biased agonist for β -arrestin signaling, and as an inverse agonist for G protein signaling, this signaling pathway may be taking place in the retina. β -arrestin is capable of inducing signaling through SRC, AKT, and MAPK pathways which have been shown to be capable of anti-apoptotic signaling. Carvedilol is a β -blocker and capable of inhibiting endogenous epinephrine binding. Since there is epinephrine present in the subretinal space, carvedilol may inhibit any endogenous signaling and suppress native $G\alpha$ activation. This could potentially lower cAMP levels in the rods. Carvedilol also acts as an α_1 -blocker and blocking endogenous agonist signaling may prevent apoptosis through PLC signaling.

More evidence is available which suggests that β -blockers may be able to treat RP. A recent study has identified that another β -blocker, metipranolol, is capable improving rod survival and electroretinogram in the *rd10* mouse (Kanan *et al.*, 2019). Another study has found that the β -blocker metoprolol can provide protection against bright light-induced retinal degeneration, and metoprolol protection can be increased by co-treatment with other GPCR agonists and antagonists (Chen *et al.*, 2016). However, the mechanism by which these β -blockers are conferring protective effects is not known. Like carvedilol, metoprolol exhibits biased agonism which may play a role in its protective effects in the retina similar to carvedilol (Nakaya *et al.*, 2012). Metipranolol (also Optipranolol) is currently used for treating glaucoma indicating that the drug targets are expressed in the eye. Carvedilol has already been shown to have beneficial effects with treating other eye-disease models. Carvedilol can lower intraocular pressure (IOP) in the eye of rabbits (Nakaya *et al.*, 2012). Also, carvedilol has neuroprotective effects on retinal ganglion cells in an optic nerve injury mouse model (Liu and Liu, 2019). These studies support the likelihood that carvedilol can be effectively repurposed to treat RP.

In this dissertation, the first evidence that visual behavior in larval zebrafish can be altered due to rod degeneration has been discovered utilizing a scotopic VMR assay. This deficit in the scotopic light-off VMR of the Q344X RP model was leveraged to perform the first drug screen to identify drugs that can potentially treat RP. This first drug screen revealed that the FDA-approved drug carvedilol improves the rod number and light sensation in the Q344X RP model. Carvedilol is a unique β -blocker that can induce biased β -adrenergic signaling as well as α 1-blocking. The drug has already proven efficacious in other models of eye disease. As an FDA-approved drug, it can be repurposed relatively easily by physicians to treat patients suffering from RP. Given the success of utilizing the scotopic light-off VMR assay with the Q344X RP model, the assay and model were employed to scale-up the drug screen to encompass a library of over 1,400 FDA-approved drugs to identify more drugs that can be quickly repurposed. The first-pass screen of this library has identified more than 200 drugs that may be able to treat RP. Additionally, the scotopic light-off VMR assay has proven to be useful in identifying a deficit in this behavior in the P23H zebrafish RP model. Taken together, the results of this work have laid the foundation for effective phenotypic drug screening with zebrafish models of RP that can identify the first drug treatments that can treat RP patients.

REFERENCES

- Ahn, S., Kim, J., Hara, M. R., Ren, X.-R., & Lefkowitz, R. J. (2009). β -Arrestin-2 Mediates Anti-apoptotic Signaling through Regulation of BAD Phosphorylation. *Journal of Biological Chemistry*, 284(13), 8855–8865. <https://doi.org/10.1074/jbc.M808463200>
- Ahuja, A. K., Dorn, J. D., Caspi, A., McMahon, M. J., Dagnelie, G., daCruz, L., Stanga, P., Humayun, M. S., Greenberg, R. J., & Argus II Study Group. (2011). Blind subjects implanted with the Argus II retinal prosthesis are able to improve performance in a spatial-motor task. *British Journal of Ophthalmology*, 95(4), 539–543. <https://doi.org/10.1136/bjo.2010.179622>
- Alfinito, P. D., & Townes-Anderson, E. (2002). Activation of mislocalized opsin kills rod cells: A novel mechanism for rod cell death in retinal disease. *Proceedings of the National Academy of Sciences*, 99(8), 5655–5660. <https://doi.org/10.1073/pnas.072557799>
- Ali, S., Champagne, D. L., & Richardson, M. K. (2012). Behavioral profiling of zebrafish embryos exposed to a panel of 60 water-soluble compounds. *Behavioural Brain Research*, 228(2), 272–283. <https://doi.org/10.1016/j.bbr.2011.11.020>
- An, W. F., & Tolliday, N. (2010). Cell-Based Assays for High-Throughput Screening. *Molecular Biotechnology*, 45(2), 180–186. <https://doi.org/10.1007/s12033-010-9251-z>
- Anasagasti, A., Irigoyen, C., Barandika, O., López de Munain, A., & Ruiz-Ederra, J. (2012). Current mutation discovery approaches in Retinitis Pigmentosa. *Vision Research*, 75, 117–129. <https://doi.org/10.1016/j.visres.2012.09.012>
- Angueyra, J. M., & Kindt, K. S. (2018). Leveraging zebrafish to study retinal degenerations. In *Frontiers in Cell and Developmental Biology*. <https://doi.org/10.3389/fcell.2018.00110>
- Athanasiou, D., Aguila, M., Bellingham, J., Li, W., McCulley, C., Reeves, P. J., & Cheetham, M. E. (2018). The molecular and cellular basis of rhodopsin retinitis pigmentosa reveals potential strategies for therapy. *Progress in Retinal and Eye Research*, 62, 1–23. <https://doi.org/10.1016/j.preteyeres.2017.10.002>
- Athanasiou, D., Kosmaoglou, M., Kanuga, N., Novoselov, S. S., Paton, A. W., Paton, J. C., Chapple, J. P., & Cheetham, M. E. (2012). BiP prevents rod opsin aggregation. *Molecular Biology of the Cell*. <https://doi.org/10.1091/mbc.E12-02-0168>
- Barber, A. C., Hippert, C., Duran, Y., West, E. L., Bainbridge, J. W. B., Warre-Cornish, K., Luhmann, U. F. O., Lakowski, J., Sowden, J. C., Ali, R. R., & Pearson, R. A. (2013). Repair

- of the degenerate retina by photoreceptor transplantation. *Proceedings of the National Academy of Sciences of the United States of America*, 110(1), 354–359. <https://doi.org/10.1073/pnas.1212677110>
- Baxendale, S., Holdsworth, C. J., Meza Santoscoy, P. L., Harrison, M. R. M., Fox, J., Parkin, C. A., Ingham, P. W., & Cunliffe, V. T. (2012). Identification of compounds with anti-convulsant properties in a zebrafish model of epileptic seizures. *Disease Models & Mechanisms*, 5(6), 773–784. <https://doi.org/10.1242/dmm.010090>
- Beatty, S., Koh, H., Phil, M., Henson, D., & Boulton, M. (n.d.). The role of oxidative stress in the pathogenesis of age-related macular degeneration. *Survey of Ophthalmology*, 45(2), 115–134. <http://www.ncbi.nlm.nih.gov/pubmed/11033038>
- Beker van Woudenberg, A., Wolterbeek, A., te Brake, L., Snel, C., Menke, A., Rubingh, C., de Groot, D., & Kroese, D. (2013). A category approach to predicting the developmental (neuro) toxicity of organotin compounds: The value of the zebrafish (*Danio rerio*) embryotoxicity test (ZET). *Reproductive Toxicology*, 41, 35–44. <https://doi.org/10.1016/j.reprotox.2013.06.067>
- Bibliowicz, J., Tittle, R. K., & Gross, J. M. (2011). Toward a better understanding of human eye disease insights from the zebrafish, *Danio rerio*. In *Progress in molecular biology and translational science* (Vol. 100, pp. 287–330). NIH Public Access. <https://doi.org/10.1016/B978-0-12-384878-9.00007-8>
- Bill, A., Sperber, G., & Ujiie, K. (1983). Physiology of the choroidal vascular bed. *International Ophthalmology*. <https://doi.org/10.1007/BF00127638>
- Bilotta, J. (2000). Effects of abnormal lighting on the development of zebrafish visual behavior. *Behavioural Brain Research*, 116(1), 81–87. <http://www.ncbi.nlm.nih.gov/pubmed/11090887>
- Bilotta, Joseph, Saszik, S., & Sutherland, S. E. (2001). Rod contributions to the electroretinogram of the dark-adapted developing zebrafish. *Developmental Dynamics*, 222(4), 564–570. <https://doi.org/10.1002/dvdy.1188>
- Brockerhoff, S E. (2006). Measuring the optokinetic response of zebrafish larvae. *Nature Protocols*, 1(5), 2448–2451. <https://doi.org/10.1038/nprot.2006.255>
- Brockerhoff, S E, Hurley, J. B., Janssen-Bienhold, U., Neuhauss, S. C., Driever, W., & Dowling, J. E. (1995). A behavioral screen for isolating zebrafish mutants with visual system defects. *Proceedings of the National Academy of Sciences of the United States of America*, 92(23),

- 10545–10549. <http://www.ncbi.nlm.nih.gov/pubmed/7479837>
- Brockerhoff, S E, Hurley, J. B., Niemi, G. A., & Dowling, J. E. (1997). A new form of inherited red-blindness identified in zebrafish. *The Journal of Neuroscience : The Official Journal of the Society for Neuroscience*, 17(11), 4236–4242. <http://www.ncbi.nlm.nih.gov/pubmed/9151740>
- Brockerhoff, Susan E, & Fadool, J. M. (2011). Genetics of photoreceptor degeneration and regeneration in zebrafish. *Cellular and Molecular Life Sciences*, 68(4), 651–659. <https://doi.org/10.1007/s00018-010-0563-8>
- Bruni, G., Rennekamp, A. J., Velenich, A., McCarroll, M., Gendele, L., Fertsch, E., Taylor, J., Lakhani, P., Lensen, D., Evron, T., Lorello, P. J., Huang, X.-P., Kolczewski, S., Carey, G., Caldarone, B. J., Prinssen, E., Roth, B. L., Keiser, M. J., Peterson, R. T., & Kokel, D. (2016). Zebrafish behavioral profiling identifies multitarget antipsychotic-like compounds. *Nature Chemical Biology*, 12(7), 559–566. <https://doi.org/10.1038/nchembio.2097>
- Burnight, E. R., Gupta, M., Wiley, L. A., Anfinson, K. R., Tran, A., Triboulet, R., Hoffmann, J. M., Klaahsen, D. L., Andorf, J. L., Jiao, C., Sohn, E. H., Adur, M. K., Ross, J. W., Mullins, R. F., Daley, G. Q., Schlaeger, T. M., Stone, E. M., & Tucker, B. A. (2017). Using CRISPR-Cas9 to Generate Gene-Corrected Autologous iPSCs for the Treatment of Inherited Retinal Degeneration. *Molecular Therapy*. <https://doi.org/10.1016/j.ymthe.2017.05.015>
- Cachafeiro, M., Bemelmans, A. P., Canola, K., Pignat, V., Crippa, S. V., Kostic, C., & Arsenijevic, Y. (2010). Remaining rod activity mediates visual behavior in adult rpe65 ^{-/-} mice. *Investigative Ophthalmology and Visual Science*. <https://doi.org/10.1167/iovs.09-3870>
- Cameron, D. A., & Carney, L. H. (2000). Cell mosaic patterns in the native and regenerated inner retina of zebrafish: implications for retinal assembly. *The Journal of Comparative Neurology*, 416(3), 356–367. <http://www.ncbi.nlm.nih.gov/pubmed/10602094>
- Chadderton, N., Millington-Ward, S., Palfi, A., O'Reilly, M., Tuohy, G., Humphries, M. M., Li, T., Humphries, P., Kenna, P. F., & Farrar, G. J. (2009). Improved Retinal Function in a Mouse Model of Dominant Retinitis Pigmentosa Following AAV-delivered Gene Therapy. *Molecular Therapy*, 17(4), 593–599. <https://doi.org/10.1038/mt.2008.301>
- Chang, J., Zheng, C., Zhou, W. X., & Zhou, W. X. (2017). Simulation-based hypothesis testing of high dimensional means under covariance heterogeneity. *Biometrics*. <https://doi.org/10.1111/biom.12695>

- Chen, Y., Palczewska, G., Masuho, I., Gao, S., Jin, H., Dong, Z., Gieser, L., Brooks, M. J., Kiser, P. D., Kern, T. S., Martemyanov, K. A., Swaroop, A., & Palczewski, K. (2016). Synergistically acting agonists and antagonists of G protein-coupled receptors prevent photoreceptor cell degeneration. *Science Signaling*, 9(438), ra74--ra74. <https://doi.org/10.1126/scisignal.aag0245>
- Chen, Y., Palczewska, G., Mustafi, D., Golczak, M., Dong, Z., Sawada, O., Maeda, T., Maeda, A., & Palczewski, K. (2013). Systems pharmacology identifies drug targets for Stargardt disease-associated retinal degeneration. *Journal of Clinical Investigation*, 123(12), 5119–5134. <https://doi.org/10.1172/JCI69076>
- Chhetri, J., Jacobson, G., & Gueven, N. (2014). Zebrafish—on the move towards ophthalmological research. *Eye*, 28(4), 367–380. <https://doi.org/10.1038/eye.2014.19>
- Chopra, S. S., Stroud, D. M., Watanabe, H., Bennett, J. S., Burns, C. G., Wells, K. S., Yang, T., Zhong, T. P., & Roden, D. M. (2010). Voltage-gated sodium channels are required for heart development in zebrafish. *Circulation Research*, 106(8), 1342–1350. <https://doi.org/10.1161/CIRCRESAHA.109.213132>
- Chuang, J.-Z., Vega, C., Jun, W., & Sung, C.-H. (2004). Structural and functional impairment of endocytic pathways by retinitis pigmentosa mutant rhodopsin-arrestin complexes. *Journal of Clinical Investigation*. <https://doi.org/10.1172/jci21136>
- Chucair, A. J., Rotstein, N. P., SanGiovanni, J. P., During, A., Chew, E. Y., & Politi, L. E. (2007). Lutein and Zeaxanthin Protect Photoreceptors from Apoptosis Induced by Oxidative Stress: Relation with Docosahexaenoic Acid. *Investigative Ophthalmology & Visual Science*, 48(11), 5168–5177. <https://doi.org/10.1167/iovs.07-0037>
- Colwill, R. M., & Creton, R. (2011). Locomotor behaviors in zebrafish (*Danio rerio*) larvae. *Behavioural Processes*, 86(2), 222–229. <https://doi.org/10.1016/j.beproc.2010.12.003>
- Concepcion, F., & Chen, J. (2010). Q344ter Mutation Causes Mislocalization of Rhodopsin Molecules That Are Catalytically Active: A Mouse Model of Q344ter-Induced Retinal Degeneration. *PLoS ONE*, 5(6), e10904. <https://doi.org/10.1371/journal.pone.0010904>
- Cottet, S., & Schorderet, D. (2009). Mechanisms of Apoptosis in Retinitis Pigmentosa. *Current Molecular Medicine*. <https://doi.org/10.2174/156652409787847155>
- Curran, J. (2018). *Hotelling: Hotelling's T² Test and Variants*.
- Daiger, S P, Sullivan, L. S., & Bowne, S. J. (2013). Genes and mutations causing retinitis

- pigmentosa. *Clinical Genetics*, 84(2), 132–141. <https://doi.org/10.1111/cge.12203>
- Daiger, Stephen P., Bowne, S. J., & Sullivan, L. S. (2007). Perspective on genes and mutations causing retinitis pigmentosa. In *Archives of Ophthalmology*. <https://doi.org/10.1001/archophth.125.2.151>
- Daiger, Stephen P., Bowne, S. J., & Sullivan, L. S. (2014). Genes and Mutations Causing Autosomal Dominant Retinitis Pigmentosa. *Cold Spring Harbor Perspectives in Medicine*, 5(10). <https://doi.org/10.1101/cshperspect.a017129>
- DAVSON, H. (1973). The Physiology of the Eye. *Optometry and Vision Science*. <https://doi.org/10.1097/00006324-197306000-00014>
- de Esch, C., van der Linde, H., Slieker, R., Willemsen, R., Wolterbeek, A., Woutersen, R., & De Groot, D. (2012). Locomotor activity assay in zebrafish larvae: Influence of age, strain and ethanol. *Neurotoxicology and Teratology*, 34(4), 425–433. <https://doi.org/10.1016/j.ntt.2012.03.002>
- Deeti, S., O'Farrell, S., & Kennedy, B. N. (2014). Early safety assessment of human oculotoxic drugs using the zebrafish visualmotor response. *Journal of Pharmacological and Toxicological Methods*, 69(1), 1–8. <https://doi.org/10.1016/j.vascn.2013.09.002>
- DeFea, K. A., Zalevsky, J., Thoma, M. S., Déry, O., Mullins, R. D., & Bunnett, N. W. (2000). beta-arrestin-dependent endocytosis of proteinase-activated receptor 2 is required for intracellular targeting of activated ERK1/2. *The Journal of Cell Biology*, 148(6), 1267–1281. <https://doi.org/10.1083/jcb.148.6.1267>
- Deretic, D., Williams, A. H., Ransom, N., Morel, V., Hargrave, P. A., & Arendt, A. (2005). Rhodopsin C terminus, the site of mutations causing retinal disease, regulates trafficking by binding to ADP-ribosylation factor 4 (ARF4). *Proceedings of the National Academy of Sciences of the United States of America*. <https://doi.org/10.1073/pnas.0500095102>
- Di Polo, A., & Farber, D. B. (1995). Rod photoreceptor-specific gene expression in human retinoblastoma cells. *Proceedings of the National Academy of Sciences*, 92(9), 4016–4020. <https://doi.org/10.1073/pnas.92.9.4016>
- Dinday, M. T., & Baraban, S. C. (2015). Large-Scale Phenotype-Based Antiepileptic Drug Screening in a Zebrafish Model of Dravet Syndrome. *ENeuro*, 2(4). <https://doi.org/10.1523/ENEURO.0068-15.2015>
- Drews, J. (2000). Drug discovery: a historical perspective. *Science (New York, N.Y.)*, 287(5460),

- 1960–1964. <http://www.ncbi.nlm.nih.gov/pubmed/10720314>
- Duncan, J. L., Richards, T. P., Arditi, A., da Cruz, L., Dagnelie, G., Dorn, J. D., Ho, A. C., Olmos de Koo, L. C., Barale, P.-O., Stanga, P. E., Thumann, G., Wang, Y., & Greenberg, R. J. (2016). Improvements in vision-related quality of life in blind patients implanted with the Argus II Epiretinal Prosthesis. *Clinical and Experimental Optometry, In press*(2), 144–150. <https://doi.org/10.1111/cxo.12444>
- Easter, S S, & Nicola, G. N. (1997). The development of eye movements in the zebrafish (*Danio rerio*). *Developmental Psychobiology*, 31(4), 267–276. <http://www.ncbi.nlm.nih.gov/pubmed/9413674>
- Easter, Stephen S, & Gregory Nicola, J. N. (1997). The Development of Eye Movements in the Zebrafish (*Danio rerio*). *Dev Psychobiol*, 31, 267–276.
- Emran, F, Rihel, J., Adolph, A. R., & Dowling, J. E. (2010). Zebrafish larvae lose vision at night. *Proceedings of the National Academy of Sciences*, 107(13), 6034–6039. <https://doi.org/10.1073/pnas.0914718107>
- Emran, Farida, Rihel, J., Adolph, A. R., Wong, K. Y., Kraves, S., & Dowling, J. E. (2007). OFF ganglion cells cannot drive the optokinetic reflex in zebrafish. *Proceedings of the National Academy of Sciences of the United States of America*, 104(48), 19126–19131. <https://doi.org/10.1073/pnas.0709337104>
- Emran, Farida, Rihel, J., & Dowling, J. E. (2008). A Behavioral Assay to Measure Responsiveness of Zebrafish to Changes in Light Intensities. *Journal of Visualized Experiments*, 20, e923. <https://doi.org/10.3791/923>
- Fadool, J. M. (2003). Development of a rod photoreceptor mosaic revealed in transgenic zebrafish. *Developmental Biology*, 258(2), 277–290. <http://www.ncbi.nlm.nih.gov/pubmed/12798288>
- Fahim, A. T., Daiger, S. P., & Weleber, R. G. (1993). Nonsyndromic Retinitis Pigmentosa Overview. In *GeneReviews®*. University of Washington, Seattle. <http://www.ncbi.nlm.nih.gov/pubmed/20301590>
- Fernandes, A. M., Fero, K., Arrenberg, A. B., Bergeron, S. A., Driever, W., & Burgess, H. A. (2012). Deep Brain Photoreceptors Control Light-Seeking Behavior in Zebrafish Larvae. *Current Biology*, 22(21), 2042–2047. <https://doi.org/10.1016/j.cub.2012.08.016>
- Frick, K. D., Roebuck, M. C., Feldstein, J. I., McCarty, C. A., & Grover, L. L. (2012). Health Services Utilization and Cost of Retinitis Pigmentosa. *Archives of Ophthalmology*, 130(5),

- 629–634. <https://doi.org/10.1001/archophthalmol.2011.2820>
- Gallardo, V. E., Varshney, G. K., Lee, M., Bupp, S., Xu, L., Shinn, P., Crawford, N. P., Inglese, J., & Burgess, S. M. (2015). Phenotype-driven chemical screening in zebrafish for compounds that inhibit collective cell migration identifies multiple pathways potentially involved in metastatic invasion. *Disease Models & Mechanisms*, 8(6), 565–576. <https://doi.org/10.1242/dmm.018689>
- Ganzen, L., Venkatraman, P., Pang, C. P., Leung, Y. F., & Zhang, M. (2017). Utilizing Zebrafish Visual Behaviors in Drug Screening for Retinal Degeneration. *International Journal of Molecular Sciences*, 18(6). <https://doi.org/10.3390/ijms18061185>
- Gao, Y., Chan, R. H. M., Chow, T. W. S., Zhang, L., Bonilla, S., Pang, C.-P., Zhang, M., & Leung, Y. F. (2014). A High-Throughput Zebrafish Screening Method for Visual Mutants by Light-Induced Locomotor Response. *IEEE/ACM Transactions on Computational Biology and Bioinformatics*, 11(4), 693–701. <https://doi.org/10.1109/TCBB.2014.2306829>
- Gao, Y., Zhang, G., Jelfs, B., Carmer, R., Venkatraman, P., Ghadami, M., Brown, S. A., Pang, C. P., Leung, Y. F., Chan, R. H. M., & Zhang, M. (2016). Computational classification of different wild-type zebrafish strains based on their variation in light-induced locomotor response. *Computers in Biology and Medicine*, 69, 1–9. <https://doi.org/10.1016/j.compbiomed.2015.11.012>
- Giannattasio, C., Cattaneo, B. M., Seravalle, G., Carugo, S., Mangoni, A. A., Grassi, G., Zanchetti, A., & Mancina, G. (1992). α 1-Blocking Properties of Carvedilol During Acute and Chronic Administration. *Journal of Cardiovascular Pharmacology*, 19(Supplement 1), S18–S22. <https://doi.org/10.1097/00005344-199219001-00005>
- Gilman, A. (1987). G Proteins: Transducers Of Receptor-Generated Signals. *Annual Review of Biochemistry*. <https://doi.org/10.1146/annurev.biochem.56.1.615>
- Gower, A. J., Noyer, M., Verloes, R., Gobert, J., & Wülfert, E. (1992). ucb L059, a novel anti-convulsant drug: pharmacological profile in animals. *European Journal of Pharmacology*, 222(2–3), 193–203. <http://www.ncbi.nlm.nih.gov/pubmed/1451732>
- Gross, J. M., & Perkins, B. D. (2008). Zebrafish mutants as models for congenital ocular disorders in humans. *Molecular Reproduction and Development*, 75(3), 547–555. <https://doi.org/10.1002/mrd.20831>
- Hadjiconstantinou, M., Cohen, J., & Neff, N. H. (1983). Epinephrine: A Potential Neurotransmitter

- in Retina. *Journal of Neurochemistry*, 41(5), 1440–1444. <https://doi.org/10.1111/j.1471-4159.1983.tb00843.x>
- Hamaoka, T., Takechi, M., Chinen, A., Nishiwaki, Y., & Kawamura, S. (2002). Visualization of rod photoreceptor development using GFP-transgenic zebrafish. *Genesis*, 34(3), 215–220. <https://doi.org/10.1002/gene.10155>
- Hamel, C. (2006). Retinitis pigmentosa. *Orphanet Journal of Rare Diseases*, 1(1), 40. <https://doi.org/10.1186/1750-1172-1-40>
- Hartmann, S., Vogt, R., Kunze, J., Rauschert, A., Kuhnert, K. D., Wanzenböck, J., Lamatsch, D. K., & Witte, K. (2018). Zebrafish larvae show negative phototaxis to near-infrared light. *PLoS ONE*. <https://doi.org/10.1371/journal.pone.0207264>
- Hartong, D. T., Berson, E. L., & Dryja, T. P. (2006). Retinitis pigmentosa. *The Lancet*, 368(9549), 1795–1809. [https://doi.org/10.1016/S0140-6736\(06\)69740-7](https://doi.org/10.1016/S0140-6736(06)69740-7)
- Ho, A. C., Humayun, M. S., Dorn, J. D., da Cruz, L., Dagnelie, G., Handa, J., Barale, P.-O., Sahel, J.-A., Stanga, P. E., Hafezi, F., Safran, A. B., Salzmann, J., Santos, A., Birch, D., Spencer, R., Cideciyan, A. V., de Juan, E., Duncan, J. L., Elliott, D., ... Argus II Study Group. (2015). Long-Term Results from an Epiretinal Prosthesis to Restore Sight to the Blind. *Ophthalmology*, 122(8), 1547–1554. <https://doi.org/10.1016/j.opthta.2015.04.032>
- Hotelling, H. (1931). The Generalization of Student's Ratio. *The Annals of Mathematical Statistics*. <https://doi.org/10.1214/aoms/1177732979>
- Huang, Y.-Y., & Neuhauss, S. C. F. (2008). The optokinetic response in zebrafish and its applications. *Frontiers in Bioscience: A Journal and Virtual Library*, 13, 1899–1916. <http://www.ncbi.nlm.nih.gov/pubmed/17981678>
- Hughes, J. P., Rees, S., Kalindjian, S. B., & Philpott, K. L. (2011). Principles of early drug discovery. *British Journal of Pharmacology*, 162(6), 1239–1249. <https://doi.org/10.1111/j.1476-5381.2010.01127.x>
- Ingebretson, J. J., & Masino, M. A. (2013). Quantification of locomotor activity in larval zebrafish: considerations for the design of high-throughput behavioral studies. *Frontiers in Neural Circuits*, 7, 109. <https://doi.org/10.3389/fncir.2013.00109>
- Jacobson, S. G., Kemp, C. M., Sung, C. H., & Nathans, J. (1991). Retinal function and rhodopsin levels in autosomal dominant retinitis pigmentosa with rhodopsin mutations. *American Journal of Ophthalmology*, 112(3), 256–271. [https://doi.org/10.1016/s0002-9394\(14\)76726-](https://doi.org/10.1016/s0002-9394(14)76726-)

- Jin, S., Sarkar, K. S., Jin, Y. N., Liu, Y., Kokel, D., Van Ham, T. J., Roberts, L. D., Gerszten, R. E., MacRae, C. A., & Peterson, R. T. (2013). An In Vivo Zebrafish Screen Identifies Organophosphate Antidotes with Diverse Mechanisms of Action. *Journal of Biomolecular Screening*, 18(1), 108–115. <https://doi.org/10.1177/1087057112458153>
- Jonas, J. B., Schneider, U., & Naumann, G. O. (1992). Count and density of human retinal photoreceptors. *Graefe's Archive for Clinical and Experimental Ophthalmology = Albrecht von Graefes Archiv Fur Klinische Und Experimentelle Ophthalmologie*, 230(6), 505–510. <http://www.ncbi.nlm.nih.gov/pubmed/1427131>
- Kanan, Y., Khan, M., Lorenc, V. E., Long, D., Chadha, R., Sciamanna, J., Green, K., & Campochiaro, P. A. (2019). Metipranolol promotes structure and function of retinal photoreceptors in the *rd10* mouse model of human retinitis pigmentosa. *Journal of Neurochemistry*, 148(2), 307–318. <https://doi.org/10.1111/jnc.14613>
- Kasibhatla, S., Gourdeau, H., Meerovitch, K., Drewe, J., Reddy, S., Qiu, L., Zhang, H., Bergeron, F., Bouffard, D., Yang, Q., Herich, J., Lamothe, S., Cai, S. X., & Tseng, B. (2004). Discovery and mechanism of action of a novel series of apoptosis inducers with potential vascular targeting activity. *Molecular Cancer Therapeutics*, 3(11), 1365–1374. <http://www.ncbi.nlm.nih.gov/pubmed/15542775>
- Kim, I.-M., Tilley, D. G., Chen, J., Salazar, N. C., Whalen, E. J., Violin, J. D., & Rockman, H. A. (2008). β -Blockers alprenolol and carvedilol stimulate β -arrestin-mediated EGFR transactivation. *Proceedings of the National Academy of Sciences*, 105(38), 14555–14560. <https://doi.org/10.1073/pnas.0804745105>
- Kobayashi, M., Takezawa, S. I., Hara, K., Yu, R. T., Umesono, Y., Agata, K., Taniwaki, M., Yasuda, K., & Umesono, K. (1999). Identification of a photoreceptor cell-specific nuclear receptor. *Proceedings of the National Academy of Sciences of the United States of America*. <https://doi.org/10.1073/pnas.96.9.4814>
- Kokel, D., Bryan, J., Laggner, C., White, R., Cheung, C. Y. J., Mateus, R., Healey, D., Kim, S., Werdich, A. A., Haggarty, S. J., MacRae, C. A., Shoichet, B., & Peterson, R. T. (2010). Rapid behavior-based identification of neuroactive small molecules in the zebrafish. *Nature Chemical Biology*, 6(3), 231–237. <https://doi.org/10.1038/nchembio.307>
- Kokel, D., Cheung, C. Y. J., Mills, R., Coutinho-Budd, J., Huang, L., Setola, V., Sprague, J., Jin,

- S., Jin, Y. N., Huang, X.-P., Bruni, G., Woolf, C. J., Roth, B. L., Hamblin, M. R., Zylka, M. J., Milan, D. J., & Peterson, R. T. (2013). Photochemical activation of TRPA1 channels in neurons and animals. *Nature Chemical Biology*, 9(4), 257–263. <https://doi.org/10.1038/nchembio.1183>
- Komeima, K, Rogers, B. S., Lu, L., & Campochiaro, P. A. (2006). Antioxidants reduce cone cell death in a model of retinitis pigmentosa. *Proceedings of the National Academy of Sciences*, 103(30), 11300–11305. <https://doi.org/10.1073/pnas.0604056103>
- Komeima, Keiichi, Rogers, B. S., & Campochiaro, P. A. (2007). Antioxidants slow photoreceptor cell death in mouse models of retinitis pigmentosa. *Journal of Cellular Physiology*, 213(3), 809–815. <https://doi.org/10.1002/jcp.21152>
- Kremmer, S., Eckstein, A., Gal, A., Apfelstedt-Sylla, E., Wedemann, H., Rütther, K., & Zrenner, E. (1997). Ocular findings in patients with autosomal dominant retinitis pigmentosa and Cys110Phe, Arg135Gly, and Gln344stop mutations of rhodopsin. *Graefes's Archive for Clinical and Experimental Ophthalmology = Albrecht von Graefes Archiv Fur Klinische Und Experimentelle Ophthalmologie*, 235(9), 575–583. <https://doi.org/10.1007/bf00947087>
- Lange, M., Neuzeret, F., Fabreges, B., Froc, C., Bedu, S., Bally-Cuif, L., & Norton, W. H. J. (2013). Inter-Individual and Inter-Strain Variations in Zebrafish Locomotor Ontogeny. *PLoS ONE*, 8(8), e70172. <https://doi.org/10.1371/journal.pone.0070172>
- Lewis, A., Williams, P., Lawrence, O., Wong, R. O. L., & Brockerhoff, S. E. (2010). Wild-Type Cone Photoreceptors Persist Despite Neighboring Mutant Cone Degeneration. *Journal of Neuroscience*, 30(1), 382–389. <https://doi.org/10.1523/JNEUROSCI.5019-09.2010>
- Li, P., Kleinstiver, B. P., Leon, M. Y., Prew, M. S., Navarro-Gomez, D., Greenwald, S. H., Pierce, E. A., Joung, J. K., & Liu, Q. (2018). Allele-Specific CRISPR-Cas9 Genome Editing of the Single-Base P23H Mutation for Rhodopsin-Associated Dominant Retinitis Pigmentosa. *The CRISPR Journal*. <https://doi.org/10.1089/crispr.2017.0009>
- Li, Xiang, Rhee, D. K., Malhotra, R., Mayeur, C., Hurst, L. A., Ager, E., Shelton, G., Kramer, Y., McCulloh, D., Keefe, D., Bloch, K. D., Bloch, D. B., & Peterson, R. T. (2015). Progesterone receptor membrane component-1 regulates hepcidin biosynthesis. *Journal of Clinical Investigation*, 126(1), 389–401. <https://doi.org/10.1172/JCI83831>
- Li, Xinle, Montgomery, J., Cheng, W., Noh, J. H., Hyde, D. R., & Li, L. (2012). Pineal photoreceptor cells are required for maintaining the circadian rhythms of behavioral visual

- sensitivity in zebrafish. *PLoS ONE*. <https://doi.org/10.1371/journal.pone.0040508>
- Link, B. A., & Collery, R. F. (2015). Zebrafish Models of Retinal Disease. *Annual Review of Vision Science*, 1(1), 125–153. <https://doi.org/10.1146/annurev-vision-082114-035717>
- Liu, B., & Liu, Y.-J. (2019). Carvedilol promotes retinal ganglion cell survival following optic nerve injury via ASK1-p38 MAPK pathway. *CNS & Neurological Disorders - Drug Targets*, 18. <https://doi.org/10.2174/1871527318666191002095456>
- Liu, Y., Asnani, A., Zou, L., Bentley, V. L., Yu, M., Wang, Y., Dellaire, G., Sarkar, K. S., Dai, M., Chen, H. H., Sosnovik, D. E., Shin, J. T., Haber, D. A., Berman, J. N., Chao, W., & Peterson, R. T. (2014). Visnagin protects against doxorubicin-induced cardiomyopathy through modulation of mitochondrial malate dehydrogenase. *Science Translational Medicine*, 6(266), 266ra170. <https://doi.org/10.1126/scitranslmed.3010189>
- Liu, Yiwen, Carmer, R., Zhang, G., Venkatraman, P., Brown, S. A., Pang, C.-P., Zhang, M., Ma, P., & Leung, Y. F. (2015). Statistical Analysis of Zebrafish Locomotor Response. *PLOS ONE*, 10(10), e0139521. <https://doi.org/10.1371/journal.pone.0139521>
- Loosli, F., Staub, W., Finger-Baier, K. C., Ober, E. A., Verkade, H., Wittbrodt, J., & Baier, H. (2003). Loss of eyes in zebrafish caused by mutation of *chokh/rx3*. *EMBO Reports*, 4(9), 894–899. <https://doi.org/10.1038/sj.embor.embor919>
- MacLaren, R. E., Pearson, R. A., MacNeil, A., Douglas, R. H., Salt, T. E., Akimoto, M., Swaroop, A., Sowden, J. C., & Ali, R. R. (2006). Retinal repair by transplantation of photoreceptor precursors. *Nature*, 444(7116), 203–207. <https://doi.org/10.1038/nature05161>
- Maurer, C. M., Schonthaler, H. B., Mueller, K. P., & Neuhauss, S. C. F. (2010). Distinct Retinal Deficits in a Zebrafish Pyruvate Dehydrogenase-Deficient Mutant. *Journal of Neuroscience*, 30(36), 11962–11972. <https://doi.org/10.1523/JNEUROSCI.2848-10.2010>
- McTavish, D., Campoli-Richards, D., & Sorkin, E. M. (1993). Carvedilol. A review of its pharmacodynamic and pharmacokinetic properties, and therapeutic efficacy. *Drugs*, 45(2), 232–258. <https://doi.org/10.2165/00003495-199345020-00006>
- Meier, A., Nelson, R., & Connaughton, V. P. (2018). Color Processing in Zebrafish Retina. *Frontiers in Cellular Neuroscience*, 12, 327. <https://doi.org/10.3389/fncel.2018.00327>
- Michelini, E., Cevenini, L., Mezzanotte, L., Coppa, A., & Roda, A. (2010). Cell-based assays: fuelling drug discovery. *Analytical and Bioanalytical Chemistry*, 398(1), 227–238. <https://doi.org/10.1007/s00216-010-3933-z>

- Mitchell, D., Lovel, A., & Lambert, J. (2019). Rapid macrophage-mediated clearance of apoptosis-fated cells during zebrafish retinal development. *Investigative Ophthalmology & Visual Science*, 60(9).
- Moore, K., & Rees, S. (2001). Cell-Based Versus Isolated Target Screening: How Lucky Do You Feel? *Journal of Biomolecular Screening*, 6(2), 69–74. <https://doi.org/10.1089/108705701750160200>
- Morris, A C, & Fadool, J. M. (2005). Studying rod photoreceptor development in zebrafish. *Physiology & Behavior*, 86(3), 306–313. <https://doi.org/10.1016/j.physbeh.2005.08.020>
- Morris, Ann C., Scholz, T. L., Brockerhoff, S. E., & Fadool, J. M. (2008). Genetic dissection reveals two separate pathways for rod and cone regeneration in the teleost retina. *Developmental Neurobiology*. <https://doi.org/10.1002/dneu.20610>
- Morris, Ann C. (2011). The genetics of ocular disorders: Insights from the zebrafish. *Birth Defects Research Part C: Embryo Today: Reviews*, 93(3), 215–228. <https://doi.org/10.1002/bdrc.20211>
- Moyano, M., Porteros, Á., & Dowling, J. E. (2013). The effects of nicotine on cone and rod b-wave responses in larval zebrafish. *Visual Neuroscience*, 30(04), 141–145. <https://doi.org/10.1017/S0952523813000187>
- Mueller, H., Kassack, M. U., & Wiese, M. (2004). Comparison of the Usefulness of the MTT, ATP, and Calcein Assays to Predict the Potency of Cytotoxic Agents in Various Human Cancer Cell Lines. *Journal of Biomolecular Screening*, 9(6), 506–515. <https://doi.org/10.1177/1087057104265386>
- Muto, A., Orger, M. B., Wehman, A. M., Smear, M. C., Kay, J. N., Page-McCaw, P. S., Gahtan, E., Xiao, T., Nevin, L. M., Gosse, N. J., Staub, W., Finger-Baier, K., & Baier, H. (2005). Forward Genetic Analysis of Visual Behavior in Zebrafish. *PLoS Genetics*, 1(5), e66. <https://doi.org/10.1371/journal.pgen.0010066>
- Nakao, T., Tsujikawa, M., Notomi, S., Ikeda, Y., & Nishida, K. (2012). *The Role of Mislocalized Phototransduction in Photoreceptor Cell Death of Retinitis Pigmentosa*. 7(4), e32472. <https://doi.org/10.1371/journal.pone.0032472>
- Nakaya, M., Chikura, S., Watari, K., Mizuno, N., Mochinaga, K., Mangmool, S., Koyanagi, S., Ohdo, S., Sato, Y., Ide, T., Nishida, M., & Kurose, H. (2012). Induction of Cardiac Fibrosis by β -Blocker in G Protein-independent and G Protein-coupled Receptor Kinase 5/ β -

- Arrestin2-dependent Signaling Pathways. *Journal of Biological Chemistry*, 287(42), 35669–35677. <https://doi.org/10.1074/jbc.M112.357871>
- Nath, A. K., Ryu, J. H., Jin, Y. N., Roberts, L. D., Dejam, A., Gerszten, R. E., & Peterson, R. T. (2016). PTPMT1 Inhibition Lowers Glucose through Succinate Dehydrogenase Phosphorylation. *Cell Reports*, 10(5), 694–701. <https://doi.org/10.1016/j.celrep.2015.01.010>
- Nemet, I., Ropelewski, P., & Imanishi, Y. (2015). Rhodopsin trafficking and mistrafficking: Signals, molecular components, and mechanisms. *Progress in Molecular Biology and Translational Science*. <https://doi.org/10.1016/bs.pmbts.2015.02.007>
- Neuhauss, S. C. F., Biehlmaier, O., Seeliger, M. W., Das, T., Kohler, K., Harris, W. A., & Baier, H. (1999). Genetic disorders of vision revealed by a behavioral screen of 400 essential loci in zebrafish. *Journal of Neuroscience*, 19(19), 8603–8615. <https://doi.org/10.1523/jneurosci.19-19-08603.1999>
- Noldus. (n.d.). Retrieved May 23, 2017, from <http://www.noldus.com>
- Noma, T., Lemaire, A., Naga Prasad, S. V, Barki-Harrington, L., Tilley, D. G., Chen, J., Le Corvoisier, P., Violin, J. D., Wei, H., Lefkowitz, R. J., & Rockman, H. A. (2007). Beta-arrestin-mediated beta1-adrenergic receptor transactivation of the EGFR confers cardioprotection. *The Journal of Clinical Investigation*, 117(9), 2445–2458. <https://doi.org/10.1172/JCI31901>
- Novodvorsky, P., Da Costa, M. M. J., & Chico, T. J. A. (2013). Zebrafish-based small molecule screens for novel cardiovascular drugs. *Drug Discovery Today: Technologies*, 10(1), e109--e114. <https://doi.org/10.1016/j.ddtec.2012.01.005>
- O’Neal, T. B., & Luther, E. E. (2019). Retinitis Pigmentosa. In *StatPearls*. StatPearls Publishing. <http://www.ncbi.nlm.nih.gov/pubmed/30137803>
- O’Reilly, M., Millington-Ward, S., Palfi, A., Chadderton, N., Cronin, T., McNally, N., Humphries, M. M., Humphries, P., Kenna, P. F., & Farrar, G. J. (2008). A transgenic mouse model for gene therapy of rhodopsin-linked Retinitis Pigmentosa. *Vision Research*, 48(3), 386–391. <https://doi.org/10.1016/j.visres.2007.08.014>
- Olsson, J. E., Gordon, J. W., Pawlyk, B. S., Roof, D., Hayes, A., Molday, R. S., Mukai, S., Cowley, G. S., Berson, E. L., & Dryja, T. P. (1992). Transgenic mice with a rhodopsin mutation (Pro23His): A mouse model of autosomal dominant retinitis pigmentosa. *Neuron*. [https://doi.org/10.1016/0896-6273\(92\)90236-7](https://doi.org/10.1016/0896-6273(92)90236-7)

- Orger, M. B., Gahtan, E., Muto, A., Page-McCaw, P., Smear, M. C., & Baier, H. (2004). Behavioral screening assays in zebrafish. *Methods in Cell Biology*, 77, 53–68. <http://www.ncbi.nlm.nih.gov/pubmed/15602905>
- Overington, J. P., Al-Lazikani, B., & Hopkins, A. L. (2006). How many drug targets are there? *Nature Reviews Drug Discovery*. <https://doi.org/10.1038/nrd2199>
- Owens, K. N., Santos, F., Roberts, B., Linbo, T., Coffin, A. B., Knisely, A. J., Simon, J. A., Rubel, E. W., & Raible, D. W. (2008). Identification of genetic and chemical modulators of zebrafish mechanosensory hair cell death. *PLoS Genetics*, 4(2), e1000020. <https://doi.org/10.1371/journal.pgen.1000020>
- Parmeggiani, F., S. Sorrentino, F., Ponzin, D., Barbaro, V., Ferrari, S., & Di Iorio, E. (2011). Retinitis Pigmentosa: Genes and Disease Mechanisms. *Current Genomics*. <https://doi.org/10.2174/138920211795860107>
- Patton, E. E., & Zon, L. I. (2001). The art and design of genetic screens: zebrafish. *Nature Reviews Genetics*, 2(12), 956–966. <https://doi.org/10.1038/35103567>
- Pearson, R A, Barber, A. C., Rizzi, M., Hippert, C., Xue, T., West, E. L., Duran, Y., Smith, A. J., Chuang, J. Z., Azam, S. A., Luhmann, U. F. O., Benucci, A., Sung, C. H., Bainbridge, J. W., Carandini, M., Yau, K.-W., Sowden, J. C., & Ali, R. R. (2012). Restoration of vision after transplantation of photoreceptors. *Nature*, 485(7396), 99–103. <https://doi.org/10.1038/nature10997>
- Pearson, Rachael A. (2014). Advances in repairing the degenerate retina by rod photoreceptor transplantation. *Biotechnology Advances*, 32(2), 485–491. <https://doi.org/10.1016/j.biotechadv.2014.01.001>
- Pellegrini, G., De Luca, M., & Arsenijevic, Y. (2007). Towards therapeutic application of ocular stem cells. *Seminars in Cell & Developmental Biology*, 18(6), 805–818. <https://doi.org/10.1016/j.semcdb.2007.09.011>
- Peterson, R T, Link, B. A., Dowling, J. E., & Schreiber, S. L. (2000). Small molecule developmental screens reveal the logic and timing of vertebrate development. *Proceedings of the National Academy of Sciences of the United States of America*, 97(24), 12965–12969. <https://doi.org/10.1073/pnas.97.24.12965>
- Peterson, Randall T, Shaw, S. Y., Peterson, T. A., Milan, D. J., Zhong, T. P., Schreiber, S. L., MacRae, C. A., & Fishman, M. C. (2004). Chemical suppression of a genetic mutation in a

- zebrafish model of aortic coarctation. *Nature Biotechnology*, 22(5), 595–599. <https://doi.org/10.1038/nbt963>
- Portera-Cailliau, C., Sung, C. H., Nathans, J., & Adler, R. (1994). Apoptotic photoreceptor cell death in mouse models of retinitis pigmentosa. *Proceedings of the National Academy of Sciences of the United States of America*, 91(3), 974–978. <https://doi.org/10.1073/pnas.91.3.974>
- Povsic, T. J., Kohout, T. A., & Lefkowitz, R. J. (2003). β -Arrestin1 Mediates Insulin-like Growth Factor 1 (IGF-1) Activation of Phosphatidylinositol 3-Kinase (PI3K) and Anti-apoptosis. *Journal of Biological Chemistry*, 278(51), 51334–51339. <https://doi.org/10.1074/jbc.M309968200>
- Punzo, C., Xiong, W., & Cepko, C. L. (2012). Loss of Daylight Vision in Retinal Degeneration: Are Oxidative Stress and Metabolic Dysregulation to Blame? *Journal of Biological Chemistry*, 287(3), 1642–1648. <https://doi.org/10.1074/jbc.R111.304428>
- Purves, D., Augustine, G. J., & Fitzpatrick, D. (2001). Anatomical Distribution of Rods and Cones. In *Neuroscience*. Sinauer Associates. <https://www.ncbi.nlm.nih.gov/books/NBK10848/>
- Rajagopal, S., Rajagopal, K., & Lefkowitz, R. J. (2010). Teaching old receptors new tricks: biasing seven-transmembrane receptors. *Nature Reviews Drug Discovery*, 9(5), 373–386. <https://doi.org/10.1038/nrd3024>
- Raymond, P. A., Colvin, S. M., Jabeen, Z., Nagashima, M., Barthel, L. K., Hadidjojo, J., Popova, L., Pejaver, V. R., & Lubensky, D. K. (2014). Patterning the Cone Mosaic Array in Zebrafish Retina Requires Specification of Ultraviolet-Sensitive Cones. *PLoS ONE*, 9(1), e85325. <https://doi.org/10.1371/journal.pone.0085325>
- Revankar, C. M., Vines, C. M., Cimino, D. F., & Prossnitz, E. R. (2004). Arrestins Block G Protein-coupled Receptor-mediated Apoptosis. *Journal of Biological Chemistry*, 279(23), 24578–24584. <https://doi.org/10.1074/jbc.M402121200>
- Richards, F. M., Alderton, W. K., Kimber, G. M., Liu, Z., Strang, I., Redfern, W. S., Valentin, J.-P., Winter, M. J., & Hutchinson, T. H. (2008). Validation of the use of zebrafish larvae in visual safety assessment. *Journal of Pharmacological and Toxicological Methods*, 58(1), 50–58. <https://doi.org/10.1016/j.vascn.2008.04.002>
- Richman, E. A. (2007). The economic impact of vision problems: The toll of major adult eye disorders, visual impairment, and blindness on the U.S. economy. *Prevent Blindness America*.

- Rihel, J., Prober, D. A., Arvanites, A., Lam, K., Zimmerman, S., Jang, S., Haggarty, S. J., Kokel, D., Rubin, L. L., Peterson, R. T., & Schier, A. F. (2010). Zebrafish behavioral profiling links drugs to biological targets and rest/wake regulation. *Science (New York, NY)*, 327(5963), 348–351. <https://doi.org/10.1126/science.1183090>
- Rihel, J., & Schier, A. F. (2012). Behavioral screening for neuroactive drugs in zebrafish. *Developmental Neurobiology*, 72(3), 373–385. <https://doi.org/10.1002/dneu.20910>
- Rinner, O., Rick, J. M., & Neuhauss, S. C. F. (2005). Contrast sensitivity, spatial and temporal tuning of the larval zebrafish optokinetic response. *Investigative Ophthalmology and Visual Science*. <https://doi.org/10.1167/iovs.04-0682>
- Robinson, J., Schmitt, E. A., Hárosi, F. I., Reece, R. J., & Dowling, J. E. (1993). Zebrafish ultraviolet visual pigment: absorption spectrum, sequence, and localization. *Proceedings of the National Academy of Sciences of the United States of America*, 90(13), 6009–6012. <http://www.ncbi.nlm.nih.gov/pubmed/8327475>
- Rossmiller, B., Mao, H., & Lewin, A. S. (2012). Gene therapy in animal models of autosomal dominant retinitis pigmentosa. *Molecular Vision*, 18, 2479–2496. <http://www.ncbi.nlm.nih.gov/pubmed/23077406>
- Rotstein, N. P., Politi, L. E., German, O. L., & Girotti, R. (2003). Protective effect of docosahexaenoic acid on oxidative stress-induced apoptosis of retina photoreceptors. *Investigative Ophthalmology & Visual Science*, 44(5), 2252–2259. <https://doi.org/10.1167/iovs.02-0901>
- Ruan, G.-X., Barry, E., Yu, D., Lukason, M., Cheng, S. H., & Scaria, A. (2017). CRISPR/Cas9-Mediated Genome Editing as a Therapeutic Approach for Leber Congenital Amaurosis 10. *Molecular Therapy*, 25(2), 331–341. <https://doi.org/10.1016/j.ymthe.2016.12.006>
- Saade, C. J., Alvarez-Delfin, K., & Fadool, J. M. (2013). Rod Photoreceptors Protect from Cone Degeneration-Induced Retinal Remodeling and Restore Visual Responses in Zebrafish. *Journal of Neuroscience*, 33(5), 1804–1814. <https://doi.org/10.1523/JNEUROSCI.2910-12.2013>
- Sakaguchi, D. S., Van Hoffelen, S. J., & Young, M. J. (2003). Differentiation and morphological integration of neural progenitor cells transplanted into the developing mammalian eye. *Annals of the New York Academy of Sciences*, 995(1), 127–139. <https://doi.org/10.1111/j.1749-6632.2003.tb03216.x>

- Salbreux, G., Barthel, L. K., Raymond, P. A., & Lubensky, D. K. (2012). Coupling Mechanical Deformations and Planar Cell Polarity to Create Regular Patterns in the Zebrafish Retina. *PLoS Computational Biology*, 8(8), e1002618. <https://doi.org/10.1371/journal.pcbi.1002618>
- Samsdodd, F. (2005). Target-based drug discovery: is something wrong? *Drug Discovery Today*, 10(2), 139–147. [https://doi.org/10.1016/S1359-6446\(04\)03316-1](https://doi.org/10.1016/S1359-6446(04)03316-1)
- Shu, X., Zeng, Z., Gautier, P., Lennon, A., Gakovic, M., Cheetham, M. E., Patton, E. E., & Wright, A. F. (2011). Knockdown of the zebrafish ortholog of the retinitis pigmentosa 2 (RP2) gene results in retinal degeneration. *Investigative Ophthalmology and Visual Science*. <https://doi.org/10.1167/iovs.10-6800>
- Siegert, S., Cabuy, E., Scherf, B. G., Kohler, H., Panda, S., Le, Y.-Z., Fehling, H. J., Gaidatzis, D., Stadler, M. B., & Roska, B. (2012). Transcriptional code and disease map for adult retinal cell types. *Nature Neuroscience*, 15(3), 487–495. <https://doi.org/10.1038/nn.3032>
- Sorrentino, F. S., Gallenga, C. E., Bonifazzi, C., & Perri, P. (2016). A challenge to the striking genotypic heterogeneity of retinitis pigmentosa: a better understanding of the pathophysiology using the newest genetic strategies. *Eye*, 30(12), 1542–1548. <https://doi.org/10.1038/eye.2016.197>
- Stainier, D. Y. R. (2001). Zebrafish genetics and vertebrate heart formation. *Nature Reviews Genetics*, 2(1), 39–48. <https://doi.org/10.1038/35047564>
- Stearns, G., Evangelista, M., Fadool, J. M., & Brockerhoff, S. E. (2007). A Mutation in the Cone-Specific pde6 Gene Causes Rapid Cone Photoreceptor Degeneration in Zebrafish. *Journal of Neuroscience*, 27(50), 13866–13874. <https://doi.org/10.1523/JNEUROSCI.3136-07.2007>
- Sung, C. H., Makino, C., Baylor, D., & Nathans, J. (1994). A rhodopsin gene mutation responsible for autosomal dominant retinitis pigmentosa results in a protein that is defective in localization to the photoreceptor outer segment. *The Journal of Neuroscience: The Official Journal of the Society for Neuroscience*, 14(10), 5818–5833. <http://www.ncbi.nlm.nih.gov/pubmed/7523628>
- Swinney, D. (2013). Phenotypic vs. Target-Based Drug Discovery for First-in-Class Medicines. *Clinical Pharmacology & Therapeutics*, 93(4), 299–301. <https://doi.org/10.1038/clpt.2012.236>
- Swinney, D. C., & Anthony, J. (2011). How were new medicines discovered? *Nature Reviews Drug Discovery*, 10(7), 507–519. <https://doi.org/10.1038/nrd3480>

- Szymański Paweł and Markowicz, M., & Mikiciuk-Olasik, E. (2011). Adaptation of High-Throughput Screening in Drug Discovery—Toxicological Screening Tests. *International Journal of Molecular Sciences*, *13*(12), 427–452. <https://doi.org/10.3390/ijms13010427>
- Tam, B. M., Xie, G., Oprian, D. D., & Moritz, O. L. (2006). Mislocalized Rhodopsin Does Not Require Activation to Cause Retinal Degeneration and Neurite Outgrowth in *Xenopus laevis*. *Journal of Neuroscience*, *26*(1), 203–209. <https://doi.org/10.1523/JNEUROSCI.3849-05.2006>
- Terstappen, G. C., Schlüpen, C., Raggiaschi, R., & Gaviraghi, G. (2007). Target deconvolution strategies in drug discovery. *Nature Reviews Drug Discovery*, *6*(11), 891–903. <https://doi.org/10.1038/nrd2410>
- Tochitsky, I., Kienzler, M. A., Isacoff, E., & Kramer, R. H. (2018). Restoring Vision to the Blind with Chemical Photoswitches. In *Chemical Reviews*. <https://doi.org/10.1021/acs.chemrev.7b00723>
- Tochitsky, I., Trautman, J., Gallerani, N., Malis, J. G., & Kramer, R. H. (2017). Restoring visual function to the blind retina with a potent, safe and long-lasting photoswitch. *Scientific Reports*. <https://doi.org/10.1038/srep45487>
- Tsujikawa, M., & Malicki, J. (2004). Genetics of photoreceptor development and function in zebrafish. *The International Journal of Developmental Biology*, *48*(8–9), 925–934. <https://doi.org/10.1387/ijdb.041890mt>
- Venkatraman, P., Cramer, R., Pang, C. P., Zhang, M., & Leung, Y. F. (2015). Understanding the contribution of photoreceptors to the Visual Motor Response. *Investigative Ophthalmology & Visual Science*, *56*(7), 998–998.
- Venkatraman, P., Mills-Henry, I., Ramaswamy, K., Pascuzzi, P., Hassan, M., Zhang, J., Zhang, X., Ma, P., Dowling, J., Pang, C. P., Zhang, M., & Leung, Y. F. (2020). Rods contribute to Visual Behaviour in Larval Zebrafish (In Revision). *Investigative Ophthalmology & Visual Science*.
- Viewpoint LifeSciences*. (n.d.). Retrieved May 23, 2017, from <http://www.viewpoint.fr/en/p/equipment/zebrabox>
- Vignet, C., Bégout, M.-L., Péan, S., Lyphout, L., Leguay, D., & Cousin, X. (2013). Systematic Screening of Behavioral Responses in Two Zebrafish Strains. *Zebrafish*, *10*(3), 365–375. <https://doi.org/10.1089/zeb.2013.0871>

- Walker, S. L., Ariga, J., Mathias, J. R., Coothankandaswamy, V., Xie, X., Distel, M., Köster, R. W., Parsons, M. J., Bhalla, K. N., Saxena, M. T., & Mumm, J. S. (2012). Automated Reporter Quantification In Vivo: High-Throughput Screening Method for Reporter-Based Assays in Zebrafish. *PLoS ONE*, 7(1), e29916. <https://doi.org/10.1371/journal.pone.0029916>
- Wang, Jialu, Hanada, K., Staus, D. P., Makara, M. A., Dahal, G. R., Chen, Q., Ahles, A., Engelhardt, S., & Rockman, H. A. (2017). Gai is required for carvedilol-induced β 1 adrenergic receptor β -arrestin biased signaling. *Nature Communications*, 8(1), 1706. <https://doi.org/10.1038/s41467-017-01855-z>
- Wang, Jing, Morita, Y., Mazelova, J., & Deretic, D. (2012). The Arf GAP ASAP1 provides a platform to regulate Arf4-and Rab11-Rab8-mediated ciliary receptor targeting. *EMBO Journal*. <https://doi.org/10.1038/emboj.2012.253>
- Westerfield, M. (2007). The Zebrafish Book. A Guide for the Laboratory Use of Zebrafish (*Danio rerio*), 5th Edition. *University of Oregon Press, Eugene (Book)*.
- White, D. T., Eroglu, A. U., Wang, G., Zhang, L., Sengupta, S., Ding, D., Rajpurohit, S. K., Walker, S. L., Ji, H., Qian, J., & Mumm, J. S. (2016). ARQiv-HTS, a versatile whole-organism screening platform enabling in vivo drug discovery at high-throughput rates. *Nature Protocols*, 11(12), 2432–2453. <https://doi.org/10.1038/nprot.2016.142>
- Wickham, H. (2016). *ggplot2: Elegant Graphics for Data Analysis*. Springer-Verlag New York.
- Wiley, D. S., Redfield, S. E., & Zon, L. I. (2017). Chemical screening in zebrafish for novel biological and therapeutic discovery. *Methods in Cell Biology*, 138, 651–679. <https://doi.org/10.1016/bs.mcb.2016.10.004>
- Wisler, J. W., DeWire, S. M., Whalen, E. J., Violin, J. D., Drake, M. T., Ahn, S., Shenoy, S. K., & Lefkowitz, R. J. (2007). A unique mechanism of beta-blocker action: Carvedilol stimulates beta-arrestin signaling. *Proceedings of the National Academy of Sciences*, 104(42), 16657–16662. <https://doi.org/10.1073/pnas.0707936104>
- Xie, R., Zhang, M., Venkatraman, P., Zhang, X., Zhang, G., Carmer, R., Kantola, S. A., Pang, C. P., Ma, P., Zhang, M., Zhong, W., & Leung, Y. F. (2019). Normalization of large-scale behavioural data collected from zebrafish. *PLOS ONE*, 14(2), e0212234. <https://doi.org/10.1371/journal.pone.0212234>
- Y. Sasamoto, T. Nakao, N. Matsumura, & M. Tsujikawa. (2010). Generation of Transgenic Zebrafish Lines With Human Rhodopsin Mutations. *Investigative Ophthalmology & Visual*

<https://iovs.arvojournals.org/article.aspx?articleid=2370047&resultClick=1>

- Young, M. J., Ray, J., Whiteley, S. J. O., Klassen, H., & Gage, F. H. (2000). Neuronal Differentiation and Morphological Integration of Hippocampal Progenitor Cells Transplanted to the Retina of Immature and Mature Dystrophic Rats. *Molecular and Cellular Neuroscience*, 16(3), 197–205. <https://doi.org/10.1006/mcne.2000.0869>
- Zhang, F., Qin, W., Zhang, J. P., & Hu, C. Q. (2015). Antibiotic toxicity and absorption in zebrafish using liquid chromatography-tandem mass spectrometry. *PLoS ONE*. <https://doi.org/10.1371/journal.pone.0124805>
- Zhang, L., Xiang, L., Liu, Y., Venkatraman, P., Chong, L., Cho, J., Bonilla, S., Jin, Z.-B., Pang, C. P., Ko, K. M., Ma, P., Zhang, M., & Leung, Y. F. (2016). A Naturally-Derived Compound Schisandrin B Enhanced Light Sensation in the pde6c Zebrafish Model of Retinal Degeneration. *PLOS ONE*, 11(3), e0149663. <https://doi.org/10.1371/journal.pone.0149663>
- Zhou, Y., Cattley, R. T., Cario, C. L., Bai, Q., & Burton, E. A. (2014). Quantification of larval zebrafish motor function in multiwell plates using open-source MATLAB applications. *Nature Protocols*, 9(7), 1533–1548. <https://doi.org/10.1038/nprot.2014.094>

VITA

Logan Ganzen was born on January 8, 1992 to Susan and Jeffery Ganzen in Fontana, California. He grew up in Oak Hills, California and graduated from Serrano High School in 2010. After high school, Logan attended the University of California Riverside and completed a Bachelor of Science in Microbiology in 2014. During this time, Logan worked in the laboratory of Dr. Bradley Hyman with then Ph.D. student Samantha Lewis to investigate the mechanism of mitochondrial DNA replication in *Caenorhabditis elegans*. Upon graduation, Logan attended Purdue University to complete a Ph.D. He joined the Purdue University Interdisciplinary Life Sciences Program, (PULSe) in 2014. In this program, Logan performed his thesis research in the laboratory Dr. Yuk Fai Leung utilizing zebrafish models of Retinitis Pigmentosa to find novel therapies to treat the disease. Logan completed his Ph.D. in April of 2020.

PUBLICATIONS

Ganzen, L.; Ko, MJ; Zhang, M; Xie, R; Chen, Y; Zhang, L; James, R; Mumm, J; Van Rijn, R; Zhong, W; Pang, CP; Zhang, M; Tsujikawa, M; Leung, YF; Drug Screening with Zebrafish Visual Behavior Identifies Carvedilol as a Potential Treatment for Retinitis Pigmentosa, Submitted.

Ko, MJ. †; Ganzen, L. †; Coskun, E.; Mukadam, A.; Leung, YF.; Van Rijn, R.; A Critical Evaluation of TRPA1-mediated Locomotor Behavior in Zebrafish as a Screening Tool for Novel Anti-nociceptive Drug Discovery. *Scientific Reports*. 2019 Feb 20;9(1):2430.

Ganzen, L.†; Venkatraman, P. †; Pang, C.P.; Leung, Y.F.; Zhang, M. Utilizing Zebrafish Visual Behaviors in Drug Screening for Retinal Degeneration. 2017 Jun 2;18(6).

Carrillo, A.; Schacht, P.; Cabrera, I.; Blahut, J.; Prudhomme, L.; Dietrich, S.; Beckman, T.; Mei, J.; Carrera, C.; Chen, V.; Clark, I.; Fierro, G.; Ganzen, L.; Orellana, J.; Wise, S.; Yang, K.; Zhong, H.; Borkovich, K. Functional Profiling of Transcription Factor Genes in *Neurospora crassa*. *G3*. 2017 Sep 7;7(9):2945-2956.